

INTERFERENCE MANAGEMENT
FOR INTERFERENCE CHANNELS:
PERFORMANCE IMPROVEMENT
AND LATTICE TECHNIQUES

MARIA CONSTANZA ESTELA ZAMORA

SUPERVISOR
DR CONG LING

A Thesis submitted in fulfilment of requirements for the degree
of Doctor of Philosophy of Imperial College London

April 2014

Communications and Signal Processing Group
Department of Electrical and Electronic Engineering
Imperial College London

To my parents, my sister and Stephane

Abstract

This thesis focuses on interference management methods for interference channels, in particular on interference alignment. The aim is to contribute to the understanding of issues such as the performance of the interference alignment scheme and lattice codes for interference channels. Interference alignment is studied from two perspectives. One is the signal space perspective where precoding methods are designed to align the interference in half of the received subspace. Cadambe and Jafar found precoding matrices to achieve the theoretical degrees of freedom. However, using an interference suppression technique over the Cadambe and Jafar scheme, yields poor performance. Thus, in this thesis precoding methods such as singular value decomposition and Tomlinson-Harashima precoding are proposed to improve performance. The second perspective is on the signal scale, where structured codes are used to align interference. For this, lattice codes are suitable. In this research, the problem was initially approached with a many-to-one interference channel. Using lattices, joint maximum-likelihood decoding of the desired signal and the sum of the interference signals is used, and the union bound of the error probability for user 1 is derived, in terms of the theta series. Later, a symmetric interference channel is studied. Jafar built a scheme for every level of interference, where interference was aligned and could be cancelled. In this thesis, Barnes-Wall lattices are used since they have a similar structure to the scheme proposed by Jafar, and it is shown to be possible to improve the performance of the technique using codes constructed with Barnes-Wall lattices. Finally, previous work has found the generalized degrees of freedom for a two-user symmetric interference channel using random codes. Here, we obtain the generalized degrees of freedom for that channel setting using lattice Gaussian

distribution.

Acknowledgment

I want to thank my supervisor Dr Cong Ling for his help during these years. His guidance, support and experience were key to the results of this thesis. I would also like to thank Dr Laura Luzzi who worked with me recently and whose mathematical knowledge was extremely useful for my learning. I would like to thank Prof. Jean-Claude Belfiore with whom I worked on many occasions: firstly in a great opportunity during an IDEA League trip to Paris, and later on some papers. His experience in the field was an immense help to my learning. I would also like to thank Dr Haishi Ning and Yanfei Yan for many fruitful discussions.

In particular, I would like to thank Yanfei Yan for providing the Matlab code for the Bounded distance decoder.

Finally, I would like to thank my parents, my sister and Stephane. Without their support, encouragement and motivation this work may not have been possible. To them I dedicate this thesis.

Statement of Originality

I hereby declare that this thesis is my own work, and to the best of my knowledge everything else it is appropriately referenced or acknowledged.

SignedMaria Constanza Estela Zamora.....

Date.....14/04/2014.....

Copyright Declaration

The copyright of this thesis rests with the author and is made available under a Creative Commons Attribution Non-Commercial No Derivatives licence. Researchers are free to copy, distribute or transmit the thesis on the condition that they attribute it, that they do not use it for commercial purposes and that they do not alter, transform or build upon it. For any reuse or redistribution, researchers must make clear to others the licence terms of this work.

Publications

1. M.C. Estela and C. Ling, "Improving Interference Alignment by Precoding Methods", in *IEEE Sensor Signal Processing for Defence (SSPD 2011)*, Sep. 2011.
2. M.C. Estela, L. Luzzi, C. Ling and J.-C. Belfiore, "Analysis of lattice codes for the Many-to-one Interference Channel", in *IEEE Information Theory Workshop, ITW 2012*, Sep. 2012.
3. M.C. Estela, C. Ling and J.-C. Belfiore, "Barnes-Wall lattices for the Symmetric Interference Channel", in *IEEE International Symposium on Information Theory, ISIT 2013*, Jul. 2013.

Contents

Abstract	5
Acknowledgment	8
Statement of Originality	10
Copyright Declaration	11
Publications	13
Contents	15
List of Figures	19
List of Tables	21
List of Algorithms	22
Abbreviations	24
Notation	26
Chapter 1. Introduction	28
1.1 Overview	28
1.2 Special interference channels	29

1.3	Types of interference and interference management techniques for interference channels	32
1.4	Interference alignment: Signal space approach	37
1.5	Interference alignment: Signal scale approach	41
1.5.1	Lattice codes	41
1.5.2	Lattice codes in interference channels: Key example [1]	49
1.6	Generalized Degrees of Freedom	50
1.7	Research objectives	51
1.8	Technical contributions	52
1.9	Thesis structure	52
 Chapter 2. Literature review		55
2.1	Interference alignment: Signal space approach	55
2.2	Interference alignment: Signal scale approach	60
2.3	Channel knowledge for interference alignment	66
 Chapter 3. Precoding methods for interference alignment		68
3.1	Introduction	68
3.2	Interference alignment [10]	68
3.3	Precoding schemes to improve performance	69
3.3.1	Singular value decomposition	73
3.3.2	Tomlinson-Harashima Precoding [17], [49]	75
3.4	Precoding methods applied to interference alignment	77
3.4.1	Simulations on precoding methods applied to interference alignment	78
3.5	Conclusions	85

Chapter 4. Lattice codes for the many-to-one interference channel	88
4.1 Introduction	88
4.2 System model and lattice alignment	88
4.3 Flatness factor	90
4.3.1 ML decoding	90
4.3.2 Gaussian measures on lattices and flatness factor	91
4.3.3 Examples	92
4.3.4 Average behaviour	93
4.4 Error probabilities	93
4.5 The good and bad lattices	97
4.6 Conclusions	99
Chapter 5. Barnes-Wall lattices for the symmetric interference channel	102
5.1 Introduction	102
5.2 Symmetric interference channel by Jafar [5]	103
5.2.1 Encoding	104
5.2.2 Decoding	107
5.3 Barnes-Wall lattices	109
5.3.1 Encoding	109
5.3.2 Decoding	109
5.4 Barnes-Wall lattices for the two-user symmetric interference channel	110
5.4.1 Preliminary idea	110
5.4.2 Decoding	113
5.4.3 General proposed scheme	116
5.4.4 Selecting the lattice that mimics the Jafar one-dimensional message	116

5.4.5	Simulations	122
5.5	Barnes-Wall lattices for the K -user symmetric interference channel	123
5.6	Conclusions	126
Chapter 6. Generalized degrees of freedom of a two-user symmetric interference channel using lattice Gaussian distribution		129
6.1	Introduction	129
6.2	Preliminary	129
6.2.1	Generalized degrees of freedom with random codes [2]	130
6.2.2	Lattice Gaussian Coding	133
6.3	Achieving the generalized degrees of freedom for the two-user symmetric interference channel using lattice Gaussian distribution	137
6.3.1	Very strong and strong interference scenarios	138
6.3.2	Moderately weak and weak interference	148
6.3.3	Noisy interference	165
6.4	Conclusions	167
Chapter 7. Conclusion and Future Work		169
7.1	Conclusions	169
7.2	Future work	170
Bibliography		174
Appendix A. Fisher-Huber optimization		182
Appendix B. Proof of $\epsilon_{\Lambda}(\sigma) = \epsilon_{g\Lambda}(g\sigma)$		185

List of Figures

1.1	Diagram of an interference channel	28
1.2	three-user interference channel	29
1.3	Many-to-one channel with three users	30
1.4	Achievable rate region for a two-user interference channel (adapted from [7])	36
1.5	Three-user interference alignment scheme (adapted from [10])	38
1.6	A two-dimensional lattice	42
1.7	Example of a three-user many-to-one interference channel [1]	49
2.1	Example of the deterministic many-to-one interference channel [2]	62
3.1	Equivalent system with SVD	73
3.2	DFE [49]	75
3.3	Equivalent system using THP [49]	76
3.4	Energy diagram before and after V	82
3.5	Bit error rate for user 1 and $n = 1$, and different precoding schemes	83
3.6	Bit error rate for user 1 and $n = 2$, and different precoding schemes	83
3.7	Bit error rate for user 2 and $n = 1$, and different precoding schemes	84
3.8	Bit error rate for user 2 and $n = 2$, and different precoding schemes	84
3.9	Bit error rate for user 3 and $n = 1$, and different precoding schemes	85

3.10	Bit error rate for user 3 and $n = 2$, and different precoding schemes	85
4.1	three-user many-to-one interference channel	89
4.2	Flatness factor for two and eight dimensional lattices	93
4.3	Function $f_{\sigma\Lambda_2}(\mathbf{t})$ using $\Lambda_2 = \mathbb{Z}^2$ and $\sigma^2 = 0.15$	94
4.4	Function $f_{\sigma,\Lambda_2}(\mathbf{t})$ using $\Lambda_2 = A_2$ and $\sigma^2 = 0.15$	95
4.5	Error probability	97
5.1	Error rate for very strong interference, when $Q = 4, M = 2, N = 2$	123
5.2	Error rate for weak interference, when $Q = 4, M = 1, N = 1$	123
5.3	Error rate for strong interference, when $Q = 8, M = 1, N = 2$	124
5.4	Error rate for weak interference, when $Q = 8, M = 1, N = 1$ and $K = 3$	126
6.1	W curve (adapted from [2])	133
6.2	System model	137
6.3	MAC1	144
6.4	MAC2	144
6.5	Intersection region for the very strong interference case	145
6.6	Intersection region for the strong interference case	146
6.7	Intersection region for the weak interference case, region 1	156
6.8	Intersection region for the weak interference case, region 2	157
6.9	Intersection region for the noisy interference case	166

List of Tables

2.1	Cadambe and Jafar scheme vs Shen and Host Madsen scheme	58
-----	---	----

List of Algorithms

3.1	Fisher-Huber algorithm [49]	74
3.2	Modified Fisher-Huber algorithm (modified from [49])	80
5.1	General decoding algorithm (adapted from [5])	108
5.2	Sequential BDD for BW lattices (modified from [26])	110

Abbreviations

AWGN:	Additive white Gaussian noise
BER:	Bit error rate
BDD:	Bounded distance decoder
BW:	Barnes-Wall
CSI:	Channel State Information
DoF:	Degree of Freedom
FH:	Fischer-Huber loading algorithm
GDoF:	Generalized Degree of Freedom
HK:	Han-Kobayashi
INR:	Interference-to-noise ratio
MAC:	Multiple access channels
MIMO	Multiple-input multiple-output
MMSE:	Minimum mean squared error
ML:	Maximum-Likelihood
PDF:	Probability density function
QAM:	Quadrature Amplitude modulation

- RM:** Reed-Muller
- SISO:** Single-input single-output
- SNR:** Signal-to-noise ratio
- SVD:** Singular value decomposition
- TDMA:** Time division multiple access
- THP:** Tomlinson-Harashima precoding
- VNR:** Volume-to-noise ratio
- ZF:** Zero forcing

Notation

The most common symbols are given below. Others are defined within the text.

a, A	: Scalar
\mathbf{a}	: Column vector
\mathbf{A}	: Matrix
$(\cdot)^H$: Hermitian transpose
$\lfloor \cdot \rfloor$: Floor operation
$\lceil \cdot \rceil$: Round operation
mod	: Modulo operation
\triangleq	: Defined as
Λ, Γ	: Lattice
Θ_Λ	: Theta series of the lattice Λ
ϵ_Λ	: Flatness factor of the lattice Λ
\subseteq	: Subset
\supseteq	: Superset
\cong	: Isomorphism
\oplus	: Binary sum
\otimes	: Kronecker product
\lim	: limit

Chapter 1

Introduction

1.1 Overview

Interference is one of the main issues in wireless communications. It can be found in different scenarios such as many transmitters and receptors pairs, known as interference channels. In an interference channel, each transmitter wishes to communicate with its correspondent receiver. However, since the channel is shared among all users, each receiver has interference from all of the other transmissions that are not intended for it.

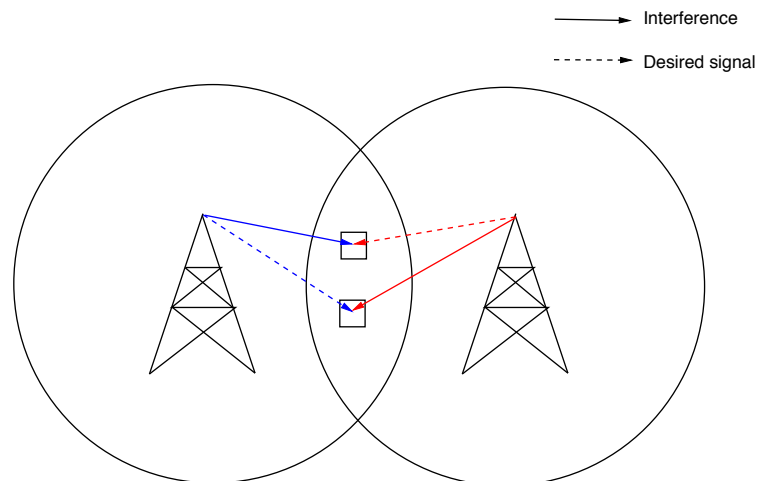


Figure 1.1: Diagram of an interference channel

A K -user fully connected interference channel is described by

$$y_i = h_{ii}x_i + \sum_{j \neq i}^K h_{ij}x_j + z_i \quad (1.1)$$

where h_{ij} is the channel gain between transmitter j and receiver i , x_i is the transmitted signal from transmitter i subject to a power constraint $E[|x_i|^2] = P_i$, and z_i is the additive white Gaussian noise (AWGN) of zero mean and variance σ^2 at receiver i , for $i, j = 1, \dots, K$. The signal-to-noise ratio (SNR) of user i is defined as

$$\text{SNR}_i = \frac{|h_{ii}|^2 P_i}{\sigma^2}, \quad (1.2)$$

and the interference-to-noise ratio (INR) from user j over user i is expressed as

$$\text{INR}_{ij} = \frac{|h_{ij}|^2 P_j}{\sigma^2}. \quad (1.3)$$

This model is represented in Fig. 1.2 for a three-user interference channel.

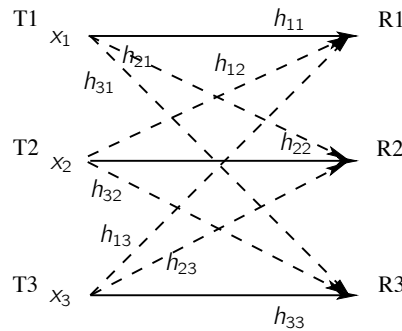


Figure 1.2: three-user interference channel

In this thesis we define the channel gains according to our purposes. These are defined in each chapter accordingly.

1.2 Special interference channels

Equation (1.1) can be simplified into special interference channels. In this section we describe some simplifications used in later chapters.

- **Many-to-one interference channel:** The many-to-one interference channel is a simplification of the fully connected interference channel, where only one user suffers from interference. In particular, and without loss of generality, we consider the following definition [1]. Given a fully connected interference channel as in (1.1), the many-to-one interference channel corresponds to the case where all channel gains are zero except h_{ii} and h_{1i} , for $1 \leq i \leq K$. Thus, only user 1 suffers from interference. Fig. 1.3 illustrates the three-user many-to-one interference channel described here. The many-to-one interference channel enables the simplification of

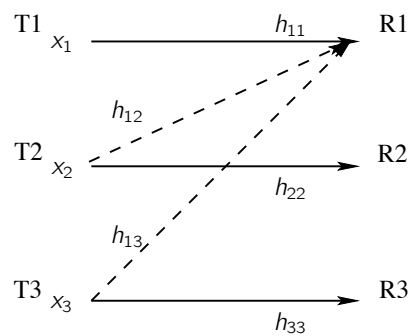


Figure 1.3: Many-to-one channel with three users

the problem of the interference channel while we can still develop tools that can be later used for the fully connected interference channel.

- **Symmetric interference channel:** The symmetric interference channel is the fully connected interference channel from (1.1) where all direct power channel gains are equal, and all indirect channel gains are equal. Thus, we can define [2] $|h_{ii}|^2 \triangleq |h_d|^2$, $|h_{ij}|^2 \triangleq |h_c|^2$ and $P_i \triangleq P$, or $\text{SNR}_i \triangleq \text{SNR}$ and $\text{INR}_{ij} \triangleq \text{INR}$, $\forall i, 1 \leq i \leq K$.
- **Deterministic and Q -base representation interference channel:** The deterministic channel was defined in [3] and consists of representing the channel at signal levels, which is equivalent to a unit of power in the Gaussian channel [1]. The idea is to write the real valued channel input in base 2. Thus, the signal is constructed in bits as

$$x = 0.b_1b_2b_3b_4 \dots \quad (1.4)$$

With this representation, the noise is truncated in such way that bits that fall under the level of noise are lost. Thus, the interference channel can be written as [1]

$$y_i = \lfloor 2^{n_{i0}} x_0 \rfloor \oplus \cdots \oplus \lfloor 2^{n_{iK}} x_K \rfloor, \quad (1.5)$$

where addition is performed on each bit. The channel also retains the superposition of transmitted signals. The signal at the receiver can be viewed as a base 2 representation, separating the effect of the interference by level.

A similar model is explained in [4] and [5], where a base Q is used instead of a base 2. Here, a symmetric interference channel is used, where $h_{ii} = 1$ while the indirect channel gains are given by $h_{ij} = Q^M$, for any integer M . The transmitted symbol at transmitter k is built as:

$$x^{[k]} = \left[x_{N-1}^{[k]} x_{N-2}^{[k]} \cdots x_1^{[k]} x_0^{[k]} \right]_Q \quad (1.6)$$

$$= Q^{N-1} x_{N-1}^{[k]} + Q^{N-2} x_{N-2}^{[k]} + \cdots + Q x_1^{[k]} + x_0^{[k]}. \quad (1.7)$$

where $x_i^{[k]} \in \{1, 2, \dots, Q-2\}$. Consider for example $1 < M < N$. At the receiver k we have

$$\begin{aligned} y^{[k]} &= \sum_{j \neq k} Q^{M+N-1} x_{N-1}^{[j]} + \cdots + \sum_{j \neq k} Q^{N-1} \left(x_{N-1-M}^{[j]} + x_{N-1}^{[k]} \right) \\ &+ \cdots + \cdots + \sum_{j \neq k} Q^M \left(x_0^{[j]} + x_M^{[k]} \right) + Q^{M-1} x_{M-1}^{[j]} \\ &+ \cdots x_0^{[k]} + z^{[k]}. \end{aligned} \quad (1.8)$$

As in the deterministic interference channel we see that the Q -base channel can also be represented with levels.

1.3 Types of interference and interference management techniques for interference channels

So far, information theory has classified interference in the following levels or types: noisy, weak, moderately weak, strong and very strong.

When interference is noisy, it is treated as noise, because it falls below the level of noise. This implies that there is no loss of data rate due to interference. When interference is strong and very strong, interference decoding is used. For the case of very strong interference, Carleial [6] showed that the capacity of a channel with very strong interference is the same as a channel with no interference at all. This is because when interference is very strong, interference is decoded before the desired signal. In a channel with no interference, the data rate is known to be given by

$$R_i < \frac{1}{2} \log \left(1 + \frac{P_i}{\sigma_i^2} \right) \equiv C_i \quad (1.9)$$

where C_i corresponds to the capacity achieved by user i when there is no interference, and P_i and σ_i^2 are the signal and noise powers respectively. Consider a two-user interference channel given by

$$y_1 = \sqrt{a_{11}}x_1 + \sqrt{a_{21}}x_2 + z_1 \quad (1.10)$$

$$y_2 = \sqrt{a_{12}}x_1 + \sqrt{a_{22}}x_2 + z_2, \quad (1.11)$$

where $a_{ii} = 1$ and $\sqrt{a_{ij}}$ are the channel gains from transmitter i to receiver j , and z_i is the AWGN of user i with zero mean and variance σ_i^2 . Carleial [6] demonstrated that in a two-user interference channel, when interference is very strong, the capacity of the channel is the same as if there was no interference at all. Here, the very strong interference condition is satisfied when $a_{12} \geq (P_2 + \sigma_2^2)/\sigma_1^2$ and $a_{21} \geq (P_1 + \sigma_1^2)/\sigma_2^2$. Then, the rate

achieved with interference is given by

$$C_1 < R_1 < \frac{1}{2} \log \left(1 + \frac{a_{12}P_1}{P_2 + \sigma_2^2} \right) \quad (1.12)$$

$$C_2 < R_2 < \frac{1}{2} \log \left(1 + \frac{a_{21}P_2}{P_1 + \sigma_1^2} \right) \quad (1.13)$$

The data rate achieved with interference in (1.12) and (1.13) is bigger than the one achieved without interference (1.9), so the data rate is, in fact, not affected by interference.

In the case of strong interference some approaches [7,8] managed to calculate the lower bound of the data achievable rate, for a two-user interference channel. As shown in [7–9] the capacity region of a two-user Gaussian interference channel under strong interference is the intersection of the capacity regions of a two-multiple access channel (MAC). The MAC consists of a channel with multiple transmitters and one receiver and, unlike the interference channel, the receiver is interested in all the received signals. The region found in [7–9] is given by

$$0 \leq R_1 \leq C_1 \quad (1.14)$$

$$0 \leq R_2 \leq C_2 \quad (1.15)$$

$$0 \leq R_1 + R_2 \leq \min \left\{ \frac{1}{2} \log \left(1 + \frac{P_1 + a_{21}P_2}{\sigma_1^2} \right), \frac{1}{2} \log \left(1 + \frac{a_{12}P_1 + P_2}{\sigma_2^2} \right) \right\}. \quad (1.16)$$

Here the conditions are given by $a_{21} \geq \sigma_1^2/\sigma_2^2$ and $a_{12} \geq \sigma_2^2/\sigma_1^2$.

The problem is still relatively open for moderate or not so strong interference. One of the main achievements so far can be seen in the work of Han and Kobayashi [7], who determined an inner bound for the two-user interference channel using superposition coding. Han and Kobayashi (HK) defined a novel method of determining the capacity of an interference channel using private and common messages from each transmitter. Both receivers can decode the common messages from each of the transmitters, leaving the private messages as noise. Once the common messages have been decoded, they are subtracted from the received signal and each receiver can decode its own private

message, leaving the other user's private message as noise. In that paper, the achievable region is defined to be equal to the polyhedron of Fig. 1.4, which consists of all the pairs (R_1, R_2) of nonnegative real numbers such that [7]:

$$R_1 \leq \rho_1 \quad (1.17)$$

$$R_2 \leq \rho_2 \quad (1.18)$$

$$R_1 + R_2 \leq \rho_{12} \quad (1.19)$$

$$2R_1 + R_2 \leq \rho_{10} \quad (1.20)$$

$$R_1 + 2R_2 \leq \rho_{20}, \quad (1.21)$$

where

$$\rho_1 = \sigma_1^* + I(Y_1; U_1 | W_1 W_2 Q) \quad (1.22)$$

$$\rho_2 = \sigma_2^* + I(Y_2; U_2 | W_1 W_2 Q) \quad (1.23)$$

$$\rho_{12} = \sigma_{12} + I(Y_1; U_1 | W_1 W_2 Q) + I(Y_2; U_2 | W_1 W_2 Q) \quad (1.24)$$

$$\begin{aligned} \rho_{10} = & 2\sigma_1^* + 2I(Y_1; U_1 | W_1 W_2 Q) + I(Y_2; U_2 | W_1 W_2 Q) \\ & - [\sigma_1^* - I(Y_2; W_1 | W_2 Q)]^+ \\ & + \min\{I(Y_2; W_2 | W_1 Q), I(Y_2; W_2 | Q)\} \\ & + [I(Y_2; W_1 | W_2 Q) - \sigma_1^*]^+, \\ & I(Y_1; W_2 | W_1 Q), I(Y_1; W_1 W_2 | Q) - \sigma_1^* \} \end{aligned} \quad (1.25)$$

$$\begin{aligned} \rho_{20} = & 2\sigma_2^* + I(Y_1; U_1 | W_1 W_2 Q) + 2I(Y_2; U_2 | W_1 W_2 Q) \\ & - [\sigma_2^* - I(Y_1; W_2 | W_1 Q)]^+ \\ & + \min\{I(Y_1; W_1 | W_2 Q), I(Y_1; W_1 | Q)\} \\ & + [I(Y_1; W_2 | W_1 Q) - \sigma_2^*]^+, \\ & I(Y_2; W_1 | W_2 Q), I(Y_2; W_1 W_2 | Q) - \sigma_2^* \}, \end{aligned} \quad (1.26)$$

and

$$[x]^+ = x \text{ if } x \geq 0, [x]^+ = 0 \text{ if } x < 0.$$

$$\sigma_1^* = \min\{I(Y_1; W_1|W_2Q), I(Y_2; W_1|U_2W_2Q)\}, \quad (1.27)$$

$$\sigma_2^* = \min\{I(Y_2; W_2|W_1Q), I(Y_1; W_2|U_1W_1Q)\}, \quad (1.28)$$

$$\begin{aligned} \sigma_{12} = \min\{ & I(Y_1; W_1W_2|Q), I(Y_2; W_1W_2|Q) , \\ & I(Y_1; W_1|W_2Q), I(Y_2; W_2|W_1Q) , \\ & I(Y_2; W_1|W_2Q), I(Y_1; W_2|W_1Q)\}, \end{aligned} \quad (1.29)$$

and Q, U_1, U_2, W_1, W_2 are random variables. W_i and U_i correspond to the common and private message for user i ($i = 1, 2$), respectively, and Q is the time sharing parameter. X_1, X_2 are defined as: $X_1 = f(U_1W_1|Q)$, $X_2 = f(U_2W_2|Q)$ and correspond to the input alphabet sets. Finally, Y_1 and Y_2 are the output alphabet sets. The points A, B, C and D in Fig. 1.4 are given by

$$A = (\rho_1, \rho_{10} - 2\rho_1), \quad (1.30)$$

$$B = (\rho_{10}, \rho_{12}, 2\rho_{12} - \rho_{10}), \quad (1.31)$$

$$C = (2\rho_{12}, \rho_{20}, \rho_{20} - \rho_{12}), \quad (1.32)$$

$$D = (\rho_{20} - 2\rho_2, \rho_2). \quad (1.33)$$

The region obtained by HK is the best known result for a two-user interference channel. Over 30 years have passed and the exact capacity for a two-user Gaussian interference channel has not yet been found. So far, an upper bound for the two-user interference channel has been identified by Etkin [2], with a difference of 1 Bit/s/Hz.

In this thesis, unless explicitly stated, we consider the following classification for different types of interference. This classification and these definitions have shown to be useful in [2] in finding an approximate region of the capacity of the two-user symmetric interference channel:

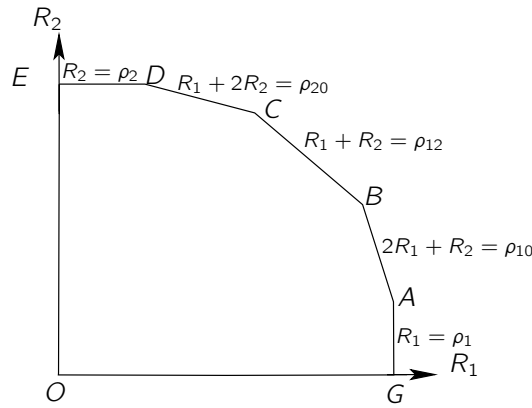


Figure 1.4: Achievable rate region for a two-user interference channel (adapted from [7])

- Noisy interference: $\text{INR}_{ij} < \sqrt{\text{SNR}_i}$
- Weak interference: $\sqrt{\text{SNR}_i} < \text{INR}_{ij} < \text{SNR}_i^2$
- Moderately weak interference: $\text{SNR}_i^{\frac{2}{3}} < \text{INR}_{ij} < \text{SNR}_i$
- Strong interference: $\text{SNR}_i < \text{INR}_{ij} < \text{SNR}_i^2$
- Very strong interference: $\text{INR}_{ij} > \text{SNR}_i^2$

Most of the previous work considers two-user interference channels, and the generalization to multiple users is not straightforward. Also to date, most of the techniques divide either time or frequency into the number of users of the interference channels, and therefore divide the available data rate among the number of users of the channel. In schemes like time division multiple access (TDMA), when interference has to be avoided, each of the K users has to communicate for a fraction of $1/K$ of the time.

A novel technique, known as interference alignment [10] has been proposed from the scope of information theory, which enables the alignment of interference at each receiver, using only half of the signal space, and leaving the other half for the intended signal, independent of the number of users that the channel has. In [10], Cadambe and Jafar characterize the network sum capacity for a K -user interference channel with interference alignment as:

$$C_{\Sigma} = \frac{K}{2} \log(\text{SNR}) + o(\log(\text{SNR})). \quad (1.34)$$

The factor $K/2$ in (1.34) represents what is defined as degree of freedom (DoF), also known as multiplexing gain, which can also be written as [11]

$$\text{DoF} = \lim_{\text{SNR} \rightarrow \infty} \frac{C_{\Sigma}(\text{SNR})}{\log(\text{SNR})} \quad (1.35)$$

This factor means that every user in a K -user interference channel can asymptotically achieve half of the capacity that it could achieve without interference. Because the exact capacity of the K -user interference channel is still an open problem, the DoF is a good representation of the capacity at high SNR. As we can see from (1.34), as the $\text{SNR} \rightarrow \infty$, the second addend of (1.34) becomes insignificant with respect to the first one, so the factor $K/2$ characterizes the capacity at high SNR. Hence, it is suitable to work with the DoF as the exact capacity is unknown.

Interference alignment is a technique properly named after Jafar's work [12] but which was actually conceived in [13] where the advantages of overlapping interference were studied. The work of Cadambe and Jafar [10] was the first to find the achievability of the technique for more than two users, which is not trivial, under certain scenarios.

The technique basically states that we can build signals, either with alignment matrices or with structured codes, such that they overlap at each of those receivers where they interfere. Interference alignment has been studied from two main approaches: 1) Interference alignment via signal space, and 2) Interference alignment via signal scale.

1.4 Interference alignment: Signal space approach

In the interference alignment technique each transmitter tries to minimize the interference to unintended receivers. This is achieved by letting all the interference signals in a given receiver align in one subspace that is different to the one for the desired signal. In interference alignment in the signal space approach, the work of Cadambe and Jafar [10] is the most followed. In that case the DoF achievability using interference alignment has been established under some scenarios:

1. The single antenna case: The $K/2$ DoF in this case has been demonstrated when

the transmitted symbols are transformed into supersymbols, or a signal vector, and where the channel is time varying or frequency fading. The channel coefficients are now represented in a diagonal channel matrix. With this scheme, each user asymptotically achieves $1/2$ DoF.

2. The multiple antenna case: For the multiple antenna case, considering a continuous channel and that each node consists of $M > 1$ antenna, the channel matrices allow the interfering signal vectors to align at the receiver where they are interfering. Interference alignment has been achieved for the $K = 3$ user case, where each user has $M/2$ DoF. For $K > 3$ only the upper bound of $M/2$ DoF has been demonstrated.

In this thesis, we consider the single antenna three-user interference channel with interference alignment given in [10] (illustrated in Fig. 1.5). In that scenario, to align

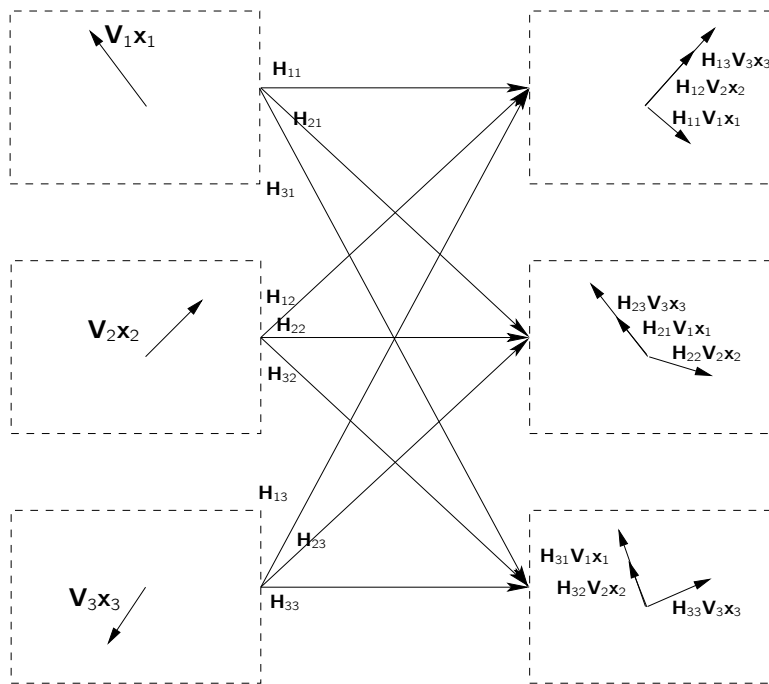


Figure 1.5: Three-user interference alignment scheme (adapted from [10])

interference it is necessary to use a symbol extension. As in [10], let user 1 take the message W_1 and encode it into a supersymbol defined by an $(n + 1)$ column vector x_1 .

Define a precoding matrix \mathbf{V}_1 of size $(2n + 1) \times (n + 1)$ such that

$$\bar{\mathbf{X}}_1 \triangleq \mathbf{V}_1 \mathbf{x}_1, \quad (1.36)$$

Similar expressions are obtained for transmitters 2 and 3, but considering n independent streams in each case.

At receiver k , the received signal is given by:

$$\mathbf{y}_k = \mathbf{H}_{kk} \mathbf{V}_k \mathbf{x}_k + \sum_{j=1, j \neq k}^3 \mathbf{H}_{kj} \mathbf{V}_j \mathbf{x}_j + \mathbf{z}_k, \quad (1.37)$$

where \mathbf{H}_{ij} is a $(2n + 1) \times (2n + 1)$ diagonal matrix composed of the channel gains correspondent to the extended symbol, and $i, j = 1, 2, 3$. At receiver 1, to obtain $(n + 1)$ interference-free dimensions corresponding to the desired signal, the dimension of the interference should not be more than n . This is assured in [10] by perfectly aligning interference from receivers 2 and 3 by

$$\mathbf{H}_{12} \mathbf{V}_2 = \mathbf{H}_{13} \mathbf{V}_3, \quad (1.38)$$

where \mathbf{V}_2 and \mathbf{V}_3 are $(2n + 1) \times (n)$ matrices.

To extract n interference free dimensions at receiver 2 and 3, the dimension of interference has to be no bigger than $n + 1$. This is accomplished in [10] by

$$\mathbf{H}_{23} \mathbf{V}_3 \prec \mathbf{H}_{21} \mathbf{V}_1 \quad (1.39)$$

$$\mathbf{H}_{32} \mathbf{V}_2 \prec \mathbf{H}_{31} \mathbf{V}_1, \quad (1.40)$$

where $\mathbf{P} \prec \mathbf{Q}$ means that a set of column vectors of \mathbf{P} is a subset of the set of column vectors of \mathbf{Q} .

Now it is necessary to solve these equations by choosing values for \mathbf{V}_1 , \mathbf{V}_2 and \mathbf{V}_3 . Cadambe and Jafar [10] solved this by

$$\mathbf{V}_1 = \begin{bmatrix} \mathbf{w} & \mathbf{T}\mathbf{w} & \mathbf{T}^2\mathbf{w} & \dots & \mathbf{T}^n\mathbf{w} \end{bmatrix} \quad (1.41)$$

$$\mathbf{H}_{21}^{-1}\mathbf{H}_{23}\mathbf{V}_3 = \begin{bmatrix} \mathbf{T}\mathbf{w} & \mathbf{T}^2\mathbf{w} & \dots & \mathbf{T}^n\mathbf{w} \end{bmatrix} \quad (1.42)$$

$$\mathbf{H}_{31}^{-1}\mathbf{H}_{32}\mathbf{V}_2 = \begin{bmatrix} \mathbf{w} & \mathbf{T}\mathbf{w} & \mathbf{T}^2\mathbf{w} & \dots & \mathbf{T}^{n-1}\mathbf{w} \end{bmatrix}, \quad (1.43)$$

where

$$\mathbf{T} = \mathbf{H}_{12}\mathbf{H}_{21}^{-1}\mathbf{H}_{23}\mathbf{H}_{32}^{-1}\mathbf{H}_{31}\mathbf{H}_{13}^{-1}, \quad (1.44)$$

and chose \mathbf{w} , $(2n+1) \times 1$ column vector as

$$\mathbf{w} = \begin{bmatrix} 1 & 1 & \dots & 1 \end{bmatrix}^T. \quad (1.45)$$

This scheme can be generalized for K users as shown in [10].

In order to suppress interference at each receiver consider a matrix \mathbf{U}_k of size $(2n+1) \times (n+1)$ for $k=1$ and a matrix of size $(2n+1) \times n$ for $k=2$ and 3, formed by columns that are the orthonormal basis of the interference-free desired signal subspace at receiver k . This matrix is designed to obtain [14]

$$\bar{\mathbf{y}}_k = \mathbf{U}_k^H \mathbf{y}_k = \mathbf{U}_k^H \mathbf{H}_{kk} \mathbf{V}_k \mathbf{x}_k + \underbrace{\mathbf{U}_k^H \sum_{j=1, j \neq k}^3 \mathbf{H}_{kj} \mathbf{V}_j \mathbf{x}_j}_{=0} + \mathbf{U}_k^H \mathbf{z}_k, \quad (1.46)$$

where

$$\mathbf{U}_k^H \mathbf{H}_{kj} \mathbf{V}_j = 0 \quad \text{for } k \neq j \quad (1.47)$$

$$\text{rank}(\mathbf{U}_k^H \mathbf{H}_{kk} \mathbf{V}_k) = \begin{cases} n+1 & \text{for } k=1 \\ n & \text{for } k=2, 3 \end{cases} \quad (1.48)$$

Thus, \mathbf{U}_k represents the subspace that is orthogonal to where the interference is projected. Condition (1.47) allows the second term of the addend of (1.46) to be zero. The condition given by (1.48) is needed for the desired user to achieve the desired DoF.

Hence, the desired signal is received through a full rank channel matrix of size $(2n + 1) \times (2n + 1)$, while the interference is completely eliminated.

1.5 Interference alignment: Signal scale approach

The case of interference alignment via signal scale was first proposed in [1] where the design of optimal structured codes were used to align interference. In [1], Bresler showed that random codes are not optimal for reaching the achievable capacity region in the way that structured codes are. The key point is that, by using structured codes such as lattices, interference can be aligned on the signal scale. With lattices, it is possible to decode the sum of the interference codewords, even when each interferer cannot be decoded.

1.5.1 Lattice codes

A lattice is a regularly spaced array of points. It can be properly defined as [15]

$$\Lambda = \left\{ \mathbf{x} = \sum_{i=1}^m \lambda_i \mathbf{v}_i, \lambda_i \in \mathbb{Z} \right\} \quad (1.49)$$

$$= \Lambda(\mathbf{M}) = \{ \mathbf{M}\lambda \mid \lambda \in \mathbb{Z}^b \}, \quad (1.50)$$

Here, the lattice has dimension m , where $\mathbf{v}_1, \mathbf{v}_2, \dots, \mathbf{v}_m$ are linearly independent vectors in \mathbb{R}^n and $\{\mathbf{v}_1, \mathbf{v}_2, \dots, \mathbf{v}_m\}$ is the basis of the lattice. The matrix

$$\mathbf{M} = \begin{bmatrix} \mathbf{v}_1 \\ \mathbf{v}_2 \\ \dots \\ \mathbf{v}_m \end{bmatrix} = \begin{pmatrix} v_{11} & v_{12} & \dots & v_{1n} \\ v_{21} & v_{22} & \dots & v_{2n} \\ \dots & \dots & \dots & \dots \\ v_{m1} & v_{m2} & \dots & v_{mn} \end{pmatrix},$$

is the generator matrix of the lattice Λ . Each row of \mathbf{M} corresponds to one of the independent vectors that define the lattice. A graphical representation of a two-dimensional lattice can be seen in Fig. 1.6.

Some important lattices are [15, 16]:

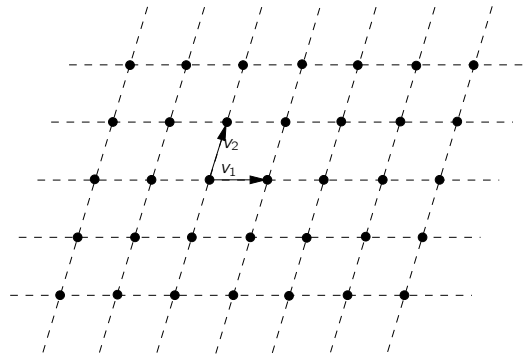


Figure 1.6: A two-dimensional lattice

- \mathbb{Z}^n : The n dimensional integer lattice is defined as

$$\mathbb{Z}^n = \{(x_1, x_2, \dots, x_n) : x_i \in \mathbb{Z}\} \quad (1.51)$$

where its generator matrix is given by $\mathbf{M} = I_{n \times n}$.

- A_n : This lattice is defined as (for $n \geq 1$):

$$A_n = \{(x_0, x_1, \dots, x_n) \in \mathbb{Z}^{n+1}, \sum_{i=0}^n x_i = 0\} \quad (1.52)$$

where its generator matrix is given by:

$$M = \begin{pmatrix} -1 & 1 & 0 & 0 & \dots & 0 & 0 \\ 0 & -1 & 1 & 0 & \dots & 0 & 0 \\ 0 & 0 & -1 & 1 & \dots & 0 & 0 \\ \dots & \dots & & & & & \dots \\ 0 & 0 & 0 & 0 & \dots & -1 & 1 \end{pmatrix}$$

- E_8 : Also called Gosset lattice, it can be defined as

$$\{(x_1, x_2, \dots, x_8) : x_i \in \mathbb{Z}^n \text{ or } x_i \in \mathbb{Z}^n + 1/2, \sum_{i=0}^8 x_i \equiv 0 \pmod{2}\} \quad (1.53)$$

Its generator matrix is given by:

$$M = \begin{pmatrix} 2 & 0 & 0 & 0 & 0 & 0 & 0 & 0 & 0 \\ -1 & 1 & 0 & 0 & 0 & 0 & 0 & 0 & 0 \\ 0 & -1 & 1 & 0 & 0 & 0 & 0 & 0 & 0 \\ 0 & 0 & -1 & 1 & 0 & 0 & 0 & 0 & 0 \\ 0 & 0 & 0 & -1 & 1 & 0 & 0 & 0 & 0 \\ 0 & 0 & 0 & 0 & -1 & 1 & 0 & 0 & 0 \\ 0 & 0 & 0 & 0 & 0 & -1 & 1 & 0 & 0 \\ \frac{1}{2} & \frac{1}{2} & \frac{1}{2} & \frac{1}{2} & \frac{1}{2} & \frac{1}{2} & \frac{1}{2} & \frac{1}{2} & \frac{1}{2} \end{pmatrix}$$

Properties of the lattices

Some important properties of the lattices are given next.

The **fundamental region** of a lattice [16] is a region that when repeated many times fills the Euclidean space without any overlap or gap.

The **Voronoi region** [17] corresponds to the fundamental region where every point is closer to the origin than to any other lattice point. It can be expressed as $\mathcal{V}(\Lambda)$.

The **volume** of the fundamental region is called the fundamental volume and can be expressed as $V(\Lambda) = |\det(\Lambda)| = \sqrt{\det(\mathbf{M}^T \mathbf{M})}$ [17].

The **fundamental or nominal coding gain** [18] is a normalized measure of the density of a lattice. It is given by

$$\gamma(\Lambda) = \frac{d_{\min}^2(\Lambda)}{V(\Lambda)^{2/m}}, \quad (1.54)$$

where $d_{\min}^2(\Lambda)$ is the **minimum squared distance** and corresponds to the minimum non-zero norm between lattice points, and m is the dimension of the lattice. Note that the fundamental coding gain is dimensionless and invariant to scaling or any orthogonal transformation.

Sublattices, partition chains and cosets [15] [18]

A **coset** of a lattice Λ , expressed as $\Lambda + c$, is the set of elements of the form $\lambda + c$, where $\lambda \in \Lambda$ and c is some constant element that specifies the coset. In other words, the coset is a translate of Λ by c .

A **sublattice** Λ' of a lattice Λ is a subset of the elements of Λ and it is also a lattice.

Let Λ' be a sublattice of Λ . The **quotient group or partition**, denoted as Λ/Λ' , is the sets of cosets of Λ' in Λ . The elements of the quotient group are written as $\Lambda' + c$, with $c \in \Lambda$.

A **partition chain** is denoted as $\Lambda/\Lambda'/\Lambda''/\dots$ where each lattice is a sublattice from the previous one. Thus $\Lambda \supseteq \Lambda' \supseteq \Lambda'' \supseteq \dots$.

The **order of the partition** Λ/Λ' is given by $|\Lambda/\Lambda'|$ represents the cardinality of the partition.

The **coset leader** (or coset representative) of Λ/Λ' is a representative from each element of Λ/Λ' . It is denoted by $[\Lambda/\Lambda']$.

Consider we have $\Lambda/\Lambda'/\Lambda''$, then the lattice Λ can be represented as $\Lambda = \Lambda'' + [\Lambda'/\Lambda''] + [\Lambda/\Lambda']$. This corresponds to a **coset decomposition**.

Constructing lattices [16]

According to the literature, a lattice can be constructed from a code or from algebraic number theory. Here we analyse some of the methods to construct a lattice from a code. For this, we consider the constructions given in [16].

- **Construction A:** Let C be an (n, M, d) binary code. $x = (x_1, \dots, x_n)$ in \mathbb{R}^n , and c a codeword in C , then x is a lattice point if and only if

$$\mathbf{x} = c + 2\mathbb{Z}^n, \quad (1.55)$$

A classical example is to construct an E_8 lattice from an extended Hamming code H_8 where $(n, k, d) = (8, 4, 4)$, where n is the length of the codeword, k are the information bits and d is the minimum hamming distance. For example we can say [19]: $E_8 = 2\mathbb{Z}^n + H_8$.

- **Construction D:** Let C_0 be the trivial code and C_i be a binary linear code with parameters (n, k_i, d_i) with $d_i \geq \frac{4^i}{\gamma}$ and $\gamma = 1$ or 2 for $i = 1, \dots, a$. Also take $C_0 \supseteq C_1 \supseteq \dots \supseteq C_a$. Then consider a basis $\{c_1, \dots, c_n\}$ for \mathbb{F}_2^n such that this basis spans C_i and forms the rows of a matrix \mathbf{B} , where the permutation of the rows of this matrix forms an upper triangular matrix.

Define the map $\delta_i : \mathbb{F}_2 \rightarrow \mathbb{R}$ by $\delta_i(x) = x/2^{i-1}$ where $x = 0$ or 1 , for $i = 1, \dots, a$ and denote the map $\mathbb{F}_2^n \rightarrow \mathbb{R}^n$ given by $\delta_i(x_1, \dots, x_n) = (\delta_i(x_1), \dots, \delta_i(x_n))$.

The lattice Λ in \mathbb{R}^n is conformed by all the vectors of the form

$$l + \sum_{i=1}^a \sum_{j=1}^{k_i} \alpha_j^{(i)} \delta_i(c_j), \quad (1.56)$$

where $l \in (2\mathbb{Z})^n$ and $\alpha_j^{(i)} = 0$ or 1 .

Theta series [16] [19]

The norm of all the lattice points can be enumerated in ascending order. This is known as the theta series of the lattice. It is defined as

$$\Theta_{\Lambda}(q) = \sum_{x \in \Lambda} q^{\|x\|^2}. \quad (1.57)$$

where $q = e^{-\frac{1}{2\sigma^2}}$.

For some lattices, there are some known theta functions such as:

$$\Theta_{\mathbb{Z}^n}(q) = \theta_3(q)^n. \quad (1.58)$$

$$\Theta_{A_2}(q) = \theta_3(q)\theta_3(q^3) + \theta_2(q)\theta_2(q^3), \quad (1.59)$$

$$\Theta_{E_8}(q) = \frac{1}{2} (\theta_2(q)^8 + \theta_3(q)^8 + \theta_4(q)^8) \quad (1.60)$$

where

$$\theta_2(q) = \sum_{n=-\infty}^{+\infty} q^{(n+\frac{1}{2})^2} \quad (1.61)$$

$$\theta_3(q) = \sum_{n=-\infty}^{+\infty} q^{(n)^2} \quad (1.62)$$

$$\theta_4(q) = \sum_{n=-\infty}^{+\infty} (-1)^n q^{n^2}, \quad (1.63)$$

are the Jacobi Theta Functions.

Flatness factor

The notion of the flatness factor of a lattice Λ was defined in [20]. The flatness factor comes from the problem of finding a maximum for a function given by

$$f_{\sigma,\Lambda}(\mathbf{w}) = \sum_{\mathbf{x} \in \Lambda} \exp\left(-\frac{\|\mathbf{w}-\mathbf{x}\|^2}{2\sigma^2}\right) \quad (1.64)$$

also defined as the Gaussian measure associated to the lattice Λ and the variance σ . Since we want to avoid the *flatness* of that function, we want to study the maximum variation of the Gaussian measure. This is actually defined as the flatness factor.

A slightly different, but equivalent definition of the flatness factor is applied in [21] and given here

$$\varepsilon_\Lambda = \frac{\max_{\mathbf{w} \in R(\Lambda)} |f_{\sigma,\Lambda}(\mathbf{w}) - E_{\mathbf{w}}[f_{\sigma,\Lambda}(\mathbf{w})]|}{E_{\mathbf{w}}[f_{\sigma,\Lambda}(\mathbf{w})]}. \quad (1.65)$$

where $E_{\mathbf{w}}[f_{\sigma,\Lambda}(\mathbf{w})]$ is the average of $f_{\sigma,\Lambda}$ over the fundamental region $R(\Lambda)$ of Λ . Using the theta series of the lattice Λ defined in (1.57), the flatness factor of Λ can be derived as [21]

$$\varepsilon_\Lambda = \lambda^{\frac{n}{2}} \Theta_\Lambda \left(e^{-\frac{1}{2\sigma^2}} \right) - 1, \quad (1.66)$$

where $\lambda = \frac{V(\Lambda)^{\frac{2}{n}}}{2\pi\sigma^2}$ is the volume-to-noise ratio, and $V(\Lambda)$ is the fundamental volume of the lattice Λ .

Reed-Muller codes [22] [23] [16]

Reed-Muller (RM) codes are a class of binary error correcting codes, where $\text{RM}(r', m+1)$ corresponds to the RM code of order r' with parameters (N, k, d) given by

$$N = 2^{m+1} \text{ (vector length)} \quad (1.67)$$

$$k = 1 + \binom{m+1}{1} + \dots + \binom{m+1}{r'} \quad (1.68)$$

$$d = 2^{m+1-r'} \text{ (minimum distance)}. \quad (1.69)$$

They can be generated by a generator matrix $G(r', m+1)$ corresponding to the RM code $\text{RM}(r', m+1)$. This matrix is obtained with the m -fold Kronecker product of $G(1, 1)$, defined as

$$G_{(m+1, m+1)} = G(m, m) \otimes \begin{bmatrix} 1 & 1 \\ 0 & 1 \end{bmatrix}$$

where

$$G_{(1,1)} = \begin{bmatrix} 1 & 1 \\ 0 & 1 \end{bmatrix}$$

Thus, the RM code $\text{RM}(m+1, 0)$ corresponds to the repetition code $(N, 1, N)$. On the other hand $\text{RM}(m+1, m+1)$ corresponds to all the binary strings of lengths 2^{m+1} , namely the code $(N, N, 1)$

The RM codes are the best binary codes of length 2^{m+1} , for $2^{m+1} \leq 32$. From the definition is it clear that the r' -th order RM code is contained in the $(r'+1)$ -th order RM code. Examples of nested RM codes of length 16 are

$$(16, 16, 1) \supseteq \underbrace{(16, 15, 2)}_{\text{RM}(3,4)} \supseteq (16, 11, 4) \supseteq \underbrace{(16, 5, 4)}_{\text{RM}(1,4)} \supseteq \dots$$

Barnes Wall lattices

Barnes-Wall (BW) lattices were originally discovered in [24] and widely explained later in [22]. They are a family of full rank lattices whose dimension is a power of 2, which correspond to the densest lattices in dimensions 2, 4, 8 and 16. These binary decompos-

able lattices can be built using RM codes. The lattice $\Lambda(0, m)$ is the m th member of the BW family of lattices, and can be expressed as a real or a complex lattice of dimension 2^{m+1} or 2^m respectively. For convenience, we consider real lattices here. The family of lattices given by $\Lambda(r, m)$ where $m \geq 0$ and $0 \leq r \leq m$ can be obtained by [25]

- $m - r$ even:

$$\begin{aligned} \Lambda(r, m) &= 2^{\frac{m-r}{2}} \mathbb{Z}^{2^{m+1}} \\ &+ \sum_{\substack{r+1 \leq r' \leq m \\ m-r' \text{ odd}}} 2^{(r'-r-1)/2} \text{RM}(r', m+1) \end{aligned} \quad (1.70)$$

- $m - r$ odd:

$$\begin{aligned} \Lambda(r, m) &= 2^{\frac{m-r+1}{2}} \mathbb{Z}^{2^{m+1}} \\ &+ \sum_{\substack{r+1 \leq r' \leq m \\ m-r' \text{ even}}} 2^{(r'-r-1)/2} \text{RM}(r', m+1). \end{aligned} \quad (1.71)$$

The BW lattice $\Lambda(0, m)$ has the following properties [26]:

- Minimum squared distance $d_{\min}^2 = 2^{m-r}$
- Volume $V(\Lambda(0, m)) = 2^{m2^{m-1}}$
- Nominal coding gain $\gamma_c(\Lambda(0, m)) = 2^{m/2}$.

These lattices are constructed using Construction D, where lower order codes are nested into bigger ones.

Some examples of BW lattices are [22]:

$$D_4 = \Lambda(0, 1) = 2\mathbb{Z}^4 + \text{RM}(1, 2) \quad (1.72)$$

$$E_8 = \Lambda(0, 2) = 2\mathbb{Z}^8 + \text{RM}(1, 3) \quad (1.73)$$

$$\Lambda_{16} = \Lambda(0, 3) = 4\mathbb{Z}^{16} + 2\text{RM}(3, 4) + \text{RM}(1, 4) \quad (1.74)$$

1.5.2 Lattice codes in interference channels: Key example [1]

Using structured codes, the cost to one user due to one interferer is the same as due to many interferers. The paper by Bresler [1] highlights the possibility of using structured codes to align interference, which is illustrated in the following example. Consider the many-to-one channel depicted in Fig. 1.7 and take P_i the average power of each transmitted symbol. Make $P_0 = P_1 = P_2 = 1$, $|h_{00}| = |h_{11}| = |h_{22}| = \sqrt{\beta}$ and $|h_{01}| = |h_{12}| = \beta$. Assume that $\beta \geq 2$.

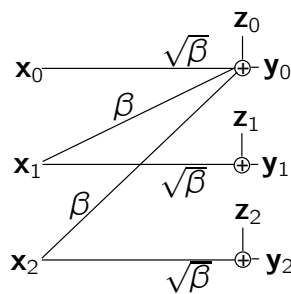


Figure 1.7: Example of a three-user many-to-one interference channel [1]

With Gaussian codes, and considering a scheme like HK, users 1 and 2 divide their messages into private and common messages. Since in this example the interference is strong, all information is common. Receiver 0 decodes all the signals x_0, x_1, x_2 as in a three-user MAC. The sum rate is thus expressed as

$$r_{\text{sum}} = r_0 + r_1 + r_2 \quad (1.75)$$

where r_i is the rate of each independent user. This can be simplified by

$$r_{\text{sum}} \leq \log(1 + 3\beta^2) \approx 2 \log \beta. \quad (1.76)$$

Consider now that $\beta = 2^{2n}$ and that each x_i , for $i = 0, 1, 2$ is given by $x_i = \sum_{k=1}^{\log \sqrt{\beta}} x_i(k) 2^{-k}$, where $x_i(k)$ are bits uniformly randomly distributed in $\{0, 1\}$. Then at receiver 0 we have (without considering noise)

$$\tilde{y}_0 = \sqrt{\beta}x_0 + \beta x_1 + \beta x_2, \quad (1.77)$$

The key point is given next. We can perfectly decode x_0 at receiver 0 since

$$\tilde{y}_0 = \sqrt{\beta}x_0 + \beta x_1 + \beta x_2 \quad (1.78)$$

$$= \sqrt{\beta}x_0 + \sqrt{\beta}(\sqrt{\beta}[x_1 + x_2]) \quad (1.79)$$

$$\in \sqrt{\beta}x_0 + \sqrt{\beta}\mathbb{Z}. \quad (1.80)$$

Then since $\sqrt{\beta}x_0 < \sqrt{\beta}$, we simply have

$$\tilde{y}_0 \bmod \sqrt{\beta} = \sqrt{\beta}x_0 \quad (1.81)$$

Since the single mutual information for a real-valued channel and signal, between input and output, is given by $I(x_i, y_i)$, and considering that the noise causes mutual information of, at most, 1.5 bits we have

$$I(x_i, \tilde{y}_i) - 1.5 \leq I(x_i, y_i). \quad (1.82)$$

If now we consider a complex-valued channel, we have that

$$r_i \geq \log \beta - 3, \quad (1.83)$$

for $i = 0, 1, 2$. The sum rate achieved in this case is therefore given by

$$r_{\text{sum}}^{\text{lattice}} = 3 \log \beta - 9 \approx 3 \log \beta. \quad (1.84)$$

This shows that the achievable region is larger when lattice codes are used [1].

1.6 Generalized Degrees of Freedom

We are now ready to understand the generalized DoF (GDoF) proposed by Tse [2] which is used in later chapters of this thesis. The GDoF is useful when there are different levels

of interference as described above. Consider the DoF definition in (1.35). The GDoF is a metric that generalizes this definition to a new metric α , where

$$\alpha \triangleq \frac{\log \text{INR}}{\log \text{SNR}} \quad (1.85)$$

and is given by

$$d(\alpha) = \lim_{\text{SNR} \rightarrow \infty} \frac{C(\text{SNR}, \alpha)}{\log(\text{SNR})} \quad (1.86)$$

Basically, it generalizes the DoF to different types of interference. Note that the classic DoF described before is the same as the GDoF when $\alpha = 1$.

With this definition, in [2] the GDoF is computed for different types of interference using the HK scheme. Thus, in [2] the GDoF for a two-user symmetric interference channel is

$$d(\alpha) = \begin{cases} 1 - \alpha & \text{for } 0 \leq \alpha \leq 1/2 & \text{for noisy interference;} \\ \alpha & \text{for } 1/2 \leq \alpha \leq 2/3 & \text{for weak interference;} \\ 1 - \frac{\alpha}{2} & \text{for } 2/3 \leq \alpha < 1 & \text{for moderately weak interference;} \\ \frac{\alpha}{2} & \text{for } 1 < \alpha \leq 2 & \text{for strong interference;} \\ 1 & \text{for } \alpha \geq 2 & \text{for very strong interference.} \end{cases}$$

1.7 Research objectives

We have seen that most researches are concerned with theoretical problems related to interference channels and interference alignment, such as the main open problem which is the capacity region, or the DoF for different scenarios and its achievability. However, little has been said about its practicality. In this thesis we are interested in finding some answers related to the error performance of the interference alignment technique under some scenarios with precoding methods, and about using lattice coding techniques for interference alignment. The purpose is either to find the performance or a bound of interference alignment in interference channels. On the other hand, and also related to the above, we also aim to design some rules for the construction of the precoders or the

codewords for interference channels, which includes using some rules that are already defined in the lattice coding theory. We aim to see if, by using lattices, we can achieve the same DoF as with random coding, but with the improved performance that using lattices can give.

1.8 Technical contributions

In this thesis we work with the performance of the interference channel and lattice coding techniques to address the problem of interference under different scenarios. The techniques in this thesis contribute to the understanding of the interference alignment problem in an interference channel and provide some answers under some scenarios using precoding methods and lattice coding techniques. The contribution of this thesis can be summarized as:

- We study the performance of the interference alignment scheme proposed by [10] and improve the performance using simple precoding schemes.
- We work with lattice codes techniques to find a bound on performance for user 1 in a many-to-one interference channel, which we relate to the theta series of the lattices.
- We extend a one-dimensional coding scheme to multiple dimensions using BW lattices in a symmetric interference channel, and we show the performance of the system can be improved when BW lattices are used.
- We extend the work of [2] where random codes are used, and derive the GDoF for a two-user symmetric interference channel using the Gaussian lattice distribution.

1.9 Thesis structure

This thesis is structured as follows. In Chapter 2, we provide a literature review of interference alignment for both the signal space and signal scale approach. In Chapter 3, we address the problem of signal space interference alignment using the scheme of

Cadambe and Jafar [10] for a SISO K -user interference channel. We work with precoding methods such as singular value decomposition (SVD) and Tomlinson-Harashima precoding (THP) with a bit and power loading strategy, and by means of simulations we show that by using precoding and bit-power loading methods, the BER can be improved compared to the original Cadambe and Jafar scheme. In Chapter 4 we address the problem of a many-to-one interference channel using lattice alignment. Assuming that the precoding matrices and the channel gain matrices are actually part of lattice codes, we produce alignment of the interference using the signal scale approach. In this chapter, we find an upper bound on the error probability for the first receiver using lattice codes. Considering joint maximum-likelihood decoding, we derive the union bound for the error probability in terms of the theta series of these lattices, and show that it is related to the flatness factor. Later, in Chapter 5 we study the performance of BW lattices in a fully connected symmetric interference channel under different types of interference. Inspired by [5] where a base Q expression for the transmitted signals is used, we work with the multilevel structure of BW lattices. Because of the good performance of lattices and the extension in bigger dimensions that using lattices enables, we propose the use of BW lattices to improve the performance of each user. In Chapter 6 we continue with the symmetric interference channel and use general lattices to obtain the GDoF. In this case, we use a lattice Gaussian distribution [27] to mimic the properties of the Gaussian random codes, but also to take advantage of the properties of the lattices. We show that we can obtain the same GDoF as the ones shown in [2] and [5] for any type of interference using the lattice Gaussian distribution properties. In Chapter 7 we conclude with some remarks and give suggestions for future work.

There are also two appendices to this thesis. Appendix A derives the rate and energy for QAM symbols for the Fischer-Huber algorithm used in Chapter 3, which is not explicit in [28], while Appendix B is a proof used in Chapter 6.

Chapter 2

Literature review

In this chapter we review the work of other researches on alignment, matrix design and structured codes for interference alignment.

2.1 Interference alignment: Signal space approach

One of the issues in interference alignment is the design of optimal precoders and decoders that allow interference alignment. Authors have worked in this area on systems that are already achievable from an algorithmic perspective [14, 29, 30] and from a closed formed perspective [31–33]. These approaches are intended to demonstrate the achievability of interference alignment by means of the DoF or sum rate obtained in each case.

In [14], distributed interference alignment algorithms are studied for an interference channel with multiple antenna nodes (M_k transmit antennae and N_k receive antennae). The first algorithm proposed seeks to find the alignment and decoding matrices \mathbf{V} and \mathbf{U} by minimizing the *leakage* produced by interference. The leakage corresponds to the interference power remaining in the desired received signal space after the interference suppressing matrix \mathbf{U} is applied. The leakage at receiver k that is caused by interference signals is measured as

$$\mathbf{I}_{k*} = \text{tr} [\mathbf{U}_k^H \mathbf{Q}_k \mathbf{U}_k], \quad (2.1)$$

where $\mathbf{Q}_k = \sum_{j=1, j \neq k}^K \frac{P_j}{d_j} \mathbf{H}_{kj} \mathbf{V}_j \mathbf{V}_j^H \mathbf{H}_{kj}^H$, and d_j represents the dimension of the transmitted

vector, where each element is defined with power $\frac{P_j}{d_j}$.

The idea of this first algorithm is to minimize the remaining interference power (leakage) at the received subspace represented by (2.1), where they start with an arbitrary \mathbf{V} . The subspace that contains less leakage is given by: $\mathbf{U}_{k,*d} = \mathbf{v}_d[\mathbf{Q}_k]$, where $\mathbf{v}_d[\mathbf{A}]$ is the eigenvector corresponding to the d_k smallest eigenvalue of \mathbf{A} , and where d_k corresponds to the degree of freedom for user k 's message¹. The next step consists on using a reciprocal channel, where \mathbf{V} and \mathbf{U} exchange roles. These two steps are repeated until convergence.

By construction, interference alignment does not maximize the desired signal power within the desired signal subspace. In fact, the algorithm just described does not depend on the direct channels \mathbf{H}_{kk} , where the desired signal is aligned, and as it is stated in [14], it is optimal when the SNR approaches infinity, but this is not necessarily true for intermediate SNR. Hence, a second algorithm is proposed in [14] to maximize the signal to interference noise ratio (SINR) at each receptor. Then \mathbf{U} is chosen as

$$\mathbf{U}_{k,*l} = \frac{\mathbf{B}_{kl}^{-1} \mathbf{H}_{kk} \mathbf{V}_{k,*l}}{\|\mathbf{B}_{kl}^{-1} \mathbf{H}_{kk} \mathbf{V}_{k,*l}\|}, \quad (2.2)$$

where

$$\mathbf{B}_{kl} = \sum_{j=1}^K \frac{P_j}{d_j} \sum_{d=1}^{d_j} \mathbf{H}_{kj} \mathbf{V}_{j,*d} \mathbf{V}_{j,*d}^H \mathbf{H}_{kj}^H - \frac{P_k}{d_k} \mathbf{H}_{kk} \mathbf{V}_{k,*d} \mathbf{V}_{k,*d}^H \mathbf{H}_{kk}^H + \mathbf{I}_{N_k} \quad (2.3)$$

and \mathbf{I}_{N_k} is the identity matrix of size $N_k \times N_k$.

The simulations in [14] show that the first algorithm is very close to the theoretical best case in terms of sum data rate. The second algorithm shows, as expected, better results than the first one in low and intermediate SNR.

Another algorithm is presented in [29] for MIMO frequency flat interference channels to minimize the distance between the interference signal and the interference sub-

¹In that paper, given a matrix \mathbf{A} , \mathbf{A}_{*d} represents its d^{th} column.

space, and to find \mathbf{V} and \mathbf{U} . For this, consider the system model defined by

$$\mathbf{y}_k = \mathbf{H}_{kk}\mathbf{V}_k\mathbf{x}_k + \sum_{j=1, j \neq k}^K \mathbf{H}_{kj}\mathbf{V}_j\mathbf{x}_j + \mathbf{z}_k, \quad (2.4)$$

similar to the one defined in (1.37) but considering K users. They are interested in minimizing

$$\min_{\forall_j \mathbf{V}_j = I, \forall_j \mathbf{U}_k^* \mathbf{U}_k = I, \forall k} \sum_{k=1}^K \sum_{j=1, j \neq k}^K \|\mathbf{H}_{kj}\mathbf{V}_j - \mathbf{U}_k \mathbf{U}_k^* \mathbf{H}_{kj}\mathbf{V}_j\|_F^2, \quad (2.5)$$

Similarly to the previous paper, the algorithm minimizes (2.5) in an alternate manner: first over \mathbf{V} , and later, over \mathbf{U} until the minimization converges. Here $\mathbf{U}_k \mathbf{U}_k^* \mathbf{H}_{kj}\mathbf{V}_j$ is the projection of the interference signal in the interference subspace and $\mathbf{H}_{kj}\mathbf{V}_j$ is the interference signal subspace. This algorithm is said to be proven to converge, but it is not clear whether or not it converges to an optimal solution.

In [32], an improved interference alignment scheme for SISO $K \geq 3$ is proposed. The DoF for the K -user interference channel with interference alignment found by Cadambe and Jafar [10] can be expressed as

$$r = \frac{(K-1)d_3 + d_1}{d_3 + d_1}, \quad (2.6)$$

where $d_1 = \frac{(n+1)^N}{(n+1)^N + n^N}$, $d_3 = \frac{n^N}{(n+1)^N + n^N}$, $N = (K-1)(K-2) - 1$ and $K \geq 3$. In [32], it is said that the DoF gets closer to the upper bound $K/2$ if d_1/d_3 gets closer to 1. Here a variation of the Cadambe and Jafar scheme is used where the DoF for each user becomes $d_1 = \binom{n^*+N+1}{N}$ and $d_3 = \binom{n^*+N}{N}$, for a nonnegative integer n^* . It was found that the proposed criterion is more efficient as d_1/d_3 gets closer to 1 than the scheme proposed by Cadambe and Jafar.

In [33], an interference alignment scheme very similar to the one presented by Cadambe and Jafar for a three-user interference channel is considered. The goal here is to optimize the alignment vectors within the subspaces constructed by Cadambe and Jafar. Variations to [10] are given in Table 2.1, where \mathbf{A}_b and \mathbf{A}_c are n column matrices chosen from $n+1$ columns of \mathbf{A} . Matrices \mathbf{E} , \mathbf{D} , and \mathbf{F} are non-singular, and $\mathbf{FD} = \mathbf{E}$.

To find matrices \mathbf{E} and \mathbf{F} , they perform a maximization of the high SNR offset

Cadambe and Jafar	Shen and Host Madsen
$\mathbf{B} = \mathbf{T}\mathbf{C}$ $\mathbf{B} \prec \mathbf{A}$ $\mathbf{C} \prec \mathbf{A}$ where: $\mathbf{A} = \tilde{\mathbf{V}}_1$ $\mathbf{B} = \mathbf{H}_{21}^{-1}\mathbf{H}_{23}\tilde{\mathbf{V}}_3$ $\mathbf{C} = \mathbf{H}_{31}^{-1}\mathbf{H}_{32}\tilde{\mathbf{V}}_2$ $\mathbf{T} = \mathbf{H}_{12}\mathbf{H}_{21}^{-1}\mathbf{H}_{23}\mathbf{H}_{32}^{-1}\mathbf{H}_{31}\mathbf{H}_{13}^{-1}$	$\mathbf{B} = \mathbf{T}\mathbf{C}\mathbf{D}$ $\mathbf{B} = \mathbf{A}_b\mathbf{E}$ $\mathbf{C} = \mathbf{A}_c\mathbf{F}$ $\mathbf{F}\mathbf{D} = \mathbf{E}$ where: $\mathbf{A} = \tilde{\mathbf{V}}_1$ $\mathbf{B} = \mathbf{H}_{21}^{-1}\mathbf{H}_{23}\tilde{\mathbf{V}}_3\mathbf{E}$ $\mathbf{C} = \mathbf{H}_{31}^{-1}\mathbf{H}_{32}\tilde{\mathbf{V}}_2\mathbf{F}$ $\mathbf{T} = \mathbf{H}_{12}\mathbf{H}_{21}^{-1}\mathbf{H}_{23}\mathbf{H}_{32}^{-1}\mathbf{H}_{31}\mathbf{H}_{13}^{-1}$ $\mathbf{V}_1 = \tilde{\mathbf{V}}_1 \left[\frac{1}{\frac{1}{2n+1}\text{trace}(\tilde{\mathbf{V}}_1\tilde{\mathbf{V}}_1^*)} \right]^{\frac{1}{2}}$ $\mathbf{V}_2 = \tilde{\mathbf{V}}_2\mathbf{F}$ $\mathbf{V}_3 = \tilde{\mathbf{V}}_3\mathbf{E}$
and $\mathbf{A}, \mathbf{B}, \mathbf{C}$ and \mathbf{w} are defined as: $\mathbf{A} = [\mathbf{w} \quad \mathbf{T}\mathbf{w} \quad \dots \quad \mathbf{T}^n\mathbf{w}]$ $\mathbf{B} = [\mathbf{T}\mathbf{w} \quad \mathbf{T}^2\mathbf{w} \quad \dots \quad \mathbf{T}^n\mathbf{w}]$ $\mathbf{C} = [\mathbf{w} \quad \mathbf{T}\mathbf{w} \quad \dots \quad \mathbf{T}^{n-1}\mathbf{w}]$ $\mathbf{w} = [1 \quad 1 \quad \dots \quad 1]^T$	and $\mathbf{A}, \mathbf{A}_b, \mathbf{A}_c$ and \mathbf{w} are defined as: $\mathbf{A} = [\mathbf{w} \quad \mathbf{T}\mathbf{w} \quad \dots \quad \mathbf{T}^n\mathbf{w}]$ $\mathbf{A}_b = [\mathbf{T}\mathbf{w} \quad \mathbf{T}^2\mathbf{w} \quad \dots \quad \mathbf{T}^n\mathbf{w}]$ $\mathbf{A}_c = [\mathbf{w} \quad \mathbf{T}\mathbf{w} \quad \dots \quad \mathbf{T}^{n-1}\mathbf{w}]$ $\mathbf{w} = [1 \quad 1 \quad \dots \quad 1]^T$

Table 2.1: Cadambe and Jafar scheme vs Shen and Host Madsen scheme

which is said to be equivalent to

$$\max \prod_{j=1}^K |(\mathbf{H}_{jj}\mathbf{V}_j - \mathbf{P}_{HV}(\mathbf{H}_{jj}\mathbf{V}_j))^* (\mathbf{H}_{jj}\mathbf{V}_j - \mathbf{P}_{HV}(\mathbf{H}_{jj}\mathbf{V}_j))| \quad (2.7)$$

$$\text{s.t.} \quad \frac{1}{N}\text{trace}(\tilde{\mathbf{V}}_i\tilde{\mathbf{V}}_i^*) = 1 \quad (2.8)$$

where \mathbf{P}_{HV} is the projection matrix for the interference subspace, and \mathbf{P}_{HV}^\perp is its orthogonal projection that enables to eliminate interference.

The solution of this optimization problem is not given explicitly, but it is said that the sum rate can be improved by orthonormalizing the alignment vectors at each transmitter.

In [34], the trade off between interference alignment, diversity and rate is studied. For this it is conjectured that the separation of the space time codes and the interference alignment precoding is optimal. Consider a multiple antenna K -user interference channel with linear detectors, separate space time codes and interference alignment. The overall

diversity of such system is claimed to be

$$D_{M_T, M_R, K}(\eta, r, m_T) = (\lfloor m_T - r + 1 \rfloor) (M_R - \min(m_T \eta, r(K - 1))), \quad (2.9)$$

where M_T and M_R correspond to the transmit and receive number of antennae, respectively, η describes the quality of interference alignment measured by $\frac{\text{rank}(\text{interference})}{\text{rank}(\text{signal})}$, r is the rate and m_T is the number of input streams. The term $M_R - m_T \eta$ corresponds to the number of antennae free of interference, ignoring space time codes and considering only interference alignment, while the term $M_R - r(K - 1)$ corresponds to the number of antennae free of interference, ignoring interference alignment and considering only space time codes.

It is important at this point to define the diversity gain [35]:

$$d = - \lim_{\text{SNR} \rightarrow \infty} \frac{\log P_e(\text{SNR})}{\log(\text{SNR})} \quad (2.10)$$

In [34], it is said that the average probability of error P_e of a system can be approximated at high SNR by:

$$P_e(\text{SNR}) \approx \alpha_{m_T, m_R} \text{SNR}^{-D_T m_R}, \quad (2.11)$$

where m_R is the number of output streams, α_{m_T, m_R} corresponds to the horizontal shift of the P_e curve, and D_T corresponds to the slope of the curve. It is said that in order to determine the diversity gain of a system it is enough to analyse the SNR exponent.

A different approach to the interference alignment problem is presented in [36]. Here the interference alignment problem is treated as proper or improper, based on the number of equations and variables the system has. For this, the problem is considered as a multivariate polynomial system, in which the system can be solved if the number of equations does not exceed the number of variables. Consider a K -user interference network with M transmitter antennae and N receiver antennae, denoted as $(M \times N)^K$.

In [36] this system is said to be proper if:

$$M + N \geq (K + 1) d, \quad (2.12)$$

where d is the DoF each user wants to achieve per channel use.

In [37], Ning visualizes the problem as zero forcing and diversity interference alignment. In the first case, the effect of the direct channel matrix \mathbf{H}_{kk} is disregarded in the interference alignment equations, while in the second case, it is part of it. For this he considers the case of [14] where the max SINR algorithm is proposed, which, as stated previously, considers the effect of the direct channel. Ning shows that when the zero forcing solution is used, the most likely event is that the subspace of the signal and the received signal have an angle of 90 degrees, which means that the SINR = 0. On the other hand, if a rotation vector is considered, this angle can be changed and some diversity can be achieved.

Our first goal in this thesis for the interference alignment via signal space is to find a scheme similar to the ones above, but we want to focus on the performance of the interference alignment scheme.

2.2 Interference alignment: Signal scale approach

The second case of interference alignment via signal scale was first proposed in [1] where the design of optimal structured codes are used in order to align interference. In [1], Bresler showed that random codes are not optimal at reaching the achievable capacity region like structured codes are. The key point is that, by using structured codes such as lattices, interference can be aligned on the signal scale. With lattices, it is possible to decode the sum of the interference codewords, even when each interferer cannot be decoded. Using structured codes, the cost to one user of one interferer is the same as the cost of many interferers. The idea is to scale the interference signals so that at each receiver, the sum of the interference signals belongs to a lattice that can be distinguished from the lattice containing the desired signal. This is referred to as *lattice alignment*,

and was defined in [1]. The key example already described in Chapter 1 was the first case where the importance of using structured codes such as lattices in an interference alignment scheme was realized. It shows that the rate is smaller when using random codes than it is when structured codes such as lattices are used.

The paper by Bresler highlights the possibility of using structured codes to align interference. From that point, work was done [4, 5, 38, 39] on these structured codes to prove DoF under different types of channels and different types of interference.

Recall the definition of the deterministic interference channel given in Chapter 1 in (1.5). Consider the following example of a deterministic channel shown in [1] and represented in Fig. 2.1. Take $n_{00} = 5$, $n_{11} = 3$, $n_{22} = 1$, $n_{33} = 4$, $n_{01} = 3$, $n_{02} = 2$ and $n_{03} = 6$. Also $x_0 = 0.d_1d_2d_3\dots$, $x_1 = 0.c_1c_2c_3\dots$, $x_2 = 0.b_1b_2b_3\dots$ and $x_3 = 0.a_1a_2a_3\dots$. For the direct channels the actual transmitted symbols are given by:

$$x_0 = 0.d_1d_2d_3d_4d_5 \quad (2.13)$$

$$x_1 = 0.c_1c_2c_3 \quad (2.14)$$

$$x_2 = 0.b_1 \quad (2.15)$$

$$x_3 = 0.a_1a_2a_3a_4. \quad (2.16)$$

Then at receiver 0 (without considering noise) we have

$$y_0 = [2^5x_0] \oplus [2^3x_1] \oplus [2^2x_2] \oplus [2^4x_3] \quad (2.17)$$

$$\begin{aligned} y_0 = & 2^5a_1 + 2^4(a_2 + d_1) + 2^3(a_3 + d_2) \\ & + 2^2(a_4 + d_3 + c_1) + 2(d_4 + c_2 + b_1) + (d_5 + c_3) \end{aligned} \quad (2.18)$$

This shows that some structure can be of use. The signal at the receiver can be viewed as a base 2 representation, separating the effect of the interference into levels.

In [4] and in later in [5] a simple idea of a coding scheme for a deterministic channel is proposed, which can be applied to a symmetric fully connected Gaussian interference channel. This was already explained in Chapter 1. Let us recall the transmitter symbols structure given previously in (1.7). Consider now the channel model given in [4]

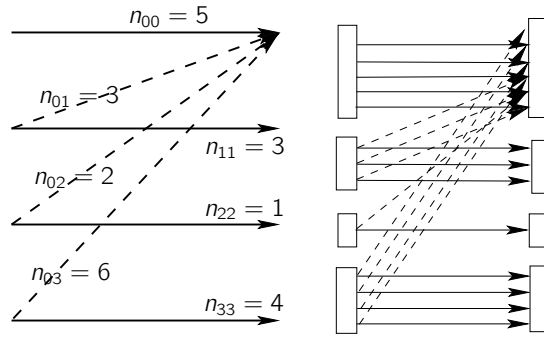


Figure 2.1: Example of the deterministic many-to-one interference channel [2]

for the symmetric Gaussian interference channel, where the direct channel gains are given as $h_{ii} = 1$ while the indirect channel gains are given by $h_{ij} = Q^{-1}$. The transmitted symbol at transmitter k is built as

$$x^{[k]} = \begin{bmatrix} x_{2N-2}^{[k]} & 0 & x_{2N-4}^{[k]} & 0 & \cdots & x_2^{[k]} & 0 & x_0^{[k]} \end{bmatrix}_Q \quad (2.19)$$

$$= Q^{2N-2} x_{2N-2}^{[k]} + Q^{2N-4} x_{2N-4}^{[k]} + \cdots + Q^4 x_4^{[k]} + Q^2 x_2^{[k]} + x_0^{[k]}. \quad (2.20)$$

where $x_q^k = 0$ if $q \notin \{0, 2, \dots, 2N-2\}$. Thus, at the receiver k we have

$$\begin{aligned} y^{[k]} &= Q^{2N-2} x_{2N-2}^{[k]} + Q^{2N-3} \sum_{l \neq k} x_{2N-2}^{[l]} + Q^{2N-4} x_{2N-4}^{[k]} \\ &+ Q^{2N-5} \sum_{l \neq k} x_{2N-4}^{[l]} + \cdots + Q^4 x_4^{[k]} + Q^3 \sum_{l \neq k} x_4^{[l]} \\ &+ Q^2 x_2^{[k]} + Q^1 \sum_{l \neq k} x_2^{[l]} + x_0^{[k]} + Q^{-1} \sum_{l \neq k} x_0^{[l]} + z^{[k]}. \end{aligned} \quad (2.21)$$

This shows that half of the levels do not have interference, achieving then a DoF of $K/2$. The channel is obviously symmetric and very simple. An important remark in this paper is that x_q^k is limited to lie between 1 and $\frac{Q}{K} - 1$. This is to avoid carry overs when the interference signals are added at the receiver.

In the paper by Etkin [2], it is shown that using a simple HK type scheme achieves the capacity of the two-user interference channel within 1 Bit/s/Hz. The method used in this paper allows to obtain the GDoF for any type of interference for the two-user symmetric interference channel. Later, in [5] the GDoF is extended to the K -user symmetric

interference channel with structured codes.

The channel model given in [2] is originally not symmetric and it is expressed as

$$y_1 = h_{11}x_1 + h_{21}x_2 + z_1 \quad (2.22)$$

$$y_2 = h_{12}x_1 + h_{22}x_2 + z_2, \quad (2.23)$$

where h_{ij} are the (complex) Gaussian channel gains, $x_i \in \mathbb{C}$ subject to a power constraint $E[|x_i|^2] = P_i$, and the noise is $z_i \sim \mathcal{CN}(0, N_0)$. Let also $\text{SNR}_i = \frac{|h_{ij}|^2 P_i}{N_0}$ be the SNR of user i , and $\text{INR}_1 = \frac{|h_{21}|^2 P_2}{N_0}$ and $\text{INR}_2 = \frac{|h_{12}|^2 P_1}{N_0}$. In the symmetric interference channel, this is simplified by: $|h_{11}|^2 = |h_{22}|^2 = |h_d|^2$, $|h_{12}|^2 = |h_{21}|^2 = |h_c|^2$ and $P_1 = P_2 = P$ or $\text{SNR}_1 = \text{SNR}_2$ and $\text{INR}_1 = \text{INR}_2$.

Initially, the idea is to find the symmetric capacity which is defined as:

$$C_{\text{sym}} = \max \min \{R_1, R_2\} \quad (2.24)$$

where $(R_1, R_2) \in R$, and R is the capacity region of the interference channel.

The region of interest is given by $0 < \text{INR}/\text{SNR} < 1$, which corresponds to the case of moderate to noisy interference, since the capacity region is known for the strong interference case.

To find the symmetric capacity they use a simple HK scheme. Consider the private message of user $i = 1, 2$ represented as u_i while the common message is represented as w_i . User i transmits the signal given by $x_i = u_i + w_i$. The private codeword u_i is meant to be decoded only by user i while at the other user it is treated as noise. Both w_1 and w_2 are decoded at both receivers. In this paper the codebooks are generated using i.i.d random Gaussian variables. The INR_p is defined as the INR created by the private message. In this paper this is chosen to be $\text{INR}_p = 1$.

In order to find the symmetric capacity, two MAC are defined. The first is formed by u_1, w_1 and w_2 at receiver 1, and the second is formed by u_2, w_2 and w_1 at receiver 2. Here, the achievable HK rates correspond to the intersection of the capacity regions of

these two MAC regions.

In Etkin's paper the decoding order is given so that the common messages are decoded first, while the private desired message is decoded last, and the other private message is treated as noise. The rates are also defined to be $R_{u,1} = R_{u,2}$ and $R_{w,1} = R_{w,2}$. With this, the following is obtained

- The rate of the private noise is given by

$$R_u = \log \left(1 + \frac{|h_c|^2 P_{u,1}}{(N_0)^2 + |h_c|^2 P_{u,2}} \right) \quad (2.25)$$

$$= \log \left(1 + \frac{\text{SNR}}{2\text{INR}} \right) \quad (2.26)$$

- The sum rate of the common messages must satisfy two conditions

$$R_{w,1} + R_{w,2} \leq \log \left(1 + \frac{|h_c|^2 P_{w,1} + |h_d|^2 P_{w,2}}{|h_c|^2 P_{u,1} + |h_d|^2 P_{u,2} + N_0} \right) \quad (2.27)$$

$$= \log \left(1 + \frac{(\text{INR} - 1)(\text{SNR} + \text{INR})}{\text{SNR} + 2\text{INR}} \right) \quad (2.28)$$

and

$$R_{w,1} + R_{w,2} \leq 2 \log \left(1 + \frac{(\text{INR})(\text{INR} - 1)}{\text{SNR} + 2\text{INR}} \right) \quad (2.29)$$

With this the following symmetric rate is obtained

$$\begin{aligned} R_{\text{HK}} &= \log \left(1 + \frac{\text{SNR}}{2\text{INR}} \right) \\ &+ \min \left\{ \frac{1}{2} \log \left(1 + \frac{(\text{INR} - 1)(\text{SNR} + \text{INR})}{\text{SNR} + 2\text{INR}} \right), \log \left(1 + \frac{(\text{INR})(\text{INR} - 1)}{\text{SNR} + 2\text{INR}} \right) \right\} \\ &= \left\{ \frac{1}{2} \log(1 + \text{SNR} + \text{INR}) + \frac{1}{2} \log \left(2 + \frac{\text{SNR}}{\text{INR}} \right) - 1, \log \left(1 + \text{INR} \frac{\text{SNR}}{\text{INR}} \right) - 1 \right\}. \end{aligned} \quad (2.30)$$

Two regimens are defined

$$B_1 = \{(\text{SNR}, \text{INR}) : \text{INR} \geq 1 \text{ and } \text{SNR}(\text{SNR} + \text{INR}) < \text{INR}^2(\text{INR} + 1)\} \quad (2.31)$$

$$B_2 = \{(\text{SNR}, \text{INR}) : \text{INR} \geq 1 \text{ and } \text{SNR}(\text{SNR} + \text{INR}) \geq \text{INR}^2(\text{INR} + 1)\}. \quad (2.32)$$

Defining a parameter α as in (1.85) and normalizing equation (2.30) by the capacity of a point-to-point AWGN channel, the following is obtained:

$$\frac{R_{\text{HK}}}{C_{\text{AWGN}}} \approx \min \left\{ 1 - \frac{\alpha}{2}, \max\{\alpha, 1 - \alpha\} \right\} \quad (2.33)$$

Equation (2.33) defines the GDoF for moderate to noisy interference, and has proved to be very useful in other papers such as [5].

It is also worth noting that later in this paper a new upper bound is derived, and is shown to be only 1 bit/s/Hz away from this rate.

Following on from the ideas of [2] and [4], in [5] the GDoFs are found for different types of interference according to the SNR and the INR for the K -user symmetric interference channel. The signals are represented in base Q , and a detailed scheme is given for the different types of interference.

Finally, in [38,39] a symmetric Gaussian K user interference channel is also considered where lattice codes are used. In the first case the authors consider the very strong interference scenario where a particular condition of the channel coefficient is given to attain the achievable rate. Lattice codes and successive interference decoding are used to achieve the optimal rate. In [39], a layered lattice coding scheme is presented which enables the determination of the DoF, not only for the very strong interference case but for a wider range of indirect channel coefficients.

In [40], Choi studies a multiple-input multiple-output (MIMO) interference channel where he is concerned with a precoder design with joint detectors at the receiver, where lattices are used to be able to decode. The focus of his paper is from a practical point of view, as to find the performance of the technique. Here, it was also remarked that using the same framework as in [10], it is possible to align (some of the) lattices.

Our goal in this part is to design lattice codes rules for interference channels using the lattice alignment technique and to find the performance or a bound of interference alignment, for certain interference channel scenarios.

2.3 Channel knowledge for interference alignment

A very important problem is that global channel knowledge is required. Some authors [34, 41] have studied the effects on interference alignment with inexact channel knowledge, and Jafar in [42] shows that only with knowledge of the statistics of the channel at the transmitter, $K/2$ DoF are achievable almost surely. This is an important problem because practical uses of interference alignment are desired. For that matter, authors have been working on feedback for interference channels. In particular, there is a branch of work where the channel state information feedback problem is equivalent to feeding back a point on the Grassmann manifold [43]. The topic of the Grassman manifold has been studied previously for MIMO beamforming in [44–46], while in [47] codebooks on the Grassmann manifolds are constructed. On a more theoretical branch, packings in the Grassmann manifold has been studied in [48].

Chapter 3

Precoding methods for interference alignment

3.1 Introduction

In this chapter, we study interference alignment from the signal space perspective. We base this part of the research on the work by Cadambe and Jafar [10] where a three-user interference channel with interference alignment is presented. In [49] precoding schemes for MIMO are analysed. A bit and power loading algorithm is used along with singular value decomposition (SVD) or Tomlinson-Harashima precoding (THP), and it is shown with simulations that these schemes improve the symbol error rate. Precoding schemes such as THP require channel knowledge at the transmitter, which is also the case for interference alignment. In this chapter we apply these techniques to interference alignment and show that the bit error rate (BER) can be improved at the cost of using precoding, but reducing the complexity of the detection methods.

3.2 Interference alignment [10]

In this chapter we consider a single antenna three-user interference channel like the one proposed by Cadambe in [10], which was previously explained in Chapter 1. For the completeness of this chapter, let us recall (1.37), (1.46), (1.47) and (1.48). We can

express the three-user interference channel as

$$\mathbf{y}_k = \mathbf{H}_{kk} \mathbf{V}_k \mathbf{x}_k + \sum_{j=1, j \neq k}^3 \mathbf{H}_{kj} \mathbf{V}_j \mathbf{x}_j + \mathbf{z}_k, \quad (3.1)$$

and obtain an interference-free signal given by

$$\bar{\mathbf{y}}_k = \mathbf{U}_k^H \mathbf{y}_k = \mathbf{U}_k^H \mathbf{H}_{kk} \mathbf{V}_k \mathbf{x}_k + \underbrace{\mathbf{U}_k^H \sum_{j=1, j \neq k}^3 \mathbf{H}_{kj} \mathbf{V}_j \mathbf{x}_j}_{=0} + \mathbf{U}_k^H \mathbf{z}_k, \quad (3.2)$$

using an interference suppressing matrix \mathbf{U}_k such that

$$\mathbf{U}_k^H \mathbf{H}_{kj} \mathbf{V}_j = 0 \quad \text{for } k \neq j \quad (3.3)$$

$$\text{rank}(\mathbf{U}_k^H \mathbf{H}_{kk} \mathbf{V}_k) = \begin{cases} n+1 & \text{for } k=1 \\ n & \text{for } k=2, 3 \end{cases} \quad (3.4)$$

where \mathbf{H}_{ij} is an $(2n+1) \times (2n+1)$ matrix ($i, j = 1, 2, 3$), \mathbf{V}_1 is an $(2n+1) \times (n+1)$ precoding matrix, \mathbf{V}_2 and \mathbf{V}_3 are $(2n+1) \times n$ precoding matrices, \mathbf{U}_1 is the $(2n+1) \times (n+1)$ interference suppressing matrix, \mathbf{U}_2 and \mathbf{U}_3 are the $(2n+1) \times n$ interference suppressing matrices, \mathbf{x}_k is the transmitted super-symbol, which is a vector of length $n+1$ for user 1, and n for user 2 and 3, and where \mathbf{z}_k is the AWGN.

After the interference suppressing matrix \mathbf{U}_k is used, the model is transformed into a channel with no interference, where the effective channel matrix is given by

$$\tilde{\mathbf{H}}_{kk} = \mathbf{U}_k^H \mathbf{H}_{kk} \mathbf{V}_k, \quad (3.5)$$

for $k = 1, 2, 3$.

3.3 Precoding schemes to improve performance

In this section, precoding schemes and a bit and power loading algorithm used for MIMO are presented. Although there are bit and power loading algorithms whose aim is to maximize the rate or optimize the energy, our aim is to minimize the error rate. This is the

reason why we have chosen the Fischer-Huber (FH) algorithm.

Fischer and Huber presented in [28] an algorithm to reallocate bits and power using D parallel Gaussian channels. Consider a system model given by $y_i = h_i x_i + z_i$ where x_i is the M-QAM transmitted symbol of rate R_i ($M_i = 2^{R_i}$), $h_i = 1, \forall i$, and z_i is the AWGN with variance N_i , and $i = 1, \dots, D$. In [28], the aim is to minimize the symbol error rate, which can be approximately derived as

$$P_r \propto Q \left(\sqrt{\frac{d_i^2/4}{N_i/2}} \right) \quad (3.6)$$

Considering the symbol error rate to be the same for all subchannels, we have $P_r = \text{constant}$. Hence

$$\text{SNR}_0 =: \frac{d_i^2/4}{N_i/2} = \text{constant}, \quad i = 1, 2, \dots, D, \quad (3.7)$$

where SNR_0 represents the squared distance to the decision threshold relative to the noise variance per dimension. The algorithm considers QAM transmission with real and imaginary parts taken from $V_i \cdot \{\pm 1, \pm 3, \dots\}$, where V_i is the gain with which the signal constellation can be scaled and the power can be adjusted. From this we can say

$$S_i = V_i^2 \frac{2}{3} 2^{R_i} \quad (3.8)$$

Since $d_i^2 = 4V_i^2$, SNR_0 can be expressed as

$$\text{SNR}_0 = \frac{V_i^2}{N_i/2}, \quad (3.9)$$

Then from (3.8) and (3.9) we have

$$S_i = V_i^2 \frac{2}{3} 2^{R_i} \quad (3.10)$$

$$= \text{SNR}_0 \frac{N_i}{2} \frac{2}{3} 2^{R_i} \quad (3.11)$$

Since we can assume that the total energy of the transmitted symbols S_T is a constant

$$S_T = \sum S_i = \text{constant}, \quad (3.12)$$

we have

$$S_T = \frac{1}{3} \text{SNR}_0 \sum_{i=1}^D N_i 2^{R_i} \quad (3.13)$$

The optimization problem is then given by [28]

$$\text{SNR}_0 = \frac{3S_T}{\sum_{i=1}^D N_i 2^{R_i}} \quad (3.14)$$

subject to

$$R_T = \sum R_i = \text{constant} \quad (3.15)$$

where R_T is the total rate of the transmitted symbols. Solving this optimization problem, gives $N_i 2^{R_i} = \text{constant}$ (see Appendix A). With this, the FH algorithm distributes the rate as [28]

$$R_i = \frac{R_T}{D} + \frac{1}{D} \cdot \log_2 \left(\frac{\prod_{l=1}^D N_l}{N_i^D} \right), \quad (3.16)$$

After this, the algorithm requires the value of R_i to be quantized (thus R_{Q_i} is defined). The power is then distributed as

$$S_i = \frac{S_T \cdot N_i \cdot 2^{R_{Q_i}}}{\sum_{l \in I} N_l \cdot 2^{R_{Q_l}}}, \quad i \in I. \quad (3.17)$$

In this document we consider a system of the form $y_i = C_i x_i + z_i$, where C_i are the parallel channel gains and z_i is AWGN with variance N_0 , for $i = 1, \dots, D$.

Hence, the optimization problem is now given by

$$\frac{d_i^2/4}{\frac{N_o/2}{|C_i|^2}} = \text{constant} \quad (3.18)$$

$$\frac{V_i^2}{\frac{N_o/2}{|C_i|^2}} = \text{constant} \quad (3.19)$$

$$\frac{N_o}{|C_i|^2} \cdot 2^{R_i} = \text{constant} \quad (3.20)$$

$$\frac{2^{R_i}}{|C_i|^2} = \text{constant} \quad (3.21)$$

Therefore, equations (3.16) and (3.17) will change to

$$R_i = \frac{R_T}{D} + \frac{1}{D} \cdot \log_2 \left(\frac{|C_i|^{2 \cdot D}}{\prod_{l=1}^D |C_l|^2} \right), \quad (3.22)$$

As before, R_i is quantized, hence the power is distributed as

$$S_i = \frac{S_T \cdot \frac{1}{|C_i|^2} \cdot 2^{R_{q_i}}}{\sum_{l \in I} \frac{1}{|C_l|^2} \cdot 2^{R_{q_l}}}, \quad i \in I. \quad (3.23)$$

The algorithm proposed by [49] is explained next and in Algorithm 3.1.

- Selection of the rate, part I: The first selection of the rate is made according to equation (3.22). If a rate is found to be $R_i < 0$ at the end of the iteration, that subchannel is removed and the iteration begins again, without that channel. Hence if a rate is 0, nothing is transmitted on that channel.
- Selection of the rate, part II: In this part the rates will be converted to integers. If a rate is found to be smaller than 0.5, then the final rate is 0. If a rate is found to be bigger than the maximum allowed rate minus 0.5, then the rate is assigned to be the maximum allowed rate. In any other case the rate is assigned to be $\text{INT}(R_i + 0.5)$, where INT represents the integer function. In this part, the difference between the original rates (R_i , assigned in part I) and the new rates (R_{q_i} , assigned by part II), is kept in a variable called Δ_R .
- In this step, the sum of the rates is checked. If the sum is the same as R_T the rates

are correct. If the sum is bigger than R_T then we find the minimum Δ_R within the values of $R_{q_i} > 0$, and subtract 1 to the correspondent value of R_{q_i} . If the sum is less than R_T then we find the maximum Δ_R within the values of $R_{q_i} > 0$, and add 1 to the correspondent value of R_{q_i} .

- The last part is the energy, which simply involves applying (3.23) within the channels in which the rate $R_{q_i} > 0$.

The FH algorithm has been applied to MIMO channels in [49]. In that paper, SVD and THP are used to obtain parallel channels.

3.3.1 Singular value decomposition

As in [49], consider a MIMO system given by

$$\tilde{\mathbf{y}} = \tilde{\mathbf{H}}\tilde{\mathbf{x}} + \tilde{\mathbf{z}}, \quad (3.24)$$

where $\tilde{\mathbf{H}}$ is a matrix that represents the MIMO channel. Applying SVD, $\tilde{\mathbf{H}}$ is given by

$$\tilde{\mathbf{H}} = \mathbf{Q}\mathbf{\Sigma}\mathbf{P}^H, \quad (3.25)$$

where \mathbf{Q} and \mathbf{P} are unitary matrices, which contain the eigenvectors of $\tilde{\mathbf{H}}\tilde{\mathbf{H}}^H$ and $\tilde{\mathbf{H}}^H\tilde{\mathbf{H}}$ respectively, while $\mathbf{\Sigma}$ is a real diagonal matrix whose components are the eigenvalues of $\tilde{\mathbf{H}}^H\tilde{\mathbf{H}}$. Thus, the parallel channels are given by

$$\mathbf{\Sigma} = \mathbf{Q}^H\tilde{\mathbf{H}}\mathbf{P}. \quad (3.26)$$

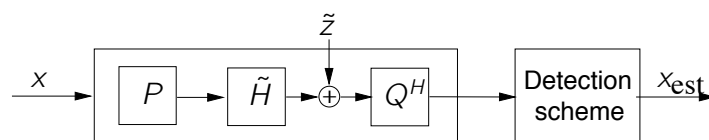


Figure 3.1: Equivalent system with SVD

Then applying the matrices \mathbf{P} and \mathbf{Q}^H to the transmitter and receiver respectively

Algorithm 3.1 Fisher-Huber algorithm [49]

```

1: function FIND  $R_i$ 
2:    $R_i = \frac{R_T}{D} + \frac{1}{D} \cdot \log_2 \left( \frac{|C_i|^{2-D}}{\prod_{l=1}^D |C_l|^2} \right)$ 
3:   if  $R_i \leq 0$  then
4:     Remove this subchannel and re-calculate  $R_i$  for all remaining valid channels
5:   else
6:     Output  $R_i$  for all valid channels
7:   end if
8: end function
9: function FIND  $R_{Q_i}$ 
10:  if  $R_i < 0.5$  then
11:     $R_{Q_i} = 0$ 
12:  else if  $R_i \geq R_{\max} - 0.5$  then
13:     $R_{Q_i} = R_{\max}$ 
14:  else
15:     $R_{Q_i} = \text{INT}(R_i + 0.5)$  ▷ where INT represents the integer function
16:  end if
17:  Define  $\Delta R_i = R_i - R_{Q_i}$ 
18: end function
19: function CHECK  $\sum_{i \in I} R_{Q_i}$ 
20:  if  $\sum_{i \in I} R_{Q_i} < R_T$  then
21:    while  $\sum_{i \in I} R_{Q_i} \neq R_T$  do
22:      Increase the rate  $R_{Q_i}$  with the biggest  $\Delta R_i$ 
23:       $\sum_{i \in I} R_{Q_i} = \sum_{i \in I} R_{Q_i} - 1$ 
24:       $\Delta R_i = \Delta R_i - 1$ 
25:    end while
26:  else if  $\sum_{i \in I} R_{Q_i} > R_T$  then
27:    while  $\sum_{i \in I} R_{Q_i} \neq R_T$  do
28:      Decrease the rate  $R_{Q_i}$  with the smallest  $\Delta R_i$ 
29:       $\sum_{i \in I} R_{Q_i} = \sum_{i \in I} R_{Q_i} + 1$ 
30:       $\Delta R_i = \Delta R_i + 1$ 
31:    end while
32:  end if
33: end function
34: function FIND  $S_j$ 
35:   $S_j = \frac{S_T \cdot \frac{1}{|C_j|^2} \cdot 2^{R_{Q_j}}}{\sum_{l \in I} \frac{1}{|C_l|^2} \cdot 2^{R_{Q_l}}}, i \in I$ 
36: end function

```

gives

$$\check{\mathbf{y}} = \mathbf{\Sigma} \mathbf{x} + \check{\mathbf{z}}, \quad (3.27)$$

where $\check{\mathbf{y}} = \mathbf{Q}^H \tilde{\mathbf{y}}$, $\check{\mathbf{z}} = \mathbf{Q}^H \tilde{\mathbf{z}}$.

3.3.2 Tomlinson-Harashima Precoding [17], [49]

The THP, as described in [17] and [49], is based on the decision feedback equalization (DFE) (shown in Fig. 3.2). Consider the system given by:

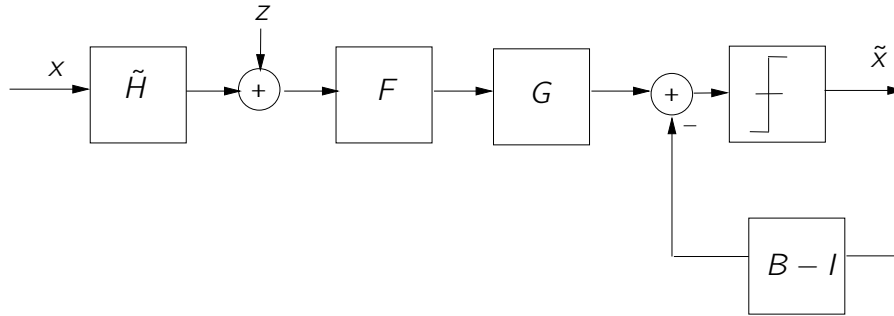


Figure 3.2: DFE [49]

$$\tilde{\mathbf{y}} = \tilde{\mathbf{H}}\mathbf{x} + \tilde{\mathbf{z}}. \quad (3.28)$$

where $\tilde{\mathbf{H}}$ is a $K \times K$ matrix.

The DFE consists of a feedforward unitary matrix \mathbf{F} , a diagonal scaling matrix \mathbf{G} , and a feedback matrix \mathbf{B} . Matrix \mathbf{F} guarantees that the noise is still white and gives spatial causality. The triangular feedback matrix $\mathbf{B} = \mathbf{G}\tilde{\mathbf{H}}$ is lower triangular and its main diagonal elements are equal to 1. This allows for the interference produced by the symbols that have already been detected, to be cancelled. The following are the relations between \mathbf{B} , \mathbf{F} and \mathbf{G} .

$$\tilde{\mathbf{H}} = \mathbf{F}^H\mathbf{S}, \text{ where } \mathbf{S} \text{ is a lower triangular matrix} \quad (3.29)$$

$$\mathbf{G} = \text{diag}(s_{11}^{-1}, \dots, s_{KK}^{-1}) \quad (3.30)$$

$$\mathbf{B} = \mathbf{G}\tilde{\mathbf{H}} = \mathbf{G}\mathbf{S}. \quad (3.31)$$

The election of the filters can be done using a criterion such as ZF or MMSE. We will focus on the ZF criterion. In that case, it is easy to see that since \mathbf{F} is a unitary matrix and by using (3.29)

$$\tilde{\mathbf{H}}^H\tilde{\mathbf{H}} = \mathbf{S}^H\mathbf{F}\mathbf{F}^H\mathbf{S} \rightarrow \tilde{\mathbf{H}}^H\tilde{\mathbf{H}} = \mathbf{S}^H\mathbf{S}. \quad (3.32)$$

where s_{11}, \dots, s_{KK} are the diagonal entries of \mathbf{S} . Therefore to obtain \mathbf{S} , a *QR-type* decomposition must be performed.

With these, the system using DFE is given by

$$\bar{y}_j = x_j + \sum_{l=1}^{j-1} b_{jl}x_l + \bar{z}_j, \quad (3.33)$$

where $\bar{z}_j = \hat{z}_j/s_{jj}$, \hat{z}_j are the entries of $\hat{\mathbf{z}}$, $\hat{\mathbf{z}} = \mathbf{F}\mathbf{z}$, \bar{y}_j are the entries of $\bar{\mathbf{y}}$, $\bar{\mathbf{y}} = \mathbf{F}\mathbf{G}\mathbf{y}$, b_{jl} are the entries of \mathbf{B} and x_j are the entries of \mathbf{x} . Using DFE, the original MIMO channel is decomposed into parallel channels, with noise variances given by $\sigma_n^2/|s_{jj}|^2$.

It is possible to use the knowledge of the channel at the transmitter to avoid propagation errors and the need for immediate decision when using equalization as it is with DFE. Bringing matrix \mathbf{B} to the transmitter, THP is shown in Fig. 3.3.

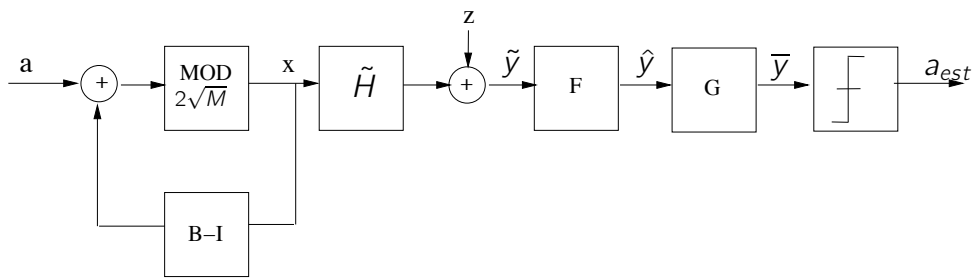


Figure 3.3: Equivalent system using THP [49]

Let us consider a constellation of the form:

$$A = \left\{ a_I + ja_Q \mid a_I, a_Q \in \left\{ \pm 1, \pm 3, \dots, \pm (\sqrt{M} - 1) \right\} \right\}, \quad (3.34)$$

which is bounded by a region $2\sqrt{M}$. The transmitted symbol is given by:

$$x_j = a_j - \sum_{l=1}^{j-1} b_{jl}x_l. \quad (3.35)$$

For the energy of the transmitted symbol not to be increased with this feedforward scheme, there is a *THP modulo*. The function of this modulo is to limit x_j by adding (or subtracting) multiples of $2\sqrt{M}$ to the real and imaginary parts of x_j , so that it falls in the

constellation region. This can be interpreted as:

$$x_j = a_j + p_j - \sum_{l=1}^{j-1} b_{jl} x_l, \quad (3.36)$$

where $p_j \in \{2\sqrt{M} \cdot (p_I + j p_Q) \mid p_I, p_Q \in \mathbb{Z}\}$. Hence, the effective symbols are $v_j = a_j + p_j$. With this, the symbols of the constellation are extended periodically and as they pass through the THP modulo they are brought back to the original symbol constellation region.

At the receiver, after passing \mathbf{F} and \mathbf{G} , the receiver signal \mathbf{r}_1 is:

$$\mathbf{r}_1 = \mathbf{v}_1 + \bar{\mathbf{z}}_1. \quad (3.37)$$

Hence, again it is possible to obtain parallel channels. The detection is then very simple. It suffices to just use another THP modulo at the receiver and a slicer.

In [49] simulations using MIMO and SVD or THP show that when no loading is used, THP is the best of both precoding schemes. However, when bit and power loading are used, SVD outperforms THP.

3.4 Precoding methods applied to interference alignment

In this section we apply what has been described in the previous section to the interference alignment technique. Here the original Cadambe and Jafar scheme is compared with the Cadambe and Jafar scheme using SVD and THP with the FH bit and power loading algorithm. By means of simulations we show that these schemes can improve the performance of the system.

Consider that (3.2) can be expressed as (3.24) and (3.28) using $\tilde{\mathbf{H}}_{kk}$ as in (3.5) by

$$\tilde{\mathbf{H}}_{kk} = \mathbf{U}_k^H \mathbf{H}_{kk} \mathbf{V}_k. \quad (3.38)$$

Thus, the matrices needed for SVD and THP can be calculated as in the MIMO case.

3.4.1 Simulations on precoding methods applied to interference alignment

Consider the Cadambe and Jafar scheme for $K = 3$ and single antenna nodes. The vectors \mathbf{x}_1 , \mathbf{x}_2 and \mathbf{x}_3 are composed of 16-QAM symbols. Each channel \mathbf{H}_{kj} is a diagonal matrix whose elements are independent and different, and like the noise, drawn from a complex Gaussian distribution with zero mean and unit variance. We use Cadambe and Jafar's alignment matrices \mathbf{V}_k and vector \mathbf{w} . For the alignment matrices \mathbf{V}_k , we run a QR decomposition to obtain a matrix whose columns are orthonormal to each other. This is to ensure that the matrices do not add energy to the system. At each receiver, an interference suppressing matrix \mathbf{U}_k^H is applied such that $\mathbf{U}_k^H \mathbf{H}_{kj} \mathbf{V}_j = 0$. On the other hand, the detection is done using either Zero Forcing (ZF) or Maximum-Likelihood (ML) estimation where for a system given by $\tilde{\mathbf{y}}_k = \tilde{\mathbf{H}}_{kk} \mathbf{x}_k + \tilde{\mathbf{z}}_k$, ZF and ML are defined as

- ZF:

$$\mathbf{x}_{k_{est}} = \tilde{\mathbf{H}}_{kk}^{-1} \cdot \tilde{\mathbf{y}}_k \quad (3.39)$$

- ML:

$$\mathbf{x}_{k_{est}} = \underset{\check{\mathbf{x}}_k \in \mathcal{C}}{\operatorname{argmin}} \|\tilde{\mathbf{H}}_{kk} \check{\mathbf{x}}_k - \tilde{\mathbf{y}}_k\|^2. \quad (3.40)$$

where \mathcal{C} corresponds to the M-QAM constellation.

In the simulations the SNR is measured after the precoding matrix \mathbf{V} . The average signal power is then measured as $\frac{2}{3}(M-1)\frac{n+1}{2n+1}$ for user 1, and $\frac{2}{3}(M-1)\frac{n}{2n+1}$ for users 2 and 3, where $\frac{2}{3}(M-1)$ is the average energy of the M-QAM symbol and $M = 16$ in these simulations. The term $\frac{n+1}{2n+1}$ (similarly the term $\frac{n}{2n+1}$) comes from re-sizing the transmitted vector after \mathbf{V} . We also consider that the noise has zero mean and variance equal to 1. Thus, in order to run the simulations with different values of SNR we have to consider another variable f_c that is used to reach said SNR given by the simulations. We prefer to use f_c instead of a given value of the variance of the noise, in order to have control over the simulations, since $\sqrt{f_c}$ is simply multiplied to the matrix \mathbf{V} . Thus, the effective SNR

for the system is defined as

$$\text{SNR}_E = \begin{cases} \frac{2}{3}(M-1)\frac{n+1}{2n+1} \cdot f_c, & \text{for the first user} \\ \frac{2}{3}(M-1)\frac{n}{2n+1} \cdot f_c, & \text{for the other users} \end{cases} \quad (3.41)$$

Simulations were performed using $n = 1$ and 2 . The aim of our result is to observe the BER obtained in each case.

Use of the Fischer-Huber algorithm in the simulations

The inputs of the algorithm are:

- The number of dimensions or parallel channels: $D = n + 1$ for the first user, $D = n$ for the other users.
- The total data rate per symbol: $(n + 1) \log_2 M$ for the first user, $n \log_2 M$ for the other users.
- The maximum data rate per dimension: $(n + 1) \log_2 M$ for the first user, $n \log_2 M$ for the other users.
- The total energy of the symbol $\frac{2}{3}(M - 1)(n + 1)$ for the first user, $\frac{2}{3}(M - 1)n$ for the other users.
- The parallel channel coefficients.

The outputs of the algorithm are:

- The rate for each of the dimensions, or components of the signal vector, R_i ($M_i = 2^{R_i}$)
- The energy per dimension.

In this section we have adapted the FH algorithm to work, for convenience, with squared constellations. The modifications are very small to the original FH algorithm described in Algorithm 3.1, corresponding only to lines 10, 12, 15, 23, 24, 29 and 30. These are highlighted in Algorithm 3.2.

Algorithm 3.2 Modified Fisher-Huber algorithm (modified from [49])

```

1: function FIND  $R_i$ 
2:    $R_i = \frac{R_T}{D} + \frac{1}{D} \cdot \log_2 \left( \frac{|C_i|^{2-D}}{\prod_{l=1}^D |C_l|^2} \right)$ 
3:   if  $R_i \leq 0$  then
4:     Remove this subchannel and re-calculate  $R_i$  for all remaining valid channels
5:   else
6:     Output  $R_i$  for all valid channels
7:   end if
8: end function
9: function FIND  $R_{Q_i}$ 
10:  if  $R_i < 1$  then ▷ Modified from Algorithm 3.1
11:     $R_{Q_i} = 0$ 
12:  else if  $R_i \geq R_{\max} - 1$  then ▷ Modified from Algorithm 3.1
13:     $R_{Q_i} = R_{\max}$ 
14:  else
15:     $R_{Q_i} = \text{EVEN}(R_i)$  ▷ Modified from Algorithm 3.1, where EVEN represents the
    next even number function
16:  end if
17:  Define  $\Delta R_i = R_i - R_{Q_i}$ 
18: end function
19: function CHECK  $\sum_{i \in I} R_{Q_i}$ 
20:  if  $\sum_{i \in I} R_{Q_i} < R_T$  then
21:    while  $\sum_{i \in I} R_{Q_i} \neq R_T$  do
22:      Increase the rate  $R_{Q_i}$  with the biggest  $\Delta R_i$ 
23:       $\sum_{i \in I} R_{Q_i} = \sum_{i \in I} R_{Q_i} - 2$  ▷ Modified from Algorithm 3.1
24:       $\Delta R_i = \Delta R_i - 2$  ▷ Modified from Algorithm 3.1
25:    end while
26:  else if  $\sum_{i \in I} R_{Q_i} > R_T$  then
27:    while  $\sum_{i \in I} R_{Q_i} \neq R_T$  do
28:      Decrease the rate  $R_{Q_i}$  with the smallest  $\Delta R_i$ 
29:       $\sum_{i \in I} R_{Q_i} = \sum_{i \in I} R_{Q_i} + 2$  ▷ Modified from Algorithm 3.1
30:       $\Delta R_i = \Delta R_i + 2$  ▷ Modified from Algorithm 3.1
31:    end while
32:  end if
33: end function
34: function FIND  $S_i$ 
35:   $S_i = \frac{S_T \cdot \frac{1}{|C_i|^2} \cdot 2^{R_{Q_i}}}{\sum_{l \in I} \frac{1}{|C_l|^2} \cdot 2^{R_{Q_l}}}, i \in I$ 
36: end function

```

Also, it is important to note that in the entire algorithm $M - 1 \approx M$. This comes from (3.8) where the energy of the QAM symbol is considered as $\frac{2}{3}M$ instead of $\frac{2}{3}(M - 1)$ to simplify the optimization problem. This approximation vanishes as the value of M increases. This is also the reason why we have chosen to work with $M = 16$, a bigger

value of M than when $M = 4$. This approximation is not considered in any other part of the simulation apart from the FH algorithm.

This algorithm is run for every new realization of the channel and the receiver must know the outputs of the algorithm. Note that the iterations converge since the algorithm initially redistributes the rates only using (3.16) and later the fine tuning is done solely by adding or subtracting values of 2.

Singular value decomposition and Fischer Huber algorithm simulations

For these simulations we consider the MIMO system to be:

$$\check{\mathbf{y}}_k = \boldsymbol{\Sigma}_k \mathbf{x}_k + \check{\mathbf{z}}_k, \quad (3.42)$$

where $\check{\mathbf{z}}_k = \mathbf{Q}_k^H \mathbf{U}_k^H \mathbf{z}_k$ and \mathbf{z}_k is AWGN, hence $\check{\mathbf{z}}_k$ is also AWGN. From (3.38), $\boldsymbol{\Sigma}_k = \mathbf{Q}_k^H \tilde{\mathbf{H}}_{kk} \mathbf{P}_k$ corresponds to the parallel channels obtained by the SVD of the MIMO channel given by $\tilde{\mathbf{H}}_{kk}$. Note that now each user has an independent (and interference-free) channel. Thus for each value of $k = 1, 2, 3$ independently, the variables \mathbf{Q}_k and \mathbf{P}_k can be computed.

The output of the FH algorithm are the rate and the energy of the transmitted M-QAM symbols \mathbf{x}_k . Note that the total rate per symbol remains constant, just like the energy.

Tomlinson-Harashima precoding and Fischer-Huber algorithm simulations

For these simulations consider, again, the channel matrix to be given by $\tilde{\mathbf{H}}_{kk} = \mathbf{U}_k^H \mathbf{H}_{kk} \mathbf{V}_k$ and the transmitted M-QAM symbols to be \mathbf{a}_k .

In this scheme, (see Fig. 3.4) the energy E_b is theoretically bigger than the energy E_a by a factor of $\frac{M}{M-1}$ for QAM constellations. Therefore, in order to be consistent with the other schemes we consider that the effective SNR is given by

$$\text{SNR}_E = \begin{cases} \frac{2}{3} M \frac{n+1}{2n+1} \cdot f_{CTHP}, & \text{for the first user} \\ \frac{2}{3} M \frac{n}{2n+1} \cdot f_{CTHP}, & \text{for the other users} \end{cases} \quad (3.43)$$

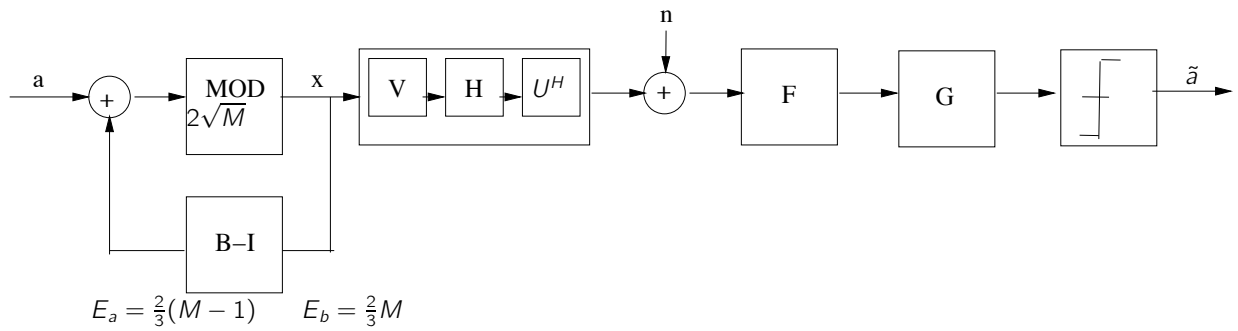


Figure 3.4: Energy diagram before and after \mathbf{V}

where again f_{CTHP} is considered and multiplied to the matrix \mathbf{V}_1 ($\mathbf{V}_1 = \sqrt{f_{CTHP}} \mathbf{V}_1$).

Note that again, each user has an independent (and interference-free) channel. Thus, for each value of $k = 1, 2, 3$ independently, the procedure for these simulations is the following:

1. Generate matrix \mathbf{S}_k for $\tilde{\mathbf{H}}_{kk}$ as shown in (3.32).
2. From \mathbf{S}_k and $\tilde{\mathbf{H}}_{kk}$ generate matrix \mathbf{G}_k , \mathbf{F}_k and \mathbf{B}_k .
3. Run the FH algorithm to determine the rate and energy for each component of \mathbf{a}_k . Note that the channel entries for the FH algorithm are given by the diagonal values of \mathbf{S}_k .
4. Given \mathbf{a}_k and \mathbf{B}_k , calculate \mathbf{x}_k and \mathbf{p}_k .
5. Calculate the noise $\bar{\mathbf{z}}_k$ where new noise variance is given by $\sigma_n^2 / |s_{jj}|^2$, where $\sigma_n^2 = 1$ as defined in (3.43), and s_{jj} corresponds to the j^{th} element of the diagonal of \mathbf{S}_k .
6. We have that $\mathbf{r}_k = \mathbf{v}_k + \bar{\mathbf{z}}_k$, where $\mathbf{v}_k = \mathbf{a}_k + \mathbf{p}_k$.
7. Pass \mathbf{r}_k through a *THP modulo* to restrict the received symbol to the region of the constellation, then use a slicer to estimate \mathbf{a}_k .

If instead of using a slicer ZF detectors are used, the results are the same since the *virtual* channel obtained with this scheme is now an identity matrix. The rate given by the FH algorithm should be applied to $\mathbf{v}_k = \mathbf{a}_k + \mathbf{p}_k$ but instead it is applied to \mathbf{a}_k .

As in [49], we sort the parallel channels for THP according to the metric proposed in [50] where a permutation matrix is found such that the minimum SNR is maximized in order to maximize the performance. The reader is referred to [50] for more details.

Simulation results

Simulation results for the first, second and third user with SVD and FH, THP and FH, and using only the Cadambe and Jafar scheme, are shown in Figs. 3.5 - 3.10.

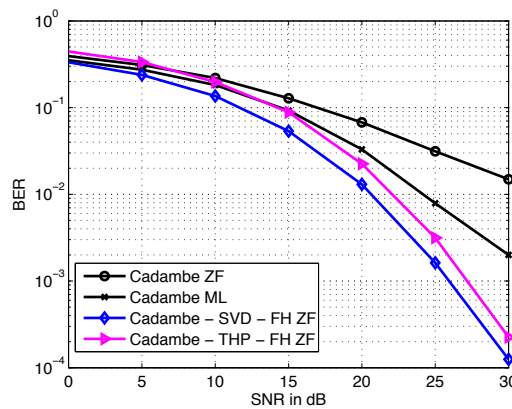


Figure 3.5: Bit error rate for user 1 and $n = 1$, and different precoding schemes

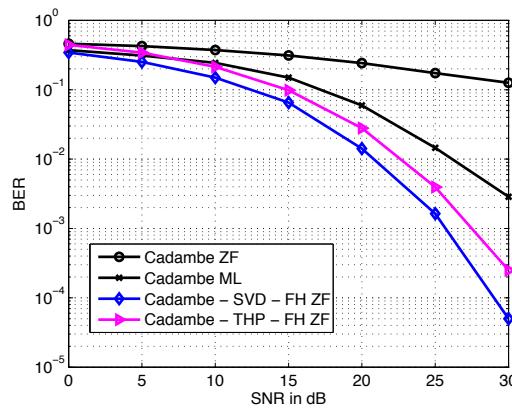


Figure 3.6: Bit error rate for user 1 and $n = 2$, and different precoding schemes

We can observe that the best scheme for user 1 is SVD FH. Obviously, for the other users, when there is no channel extension ($n = 1$), this scheme does not improve anything as there is only one (parallel) channel. It can be observed that as the channel

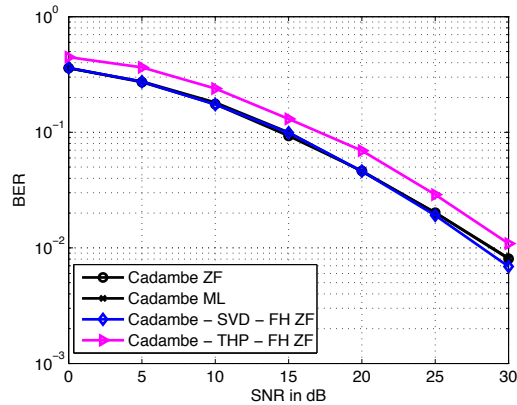


Figure 3.7: Bit error rate for user 2 and $n = 1$, and different precoding schemes

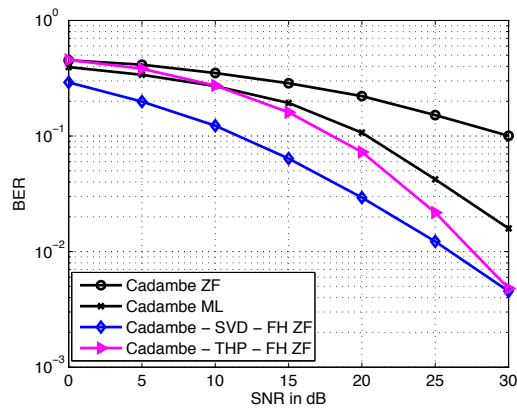


Figure 3.8: Bit error rate for user 2 and $n = 2$, and different precoding schemes

extension is increased, SVD FH is the best scheme for all users. We can also observe that using THP also improves the performance for users 2 and 3 when $n = 2$. By using bit and power loading along with these precoding techniques, compared to the Cadambe and Jafar scheme alone, additional complexity is introduced at the transmitter and receivers but the complexity of the decoding process is reduced. Using SVD and FH, the performance is improved but it requires extra processing at both the transmitter and the receiver. However, it is important to note that because now each transmission occurs in a different and parallel channel, there is no need for a complex detection scheme such as ML decoding, and therefore detection such as ZF suffices.

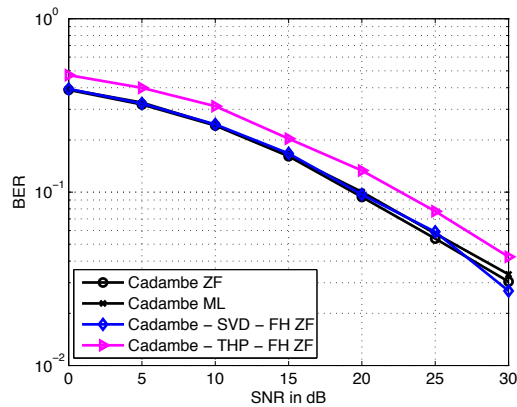


Figure 3.9: Bit error rate for user 3 and $n = 1$, and different precoding schemes

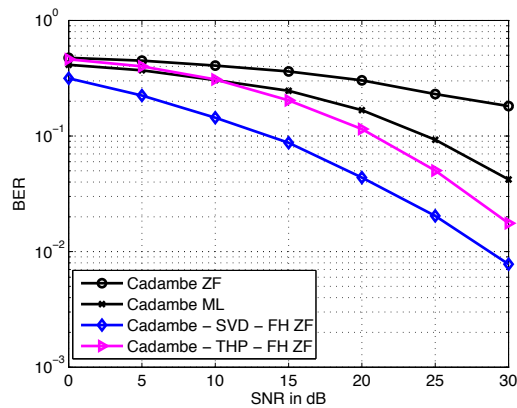


Figure 3.10: Bit error rate for user 3 and $n = 2$, and different precoding schemes

3.5 Conclusions

In this chapter we have implemented the interference alignment scheme proposed by Cadambe and Jafar in [10] for single-user antenna with symbol extension. To remove interference we have used an interference suppressing matrix like the one described in Chapter 1. We note that by doing this the Cadambe and Jafar scheme with interference suppression suffers from poor error performance even with an ML decoding strategy. Since we are interested in improving the performance of the scheme, and given the similarities with MIMO systems, we have considered SVD and THP along with a bit and power loading algorithm normally used for MIMO systems. In this case, we have applied SVD and THP with the FH algorithm to the interference alignment scheme proposed

by Cadambe and Jafar, and have observed that with these simple techniques we can improve the BER of the interference alignment scheme compared to the Cadambe and Jafar scheme alone. We considered only three users, but note that the extension to more users is possible since each of the users is seen as an independent case. The challenge, however, is to find the appropriate precoding and interference suppressing matrices \mathbf{V}_k and \mathbf{U}_k .

Finally, using these techniques increases the precoding complexity but the decoding process is achieved with simpler techniques.

Chapter 4

Lattice codes for the many-to-one interference channel

4.1 Introduction

In this chapter, we study a many-to-one interference channel where only one user suffers from interference. The many-to-one interference channel enables us to simplify the problem of the interference channel while we can still develop tools that can be later used for the fully connected interference channel. For this setting, we are interested in designing lattice codes for all users, such that the probability of error at receiver 1 is small. In [51] and [52], maximum-likelihood (ML) decoders are used for the interference channel. In particular, in [51] the performance of different decoders is analysed for a two-user interference channel. We see that we can derive a similar expression for lattice codes and that under certain conditions a relationship can be found between the union bound of the error probability of user 1, and the theta series of the interference and joint lattices.

4.2 System model and lattice alignment

Consider a many-to-one Gaussian interference channel with three users where interference is only present at receiver 1. Here, the channel model includes different scenarios, such as:

- the single antenna many-to-one Gaussian interference channel using a symbol extension, in which case the channel matrices are scalar matrices;
- the multiple antenna many-to-one Gaussian interference channel.

The model is given by

$$\mathbf{y}_1 = \mathbf{H}_{11}\mathbf{V}_1\mathbf{s}_1 + \mathbf{H}_{12}\mathbf{V}_2\mathbf{s}_2 + \mathbf{H}_{13}\mathbf{V}_3\mathbf{s}_3 + \mathbf{z}_1 \quad (4.1)$$

$$\mathbf{y}_2 = \mathbf{H}_{22}\mathbf{V}_2\mathbf{s}_2 + \mathbf{z}_2,$$

$$\mathbf{y}_3 = \mathbf{H}_{33}\mathbf{V}_3\mathbf{s}_3 + \mathbf{z}_3,$$

where \mathbf{H}_{ij} is the $n \times n$ channel matrix from transmitter j to receiver i . The transmitted symbols \mathbf{s}_j are chosen uniformly in a finite constellation $S_j \subset \mathbb{Z}^m$, $m \leq n$, and \mathbf{z}_i is the AWGN of variance σ^2 at receiver i . The matrices \mathbf{V}_j , $j = 1, 2, 3$ are $n \times m$ precoders that will allow us to align the desired lattices.

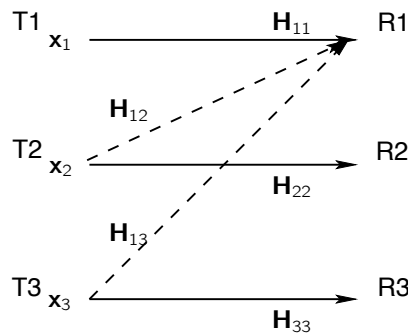


Figure 4.1: three-user many-to-one interference channel

At receiver 1, there is interference from users 2 and 3. By suitably choosing \mathbf{V}_2 and \mathbf{V}_3 and an $m \times m$ unimodular matrix \mathbf{D}_2 in such a way that

$$\mathbf{H}_{12}\mathbf{V}_2\mathbf{D}_2 = \mathbf{H}_{13}\mathbf{V}_3 \quad (4.2)$$

we can perform lattice alignment of the interfering signals from users 2 and 3 at the first receiver's end

$$L(\mathbf{H}_{12}\mathbf{V}_2) = L(\mathbf{H}_{13}\mathbf{V}_3) \quad (4.3)$$

where $L(\mathbf{M})$ is the lattice generated by the matrix \mathbf{M} .

The desired signal then belongs to the lattice $\Lambda_1 = \mathbf{H}_{11}\mathbf{V}_1\mathbb{Z}^m$, while the sum of the interfering signals $\mathbf{H}_{12}\mathbf{V}_2(\mathbf{s}_2 + \mathbf{D}_2\mathbf{s}_3)$ is aligned in the lattice $\Lambda_2 = \mathbf{H}_{12}\mathbf{V}_2\mathbb{Z}^m$. Equation (4.1) changes to:

$$\mathbf{y}_1 = \bar{\mathbf{x}}_1 + \bar{\mathbf{x}}_2 + \mathbf{z}_1, \quad (4.4)$$

where $\bar{\mathbf{x}}_1 = \mathbf{H}_{11}\mathbf{V}_1\mathbf{s}_1$ belongs to the received constellation $C_1 = \mathbf{H}_{11}\mathbf{V}_1S_1 \subset \Lambda_1$ and $\bar{\mathbf{x}}_2 = \mathbf{H}_{12}\mathbf{V}_2(\mathbf{s}_2 + \mathbf{D}_2\mathbf{s}_3)$ belongs to $C_2 \subset \Lambda_2$. We have $\bar{\mathbf{x}}_1 + \bar{\mathbf{x}}_2 \in S_1 + S_2 \subset \Lambda_1 + \Lambda_2 = \Lambda$.

In the following, we assume that Λ is a lattice¹. This can happen in several scenarios:

- If the dimension m of the signal is equal to $n/2$, it is possible (with probability 1 in the space of channel matrices) to align the interference in such a way that the $n/2$ -dimensional lattices Λ_1 and Λ_2 are in direct sum, i.e. $\Lambda_1 \cap \Lambda_2 = \{0\}$.
- If $m = n$, and the channel matrices are integer-valued, then Λ is again a lattice, even though the sum $\Lambda_1 + \Lambda_2$ cannot be a direct sum.

Note that the case of channel matrices with rational entries can be reduced to the integer-valued case by suitable scaling. The integer channel coefficient model was studied in [53], where it was shown that at finite SNR the achievable rate is less sensitive to the use of integer (or rational) channel coefficients than at very high SNR.

4.3 Flatness factor

4.3.1 ML decoding

In order to decode, in particular at receiver 1, an ML decoder can be considered as in [20]. Indeed since the symbols $\mathbf{x}_1 = \mathbf{H}_{11}\mathbf{V}_1\mathbf{s}_1$ that may have been transmitted are uniformly

¹Note that for general (real-valued) channel matrices, the set Λ may not be a discrete subset of \mathbb{R}^n since it may contain a dense set. Thus, Λ may not be a lattice.

distributed in C_1 , MAP decoding is given by

$$\begin{aligned}\hat{\mathbf{x}}_1 &= \operatorname{argmax}_{\mathbf{x}_1 \in C_1} p(\mathbf{x}_1 | \mathbf{y}_1) = \operatorname{argmax}_{\mathbf{x}_1 \in C_1} \frac{f(\mathbf{y}_1 | \mathbf{x}_1) p(\mathbf{x}_1)}{f(\mathbf{y}_1)} = \\ &= \operatorname{argmax}_{\mathbf{x}_1 \in C_1} f(\mathbf{y}_1 | \mathbf{x}_1)\end{aligned}$$

where f denotes the continuous distribution and p the discrete density.

The symbols $\mathbf{w}_2 = \mathbf{H}_{12} \mathbf{V}_2 \mathbf{s}_2$ and $\mathbf{w}_3 = \mathbf{H}_{12} \mathbf{V}_2 \mathbf{D}_2 \mathbf{s}_3$ are uniformly distributed in $A_2 = \mathbf{H}_{12} \mathbf{V}_2 S_2 \subset \Lambda_2$ and $A_3 = \mathbf{H}_{12} \mathbf{V}_2 \mathbf{D}_2 S_3 \subset \Lambda_2$ respectively. (Note that in general it is not true that $\mathbf{x}_2 = \mathbf{w}_2 + \mathbf{w}_3$ is uniformly distributed in some finite set C_2). We can write

$$\begin{aligned}f(\mathbf{y}_1 | \mathbf{x}_1) &= \sum_{\substack{\mathbf{w}_2 \in A_2 \\ \mathbf{w}_3 \in A_3}} f(\mathbf{y}_1 | \mathbf{x}_1, \mathbf{w}_2, \mathbf{w}_3) p(\mathbf{w}_2, \mathbf{w}_3 | \mathbf{x}_1) = \\ &= \frac{1}{|A_2| |A_3|} \sum_{\substack{\mathbf{w}_2 \in A_2 \\ \mathbf{w}_3 \in A_3}} \frac{1}{(\sqrt{2\pi}\sigma)^n} e^{-\frac{\|\mathbf{y}_1 - \mathbf{x}_1 - \mathbf{w}_2 - \mathbf{w}_3\|^2}{2\sigma^2}}\end{aligned}$$

since $\mathbf{w}_2, \mathbf{w}_3$ are independent of \mathbf{x}_1 . Therefore

$$\hat{\mathbf{x}}_1 = \operatorname{argmax}_{\mathbf{x}_1 \in C_1} \sum_{\substack{\mathbf{w}_2 \in A_2 \\ \mathbf{w}_3 \in A_3}} e^{-\frac{\|\mathbf{y}_1 - \mathbf{x}_1 - \mathbf{w}_2 - \mathbf{w}_3\|^2}{2\sigma^2}}$$

Since this decoding metric is too difficult to analyze, we consider the approximate metric

$$\hat{\mathbf{x}}_1 = \operatorname{argmax}_{\mathbf{x}_1 \in C_1} \sum_{\mathbf{x}_2 \in \Lambda_2} e^{-\frac{\|\mathbf{y}_1 - \mathbf{x}_1 - \mathbf{x}_2\|^2}{2\sigma^2}}, \quad (4.5)$$

where \mathbf{x}_2 is allowed to span the whole infinite lattice, thus $\mathbf{x}_2 = \mathbf{w}_2 + \mathbf{w}_3 \in \Lambda_2$, and we have assumed that $A_2 + A_3 \subseteq \Lambda_2$.

4.3.2 Gaussian measures on lattices and flatness factor

We define the Gaussian measure associated to the lattice Γ and the variance σ^2 as

$$f_{\sigma, \Gamma}(\mathbf{w}) = \sum_{\mathbf{x} \in \Gamma} e^{-\frac{\|\mathbf{w} - \mathbf{x}\|^2}{2\sigma^2}}. \quad (4.6)$$

The decoding rule (4.5) can thus be rewritten as

$$\hat{\mathbf{x}}_1 = \operatorname{argmax}_{\mathbf{x}_1} (f_{\sigma, \Lambda_2}(\mathbf{y}_1 - \mathbf{x}_1)). \quad (4.7)$$

To find one possible maximum for this function, we must be sure that the function is never flat. This problem was studied in [20] where the notion of *flatness factor* of a lattice Γ was introduced, which was presented in Chapter 1 of this document. Recall the definition of the flatness factor of Γ (1.66) given by [21]:

$$\varepsilon_\Gamma = \gamma^{\frac{n}{2}} \Theta_\Gamma \left(e^{-\frac{1}{2\sigma^2}} \right) - 1, \quad (4.8)$$

where $\gamma = \frac{V(\Gamma)^{\frac{2}{n}}}{2\pi\sigma^2}$ is the volume-to-noise ratio, $V(\Gamma)$ is the fundamental volume of the lattice Γ , and $\Theta_\Gamma \left(e^{-\frac{1}{2\sigma^2}} \right)$ is the theta series of the lattice Γ as defined in (1.57). Note that the flatness factor is only a function of the interferer lattice Γ and of the variance of the noise.

Therefore, in our case we want the flatness factor of the lattice Λ_2 to be big for a given value of σ to enable correct decoding.

4.3.3 Examples

In this subsection we compare the flatness factors of different lattices. Consider the theta series defined in Chapter 1 for $\Gamma = \mathbb{Z}^2$ and $\Gamma = \mathbb{Z}^8$ (1.58), $\Gamma = A_2$ (1.59) and $\Gamma = E_8$ (1.60). Using (4.8), we plot the respective flatness factors in Fig. 4.2, where we have normalized the volume of the lattices. The selection of the lattice Γ can be made depending on the variance of the noise σ^2 . For the two dimensional case and the eight dimensional case, the better choice is \mathbb{Z}^m ($m = 2$ or $m = 8$, respectively), for the shown values of σ^2 .

In Figs. 4.3 and 4.4, we plot $f_{\sigma, \Lambda_2}(\mathbf{t})$ for different 2-dimensional lattices Λ_2 and $\sigma^2 = 0.15$, where $\mathbf{t} = \mathbf{y}_1 - \mathbf{x}_1 \in \mathbb{R}^2$. We can see, as expected, that \mathbb{Z}^2 is the better choice.

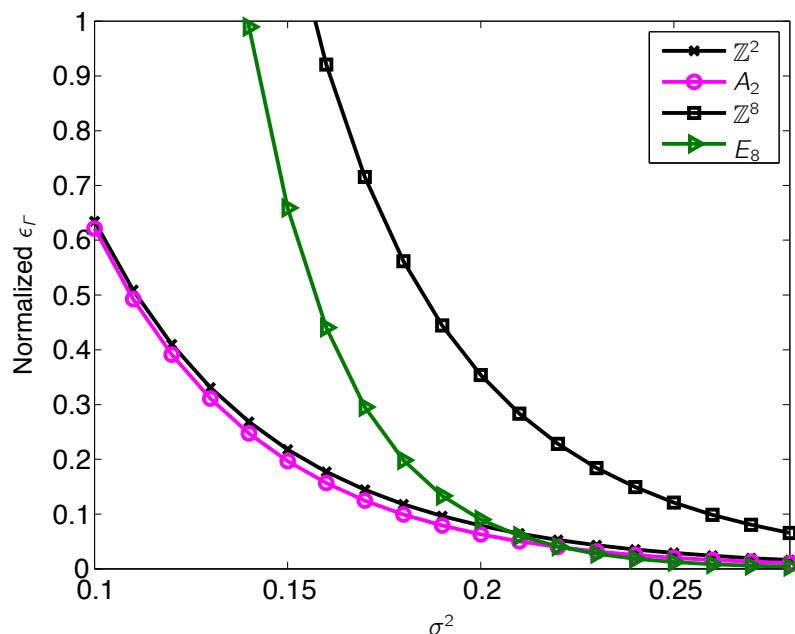


Figure 4.2: Flatness factor for two and eight dimensional lattices

4.3.4 Average behaviour

From [21], we know the average behaviour of the flatness factor for Construction-A lattices is

$$E[\epsilon_F] = \gamma^n. \quad (4.9)$$

Therefore, the average flatness factor exhibits a 'phase-transition' phenomenon: if $\gamma > 1$, then $E[\epsilon_F]$ tends to infinity exponentially with respect to n ; if $\gamma < 1$, then $E[\epsilon_F]$ tends to zero exponentially with respect to n .

4.4 Error probabilities

In this section, we describe the main contribution of this chapter. Suppose that the received signal is given by equation (4.4), where $\bar{\mathbf{x}}_1 \in C_1 \subset \Lambda_1$ and $\bar{\mathbf{x}}_2 \in C_2 \subset \Lambda_2$. We now estimate the error probability in the case in which $\Lambda = \Lambda_1 + \Lambda_2$ is a lattice. We make no assumption on the dimensions of the lattices Λ_1 and Λ_2 , which may be full-rank or not. We also do not require the sum to be a direct sum; this means that each element λ of Λ

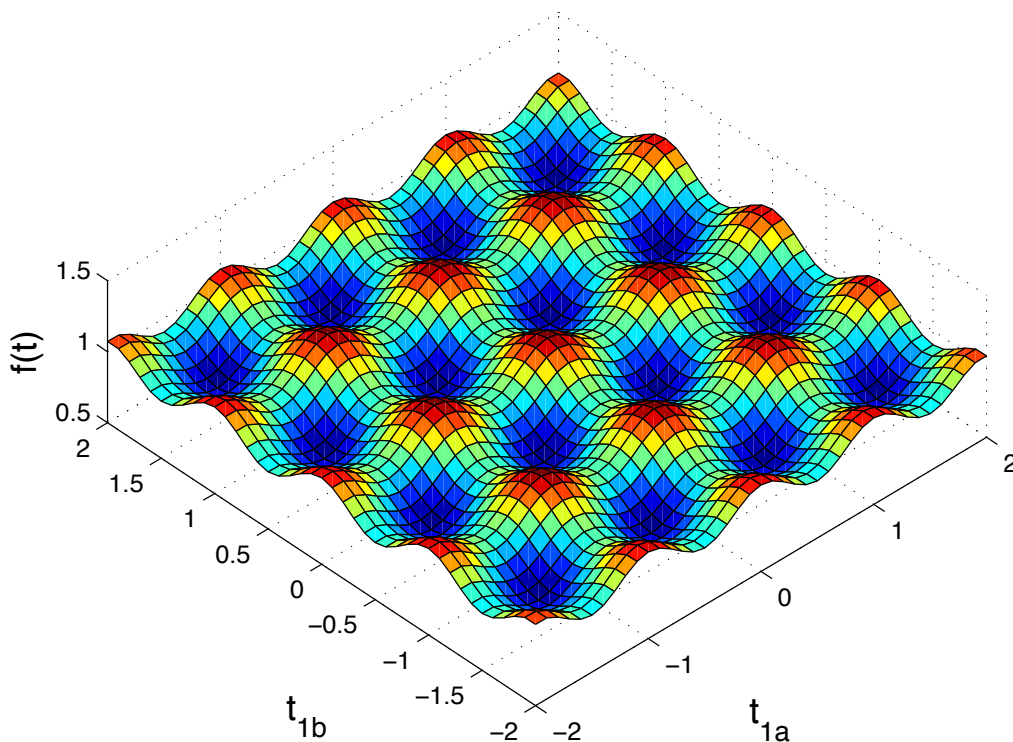


Figure 4.3: Function $f_{\sigma\Lambda_2}(\mathbf{t})$ using $\Lambda_2 = \mathbb{Z}^2$ and $\sigma^2 = 0.15$

may be written in different ways as a sum of $\lambda_1 + \lambda_2$ with $\lambda_1 \in \Lambda_1$, $\lambda_2 \in \Lambda_2$. Since such ambiguity would prevent the first receiver from decoding, the code C_1 must be chosen in such a way as to remove it.

We suppose that C_2 is any subset of Λ_2 , and that C_1 is a set of distinct coset leaders of $\Lambda_1 \cap \Lambda_2$ in Λ_1 . That is, we choose one element for each equivalence class in the quotient $\Lambda_1/(\Lambda_1 \cap \Lambda_2)$. Therefore if $\Lambda_1 \cap \Lambda_2 \neq \{0\}$, the rate of this scheme is limited by $\frac{1}{n} \log_2(|\Lambda_1/(\Lambda_1 \cap \Lambda_2)|)$. If on the contrary $\Lambda_1 \cap \Lambda_2 = \{0\}$, then C_1 can be any subset of Λ_1 and there is no a priori limitation on the rate. For the sake of simplicity, we consider the case where C_1 is the whole set of coset leaders in $\Lambda_1/(\Lambda_1 \cap \Lambda_2)$ (finite or infinite).

Since our lattices are also said to be \mathbb{Z} -modules [54], consider the definition of the \mathbb{Z} -module homomorphism [55]. Let G and H be \mathbb{Z} -modules, the mapping

$$f : G \rightarrow H \quad (4.10)$$

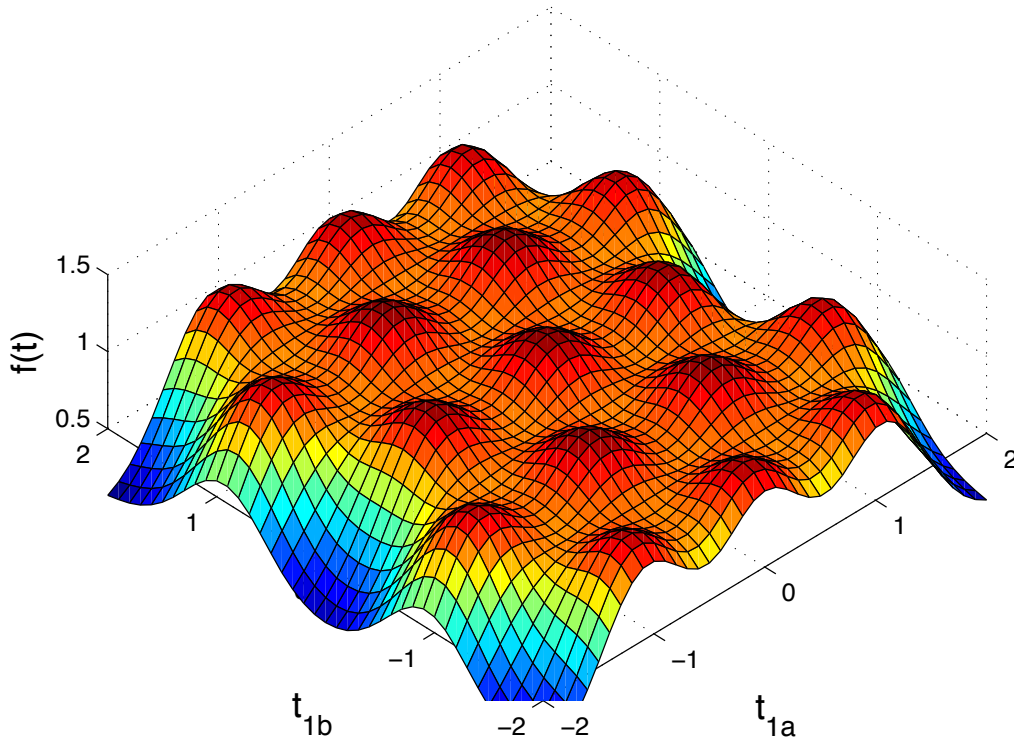


Figure 4.4: Function $f_{\sigma, \Lambda_2}(\mathbf{t})$ using $\Lambda_2 = A_2$ and $\sigma^2 = 0.15$

is a function satisfying

$$f(x + y) = f(x) + f(y), \quad \forall x, y \in G \quad (4.11)$$

$$f(rx) = rf(x), \quad \forall r \in \mathbb{Z}, x \in G. \quad (4.12)$$

A bijective homomorphism is called an isomorphism and it is denoted with \cong . Now consider the following isomorphism (second isomorphism for modules) [55]

$$\varphi : \Lambda_1 / (\Lambda_1 \cap \Lambda_2) \cong \Lambda / \Lambda_2 \quad (4.13)$$

For example, let $\Lambda_1 = 3\mathbb{Z}$, $\Lambda_2 = 2\mathbb{Z}$, thus $\Lambda = \Lambda_1 + \Lambda_2 = \mathbb{Z}$ and $\Lambda_1 \cap \Lambda_2 = 6\mathbb{Z}$. Then, $3\mathbb{Z}/6\mathbb{Z} \cong \mathbb{Z}/2\mathbb{Z}$.

From the definition of quotient group we have that $\mathbf{x} + \Lambda_2 \in \Lambda / \Lambda_2$. From the

isomorphism just described we can say that the inverse map φ^{-1} sends the equivalence class $\mathbf{x} + \Lambda_2 \in \Lambda/\Lambda_2$ to the equivalence class $(\mathbf{x} + \Lambda_2) \cap \Lambda_1 \in \Lambda_1/(\Lambda_1 \cap \Lambda_2)$.

This property allows us to define the following decoding rule. Consider the closest point in Λ to the received vector

$$\tilde{\mathbf{x}} = \operatorname{argmin}_{\mathbf{x} \in \Lambda} \|\mathbf{y}_1 - \mathbf{x}\|^2, \quad (4.14)$$

and let the output of the decoder at the first receiver be

$$\hat{\mathbf{x}}_1 = \tilde{\mathbf{x}} \bmod \Lambda_2 \quad (4.15)$$

where $\tilde{\mathbf{x}} \bmod \Lambda_2$ is defined as the (unique) element in $(\tilde{\mathbf{x}} + \Lambda_2) \cap C_1$.

The decoder (4.15) is a suboptimal approximation of the decoder (4.5), which corresponds to jointly decoding $(\mathbf{x}_1, \mathbf{x}_2)$ and then discarding \mathbf{x}_2 , but avoids ambiguities.

The conditional error probability given $\bar{\mathbf{x}}_1$ and $\bar{\mathbf{x}}_2$ can be upper bounded as follows:

$$\begin{aligned} P(e|\bar{\mathbf{x}}_1, \bar{\mathbf{x}}_2) &= \mathbb{P}\{\bar{\mathbf{x}}_1 \neq \tilde{\mathbf{x}} \bmod \Lambda_2\} = \sum_{\substack{\mathbf{x} \in \Lambda \\ \mathbf{x} - \bar{\mathbf{x}}_1 \notin \Lambda_2}} \mathbb{P}\{\tilde{\mathbf{x}} = \mathbf{x}\} \\ &\leq \sum_{\substack{\mathbf{x} \in \Lambda \\ \mathbf{x} - \bar{\mathbf{x}}_1 \notin \Lambda_2}} \mathbb{P}\left\{\|\mathbf{y}_1 - \mathbf{x}\|^2 \leq \|\mathbf{y}_1 - \bar{\mathbf{x}}_1 - \bar{\mathbf{x}}_2\|^2\right\} \\ &= \sum_{\substack{\mathbf{x} \in \Lambda \\ \mathbf{x} - \bar{\mathbf{x}}_1 \notin \Lambda_2}} \mathbb{P}\left\{\|\bar{\mathbf{x}}_1 + \bar{\mathbf{x}}_2 - \mathbf{x} + \mathbf{z}\|^2 \leq \|\mathbf{z}\|^2\right\} \\ &\leq \sum_{\substack{\mathbf{x} \in \Lambda \\ \mathbf{x} - \bar{\mathbf{x}}_1 \notin \Lambda_2}} \frac{1}{2} e^{-\frac{\|\mathbf{x} - \bar{\mathbf{x}}_1 - \bar{\mathbf{x}}_2\|^2}{8\sigma^2}} \end{aligned} \quad (4.16)$$

by the classical bound on the Gaussian tail distribution.

Observe that $\mathbf{x} - \bar{\mathbf{x}}_1 - \bar{\mathbf{x}}_2 \notin \Lambda_2$. Otherwise, we would have $(\mathbf{x} - \bar{\mathbf{x}}_1 - \bar{\mathbf{x}}_2) + \bar{\mathbf{x}}_2 = \mathbf{x} - \bar{\mathbf{x}}_1 \in \Lambda_2$, which is a contradiction.

Therefore (4.16) can be rewritten as

$$\begin{aligned} P(e|\bar{\mathbf{x}}_1, \bar{\mathbf{x}}_2) &\leq \sum_{x' \in \Lambda \setminus \Lambda_2} \frac{1}{2} e^{-\frac{\|x'\|^2}{8\sigma^2}} \\ &= \frac{1}{2} \left(\Theta_{\Lambda} \left(e^{-\frac{1}{8\sigma^2}} \right) - \Theta_{\Lambda_2} \left(e^{-\frac{1}{8\sigma^2}} \right) \right). \end{aligned} \quad (4.17)$$

Consider a toy example with only two users, where Λ_1 and Λ_2 are one-dimensional lattices in \mathbb{R}^2 . More precisely $\Lambda_1 = [1 \ 0]^T \mathbb{Z}$ and $\Lambda_2 = [1 \ 1]^T \mathbb{Z}$, and they are in direct sum, so $\Lambda = \mathbb{Z}^2$. Suppose that $S \subset \mathbb{Z}$, such that $C_1 = [1 \ 0]^T S$ and $C_2 = [1 \ 1]^T S$. Simulation results can be observed in Fig. 4.5, where we increase the size of the constellation S in each simulation to get closer to the bound given in (4.17).

Note that, even if the bound is not tight, the bound is still a contribution since it relates the theta series of the received lattice and the interference lattice, and demonstrates that to have a small error probability the flatness factor of the interference should be big.

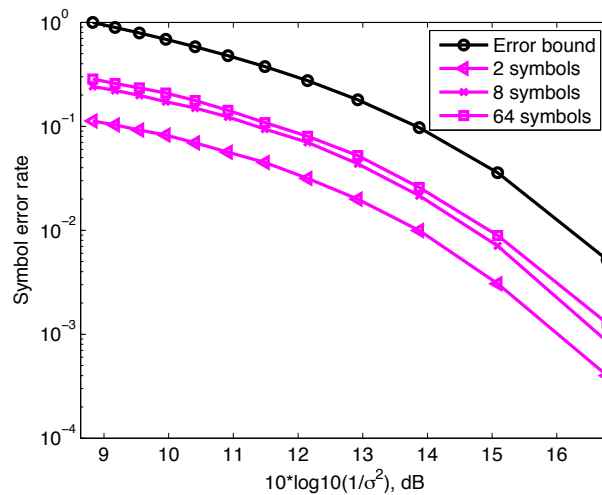


Figure 4.5: Error probability

4.5 The good and bad lattices

Based on the foregoing analysis, we now consider the design criteria of lattices for the many-to-one interference channel. The union bound (4.17) clearly indicates that to re-

duce the error probability, Λ should be a good lattice (i.e., have a small theta series), while Λ_2 should be a bad lattice (i.e., have a large theta series). The latter is consistent with the flatness factor, i.e., Λ_2 should have a large flatness factor in order to decode user 1. From the asymptotics of the flatness factor, we know that a large flatness factor is possible if

$$\gamma_{\Lambda_2} > 1. \quad (4.18)$$

Meanwhile, we also want to reliably decode at other receivers. Denote by Λ'_2 the lattice seen at receiver two. For convenience, we assume scalar channels in the following. Since in this case $V(\Lambda_2) = h_{12}$ and $V(\Lambda'_2) = h_{22}$, then $\gamma_{\Lambda_2} = \frac{V(\Lambda_2)^{\frac{2}{n}}}{2\pi\sigma^2} = \frac{h_{12}^2}{2\pi\sigma^2}$, and $\gamma_{\Lambda'_2} = \frac{V(\Lambda'_2)^{\frac{2}{n}}}{2\pi\sigma^2} = \frac{h_{22}^2}{2\pi\sigma^2}$, then Λ'_2 is a scaled version of Λ_2 , and their generalized SNR's satisfy $\gamma_{\Lambda'_2} = \frac{h_{22}^2}{h_{12}^2}\gamma_{\Lambda_2}$. We choose a lattice Λ'_2 whose generalized SNR

$$\gamma_{\Lambda'_2} = \frac{h_{22}^2}{h_{12}^2}\gamma_{\Lambda_2} > e. \quad (4.19)$$

This guarantees the existence of a lattice Λ'_2 such that the error probability at receiver 2 goes to zero as $n \rightarrow \infty$ [56].

Combining (4.18) and (4.19), we have

$$\gamma_{\Lambda_2} > \max \left\{ 1, e \cdot \frac{h_{12}^2}{h_{22}^2} \right\}. \quad (4.20)$$

We now consider two cases:

Case 1: $e \frac{h_{12}^2}{h_{22}^2} < 1$ or $h_{22} > \sqrt{e}h_{12}$, i.e., the direct link for user 2 is strong. In this case, the condition (4.20) is simply the reliability criterion $\gamma_{\Lambda_2} > 1$.

Case 2: $e \frac{h_{12}^2}{h_{22}^2} > 1$ or $h_{22} < \sqrt{e}h_{12}$, i.e., the direct link for user 2 is not strong. In this case, the condition (4.20) is $\gamma_{\Lambda_2} > e \cdot \frac{h_{12}^2}{h_{22}^2}$ so that we may need a large value of γ_{Λ_2} . This means that we have to increase the fundamental volume $V(\Lambda_2)$, hence reducing the rate of user 2 (when shaping is applied).

Similarly, the lattice Λ_3 seen by receiver 3 needs to satisfy

$$\gamma_{\Lambda'_3} = \frac{h_{33}^2}{h_{13}^2}\gamma_{\Lambda_3} > e. \quad (4.21)$$

But since $h_{13}v_3 = h_{12}v_2$, then $V(\Lambda_3) = V(\Lambda_2)$, then $\gamma_{\Lambda_2} = \gamma_{\Lambda_3}$. Thus

$$\gamma_{\Lambda'_3} = \frac{h_{33}^2}{h_{13}^2} \gamma_{\Lambda_2} > e. \quad (4.22)$$

Combining (4.18), (4.19) and (4.22), we have

$$\gamma_{\Lambda_2} > \max \left\{ 1, e \cdot \frac{h_{12}^2}{h_{22}^2}, e \cdot \frac{h_{13}^2}{h_{33}^2} \right\}. \quad (4.23)$$

Finally we summarize the design criteria of lattice alignment for the many-to-one interference channel described, where only user 1 suffers from interference:

- Good lattice: In order for user 1 to have small error probability, Λ should be a good lattice, i.e., a dense lattice.
- Bad lattice: In order to decode user 1, we require Λ_2 to have a large flatness factor. Namely, it is not dense, which is a *bad* lattice in the standard sense of coding.
- The good lattices: The lattices Λ'_2 and Λ'_3 should be good on their own channels. This can be made possible by satisfying (4.23).

4.6 Conclusions

In this chapter, we have studied lattice codes to find the error performance of a many-to-one interference channel using interference alignment at receiver 1. This work is motivated by the work of [20] in which the flatness factor concept is introduced. We see that in order to correctly decode, we need the flatness factor of the interference lattice to be big. We derive an upper bound for the error probability of user 1 by using a joint maximum-likelihood decoder of the desired signal and the sum of the interference. The resultant bound shows the relation needed between the theta series of the resultant lattice at the receiver and the theta series of the interference lattice. It shows that in order to minimize the error we need the theta series of the received lattice to be small while the theta series of the interference must be big, which is consistent with what we expect in terms of the flatness factor. We also give some design criteria for the lattices for the

many-to-one interference channel.

Chapter 5

Barnes-Wall lattices for the symmetric interference channel

5.1 Introduction

In this chapter, we extend the work of [5] in higher dimensions using lattices. In [4], a deterministic channel approach is applied to an interference channel, where signals are represented in base Q , in order to construct an interference alignment scheme. With a symmetric interference channel where the indirect channel coefficients are given by Q^{-1} and zero paddings in the signal construction, interference is perfectly aligned, leaving $K/2$ DoF for the desired signal. Following with the ideas of [2] and [4], achievable schemes for the GDoF are found in [5] for different types of interference with K users. The signals are represented in base Q , and a detailed scheme is given for the different types of interference. The construction of the schemes can serve as motivation to use lattice codes.

In this chapter we consider and focus on the performance of the symmetric fully connected interference channel. We use the base Q representation of [5] with higher dimensional lattices. In particular we use BW lattices because they have a very similar level structure to the one-dimensional lattice scheme used in [5], and because of the good performance lattices can offer. We show that it is possible to build similar schemes for different types of interference using BW lattices, with the benefit of improving the

performance.

5.2 Symmetric interference channel by Jafar [5]

Consider the K -user symmetric interference channel model given by [5]:

$$y_k = x_k + g \sum_{j=1, j \neq k}^K x_j + z_k, \quad (5.1)$$

where y_k is the received signal at receiver k , g is the real indirect channel gain, x_k is the signal transmitted by transmitter k , x_j is the interference signal from transmitter j , z_k is the AWGN with variance σ^2 and zero mean, and $k = 1, \dots, K$. In [5] g is defined as $g = \sqrt{\frac{\text{INR}}{\text{SNR}}}$. In [2] the interference is classified in types defined by means of the parameter $\alpha = \frac{\log \text{INR}}{\log \text{SNR}}$. Each type of interference is given by [2]:

- Noisy: $0 \leq \alpha \leq 1/2$
- Weak: $1/2 \leq \alpha \leq 2/3$
- Moderately weak: $2/3 \leq \alpha < 1$
- Strong: $1 < \alpha \leq 2$
- Very strong: $\alpha \geq 2$

where there is a discontinuity at 1.

In [4] and [5] the idea of quantizing the signal in *levels* is used. In the paper by Jafar [5] the problem has been addressed using a one-dimensional lattice and they are interested in a scheme to achieve the DoF found in [2], for each type of interference. The transmitted signal is constructed as $x_k = Q^{N-1}C_{N-1} + \dots + QC_1 + C_0$, where we define each level to be represented by Q^i . Here, C_i are codewords that have some properties related to Q and K , depending on the type of interference, where K , Q , M and N are positive integers. The parameter Q is also related to the SNR, since $\text{SNR} = Q^{\frac{2M}{|\alpha-1|}}$ with $Q \gg K$ and M grows to infinity. The channel gain g is given by $g = Q^{\text{sgn}(\alpha-1)M}$, where

$\text{sgn}(x) = 1$ if $x > 0$ and -1 if $x < 0$. The channel gains act as shifters, which may result in that some levels overlapping at the receivers.

With some careful properties of the codewords C_i , each level can be decoded sequentially and independently, and interference can be eliminated.

5.2.1 Encoding

The schemes presented in [5] for each type of interference manage to completely remove the interference using alignment and codeword constructions for one-dimensional symbols. Interference is then cancelled and the desired message can be decoded.

For convenience and since the channel is symmetric, we initially work with a two-user interference channel. For the rest of the chapter, the codewords will be expressed with C_i for user 1 and D_i for user 2.

Very strong interference

For the very strong interference, g is given by $g = Q^M$, and the transmitted signals are constructed as

$$x_1 = Q^{N-1}C_{N-1} + \cdots + QC_1 + C_0, \quad (5.2)$$

$$x_2 = Q^{N-1}D_{N-1} + \cdots + QD_1 + D_0, \quad (5.3)$$

where C_i and D_i are the codewords.

In order to avoid carryovers, Jafar poses another condition that for very strong interference is given by $C_i, D_i \in \{1, \dots, Q-2\}$. Note that in this case, it means that $Q \geq 4$ for a code to exist. Thus the channel coefficient g cannot be smaller than 4. Finally, the restriction that $N = \lfloor \frac{M}{\alpha-1} \rfloor$ is given to satisfy the power constraint. Since $\alpha \geq 2$, it implies that $M \geq N$.

At each receiver we have

$$y_1 = Q^{M+N-1}D_{N-1} + \cdots + Q^M D_0 + Q^{N-1}C_{N-1} + \cdots + C_0 + z_1 \quad (5.4)$$

$$y_2 = Q^{M+N-1}C_{N-1} + \cdots + Q^M C_0 + Q^{N-1}D_{N-1} + \cdots + D_0 + z_2. \quad (5.5)$$

Since the channel is symmetric, and without loss of generality from this point we will only consider the received signals at receiver 1.

Strong interference

For the strong interference, g is also given by $g = Q^M$, and the transmitted signals are constructed as

$$x_1 = Q^{2N-M-1}C_{2N-M-1} + \cdots + Q^N C_N + Q^{N-1}C_{N-1} + \cdots + C_0, \quad (5.6)$$

$$x_2 = Q^{2N-M-1}D_{2N-M-1} + \cdots + Q^N D_N + Q^{N-1}D_{N-1} + \cdots + D_0, \quad (5.7)$$

In this case, there is an extra constraint given by

$$C_{2N-M-i} = C_{i-1} \quad (5.8)$$

$$D_{2N-M-i} = D_{i-1}, \quad (5.9)$$

for $i \in \{1, \dots, N - M\}$. Equations (5.8) and (5.9) will be useful at the receiver to eliminate the interference. To avoid carryovers here, the condition is given by $C_i, D_i \in \{1, \dots, \lfloor \frac{Q-1}{K} \rfloor - 1\}$. Note that in this case, it means that $Q \geq 7$ for a code to exist. Thus the channel coefficient g cannot be smaller than 7. Finally, the restriction that $N = \lfloor \frac{\alpha M}{2(\alpha-1)} \rfloor \geq M$ is given to satisfy the power constraint.

At receiver 1 we have

$$\begin{aligned} y_1 &= Q^{2N-1}D_0 + Q^{2N-2}D_1 + \cdots + Q^{2N-M-1}(D_{2N-2M-1} + C_0) + \cdots \\ &+ Q^M(D_0 + C_M) + \cdots + QC_1 + C_0 + z_1. \end{aligned} \quad (5.10)$$

At the receiver the interference overlaps the desired signal on some levels. However, the construction and constraints presented by Jafar in (5.8) and (5.9) allows to decode each level.

Moderately weak interference

For the moderately weak interference $g = Q^{-M}$, and the transmitted signals are constructed as

$$\begin{aligned} x_1 &= Q^{2N+3M-1}C_{2N-M-1} + \cdots + Q^{N+3M}C_{N+3M} + Q^{3M+N-1}C_{3M+N-1} + \cdots \\ &+ Q^{2M+N}C_{2M+N} + Q^{2M+N-1}C_{2M+N-1} + \cdots + Q^{2M}C_{2M} \\ &+ Q^{M-1}C_{M-1} + \cdots + QC_0, \end{aligned} \quad (5.11)$$

$$\begin{aligned} x_2 &= Q^{2N+3M-1}D_{2N-M-1} + \cdots + Q^{N+3M}D_{N+3M} + Q^{3M+N-1}D_{3M+N-1} + \cdots \\ &+ Q^{2M+N}D_{2M+N} + Q^{2M+N-1}D_{2M+N-1} + \cdots + Q^{2M}D_{2M} \\ &+ Q^{M-1}D_{M-1} + \cdots + QD_0, \end{aligned} \quad (5.12)$$

In this case, there is an extra constraint given by

$$C_{2N+3M-i} = C_{2M+i-1} \quad (5.13)$$

$$D_{2N+3M-i} = D_{2M+i-1}, \quad (5.14)$$

for $i = \{1, \dots, N\}$. Here the condition is given by $C_i, D_i \in \{1, \dots, \lfloor \frac{Q-1}{K} \rfloor - 1\}$ and the restriction $N = \lfloor \frac{M(3\alpha-2)}{2(1-\alpha)} \rfloor$ is given to satisfy the power constraint.

The received signal is not as easy to express as it was before since some of the overlapping levels depend on whether M is bigger, smaller or equal to $N - 1$. To observe the overlap and the scheme presented by Jafar consider the following example. Take $N = M = 1$ and $Q \geq 7$. At transmitter 1 and 2 we have

$$x_1 = Q^4C_4 + Q^3C_3 + Q^2C_4 + C_0 \quad (5.15)$$

$$x_2 = Q^4D_4 + Q^3D_3 + Q^2D_4 + D_0, \quad (5.16)$$

where $g = Q^{-1}$. Thus, at receiver 1 we have

$$\begin{aligned} y_1 &= Q^4C_4 + Q^3(C_3 + D_4) + Q^2(C_4 + D_3) \\ &+ QD_4 + C_0 + Q^{-1}D_0 + z_1. \end{aligned} \quad (5.17)$$

where $C_1 = D_1 = 0$, and $C_4 = C_2$, $D_4 = D_2$. Thus, it is possible to decode and eliminate the interference at each receiver.

Weak interference

For the weak interference $g = Q^{-M}$, and the transmitted signals are constructed as

$$x_1 = Q^{2M+N-1}C_{2M+N-1} + \cdots + Q^{2M}C_{2M} + Q^{M-1}C_{M-1} + \cdots + QC_0, \quad (5.18)$$

$$x_2 = Q^{2M+N-1}D_{2M+N-1} + \cdots + Q^{2M}D_{2M} + Q^{M-1}D_{M-1} + \cdots + QD_0, \quad (5.19)$$

Here the condition is given by $C_i, D_i \in \{1, \dots, Q-2\}$ and the restriction that $N = \lfloor \frac{M(2\alpha-1)}{1-\alpha} \rfloor \leq M$ is given to satisfy the power constraint. At receiver 1

$$\begin{aligned} y_1 &= Q^{2M+N-1}C_{2M+N-1} + \cdots + Q^{2M}C_{2M} + \cdots \\ &+ Q^{M+N-1}D_{2M+N-1} + \cdots + Q^M D_{2M} \\ &+ Q^{M-1}C_{M-1} + \cdots + C_0 \\ &+ Q^{-1}D_{M-1} + \cdots + Q^{-M}D_0 + z_1. \end{aligned} \quad (5.20)$$

5.2.2 Decoding

The decoding of the Jafar schemes depend on the type of interference. For most types of interference, the decoding used is a multilevel decoder, starting from the lowest level. Once a level is decoded it is subtracted from the received signal and divided by Q , and the process is repeated. The decoding of each level will be shown next for the case of weak interference, and it is similar for strong and moderately weak. We will start with the very strong interference case which is different to the other three cases. For the very strong interference using (5.2) and (5.3) at receiver 1 we have (5.4). Since $M \geq N$ the interference has been shifted to *higher levels*, allowing the desired signal to be in *lower levels*, with no overlap. To decode we just need:

$$\hat{x}_1 = \lfloor y_1 \rfloor \bmod Q^N, \quad (5.21)$$

Algorithm 5.1 General decoding algorithm (adapted from [5])

```

1:  $s = y_1$  ▷ for strong interference
2:  $s = Q^M y_1$  ▷ for moderately weak and weak interference
3: for all received levels do ▷ Starting from the lowest level
4:    $c = \lfloor s \rfloor \bmod Q$ 
5:    $\hat{C}_i = c$  (or  $\hat{D}_i = c$ ) ▷ Estimated value for level  $Q^i$ 
6:    $s = (s - c)/Q$ 
7: end for

```

where $\lfloor \cdot \rfloor$ refers to the rounding operation.

Since the case of weak interference is simple (the signal and the interference do not overlap within the levels) we will analyse this case before the strong and moderate interference case. From (5.20) it can be observed that the desired signal and the interference do not overlap, so decoding can take place by levels. In fact, we decode from the lowest level upwards by applying Algorithm 5.1¹.

For the cases of strong and moderately weak interference, at the receiver in some levels there is interference overlapping the desired signal. For the case of strong interference using (5.6) and (5.7) at receiver 1 we have (5.10). However, the construction and constraints presented by Jafar allows us to decode nevertheless. Take for example level Q^0 in (5.10) where C_0 can be decoded without interference. Now take level Q^{2N-M-1} where we have the sum of $(D_{2N-2M-1} + C_0)$. Since we have already decoded C_0 , we can subtract it from $(D_{2N-2M-1} + C_0)$ and obtain $D_{2N-2M-1}$. This process is repeated on all levels where there is interference. Also note that on some levels this is facilitated by conditions (5.8) and (5.9). Since the decoding for the moderately weak interference is very similar, its analysis will be omitted here.

The schemes proposed by Jafar are very useful, however, they have some limitations. The values of Q are very limited in order to be able to construct a codebook, and therefore the values that the channel gain can take are also very limited. Also, the system is built (for simplicity) in one dimension. We can see an extension in higher dimensions if we apply lattices, in particular BW lattices which seem very useful since their construction is very similar. Finally, we do not know how is the performance of these schemes, which

¹The decoding process is not generalized to any type of interference in [5] but it can be deduced as in Algorithm 5.1

is actually hard to analyse as in some cases the SNR has to be very big and related to the value of α by $g = \text{SNR}^{\frac{\alpha-1}{2}}$. We can conjecture that higher dimensional lattices yields better performance. To simplify the problem we will assume that the interference is very strong and strong if the channel $g > 1$, while the interference is noisy, weak or moderately weak if $g < 1$.

5.3 Barnes-Wall lattices

5.3.1 Encoding

BW lattices as explained in Chapter 1 are a family of full rank lattices whose dimension is a power of 2. Recall equations (1.70) and (1.71) where BW lattices are defined as

- $m - r$ even:

$$\begin{aligned} \Lambda(r, m) &= 2^{\frac{m-r}{2}} \mathbb{Z}^{2^{m+1}} \\ &+ \sum_{\substack{r+1 \leq r' \leq m \\ m-r' \text{ odd}}} 2^{(r'-r-1)/2} \text{RM}(r', m+1) \end{aligned} \quad (5.22)$$

- $m - r$ odd:

$$\begin{aligned} \Lambda(r, m) &= 2^{\frac{m-r+1}{2}} \mathbb{Z}^{2^{m+1}} \\ &+ \sum_{\substack{r+1 \leq r' \leq m \\ m-r' \text{ even}}} 2^{(r'-r-1)/2} \text{RM}(r', m+1) \end{aligned} \quad (5.23)$$

where again for convenience we consider real lattices.

5.3.2 Decoding

A low-complexity, bounded distance decoding algorithm for Leech lattices was presented in [57], which can also be applied to decode Construction D lattices. Since BW lattices can also be constructed by Construction D, this is a useful decoder for this kind of lattices. In particular, we focus on the low-complexity bounded distance decoder (BDD) algorithm

Algorithm 5.2 Sequential BDD for BW lattices (modified from [26])

```

1:  $\mathbf{s} = \mathbf{y}_1$ 
2: for all received levels do ▷ Starting from the lowest level
3:   if  $\mathbf{C}_i$  (or  $\mathbf{D}_i$ ) to decode corresponds to a RM code then
4:      $\mathbf{b} = \lfloor \mathbf{s} \rfloor \bmod 2$ 
5:      $\rho = 1 - 2|\mathbf{s} - \lfloor \mathbf{s} \rfloor|$ 
6:      $\mathbf{c} = \text{RMdec}(j, \mathbf{b}, \rho)$  ▷ from [26, Algorithm 3], where  $j$  corresponds to
       RM( $j, m + 1$ ) to decode
7:   else If it corresponds to  $\mathbb{Z}^{2^{m+1}}/2\mathbb{Z}^{2^{m+1}}$ 
8:      $\mathbf{c} = \lfloor \mathbf{s} \rfloor \bmod 2$ 
9:   end if
10:   $\hat{\mathbf{C}}_i = \mathbf{c}$  (or  $\hat{\mathbf{D}}_i = \mathbf{c}$ ) ▷ Estimated value for level  $Q^i$ 
11:   $\mathbf{s} = (\mathbf{s} - \mathbf{c})/Q$ 
12: end for

```

for BW lattices proposed by Micciancio in [26, Algorithm 2]. The original algorithm considers complex lattices. Thus, in Algorithm 5.2, lines 4 and 5 have been modified to work with real lattices. Also, the algorithm has been slightly adapted to deliver each decoded level, if required. The decoding procedure is shown in Algorithm 5.2 for a BW lattice being transmitted on an AWGN channel.

5.4 Barnes-Wall lattices for the two-user symmetric interference channel

5.4.1 Preliminary idea

Here we show with simple examples how we can mimic the Jafar scheme to work with BW lattices. Again, the codewords are expressed with C_i for user 1 and D_i for user 2, with $i = 0$ for the lowest RM code and increasing up to the highest level represented by $\mathbb{Z}^{2^{m+1}}$. In a later section we extend this work for a K -user symmetric interference channel.

We can think of an interference channel problem as in (5.1) where each user transmits a point in the same BW lattice. Let us consider an example using $\Lambda_{16} = \Lambda(0, 3) = 4\mathbb{Z}^{16} + 2\text{RM}(3, 4) + \text{RM}(1, 4)$. Considering only two users, each transmitted signal is given

by

$$\mathbf{x}_1 = 4\mathbf{C}_2 + 2\mathbf{C}_1 + \mathbf{C}_0 \quad (5.24)$$

$$\mathbf{x}_2 = 4\mathbf{D}_2 + 2\mathbf{D}_1 + \mathbf{D}_0, \quad (5.25)$$

where $\mathbf{C}_0, \mathbf{D}_0 \in \text{RM}(1, 4)$, $\mathbf{C}_1, \mathbf{D}_1 \in \text{RM}(3, 4)$ and $\mathbf{C}_2, \mathbf{D}_2 \in \mathbb{Z}^{16}$. Let us mimic the idea of Jafar for a case where $g = 2^{-1}$. Note that in order to simplify the problem, for the rest of the chapter we assume that g is of the form 2^l where l is a negative or positive integer. Thus, g is a power of 2. Then

$$\mathbf{y}_1 = 4\mathbf{C}_2 + 2(\mathbf{C}_1 + \mathbf{D}_2) + (\mathbf{C}_0 + \mathbf{D}_1) + 2^{-1}\mathbf{D}_0 + \mathbf{z}_1. \quad (5.26)$$

In order to decode, we need some properties like before. Otherwise, we would have some interference problems. If we assume $\mathbf{C}_1 = \mathbf{D}_1 = \mathbf{0}_{16}$ we have:

$$\mathbf{y}_1 = 4\mathbf{C}_2 + 2\mathbf{D}_2 + \mathbf{C}_0 + 2^{-1}\mathbf{D}_0 + \mathbf{z}_1. \quad (5.27)$$

To keep the problem simple, we are considering that g is a power of 2. Therefore, we also have some limitations on the channels. Also, for our analysis we initially consider only two users. The reason is that, even if the schemes can work with K users, the number of users the system can accept depends on Q . This comes from [5] since to define a codebook C_i and to avoid carryovers from one level to the other, there is a relationship with Q . In that case, to prove the DoF for each type of interference Q must be very big, and in particular $Q \gg K$. So for a given set of variables, including a given channel gain, there is a given number of users the system can allocate. For the clarity and the purposes of this document, we first consider only a two-user interference channel to show that we can mimic the Jafar schemes in higher dimensions and obtain better performance, and later it is extended to a higher number of users.

We try to mimic as closely as possible the construction of Jafar by finding a lattice in a higher dimension with the same or similar structure. In the following we will see some examples for the very strong, weak and strong interference. Since the case of moderately

weak interference is similar to the strong interference case, we have omitted it.

For the very strong interference case the highest level of the Jafar symbol is given by Q^{N-1} . In order to make this easier define $Q^{N-1} = 2^\gamma$, where from (5.22) $\gamma = m/2$ if m is even or from (5.23) $\gamma = (m+1)/2$ if m is odd (note that $r = 0$). For the weak interference case we define $Q^{2M+N-1} = 2^\gamma$, and for the strong interference case $Q^{2N-M-1} = 2^\gamma$. Let us look over some examples:

- **Very strong interference:** Consider $Q = 4$, $N = 2$, $M = 2$. For Jafar we have $x_1 = 4C_1 + C_0$. Then we select a lattice with a similar structure but in higher dimensions. In that case we can see that the lattice $\Lambda(0, 3)$ is a lattice we can use. Since $\Lambda_{16} = \Lambda(0, 3) = 4\mathbb{Z}^{16} + 2\text{RM}(3, 4) + \text{RM}(1, 4)$ we can say $\mathbf{x}_1 = 4\mathbf{C}_2 + 2\mathbf{C}_1 + \mathbf{C}_0$, where $\mathbf{C}_1 = 0_{16}$ and $\mathbf{C}_2 \in \mathbb{Z}^{16}/2\mathbb{Z}^{16}$. The same is applied at transmitter 2: $\mathbf{x}_2 = 4\mathbf{D}_2 + 2\mathbf{D}_1 + \mathbf{D}_0$, where $\mathbf{D}_1 = 0_{16}$ and $\mathbf{D}_2 \in \mathbb{Z}^{16}/2\mathbb{Z}^{16}$. Then with the channel gain given by $g = 16$, at receiver 1 we have

$$\mathbf{y}_1 = 64\mathbf{D}_2 + 16\mathbf{D}_0 + 4\mathbf{C}_2 + \mathbf{C}_0 + \mathbf{z}_1. \quad (5.28)$$

- **Weak interference:** Consider $Q = 4$, $N = 1$, $M = 1$. Then for Jafar we have: $x_1 = 16C_2 + C_0$. A lattice with a similar structure is found by saying $\gamma = \log_2(16)$. Then $\Lambda(0, 8)$ satisfies what we need since $\Lambda(0, 8) = 16\mathbb{Z}^{512} + 8\text{RM}(7, 9) + 4\text{RM}(5, 9) + 2\text{RM}(3, 9) + \text{RM}(1, 9)$. Then $\mathbf{x}_1 = 16\mathbf{C}_4 + \mathbf{C}_0$, where $\mathbf{C}_3 = \mathbf{C}_2 = \mathbf{C}_1 = 0_{512}$ and $\mathbf{C}_4 \in \mathbb{Z}^{512}/2\mathbb{Z}^{512}$. Using the same idea for user 2, $\mathbf{x}_2 = 16\mathbf{D}_4 + \mathbf{D}_0$. With the channel gain given by $g = 4^{-1}$, at receiver 1 we have

$$\mathbf{y}_1 = 16\mathbf{C}_4 + 4\mathbf{D}_4 + \mathbf{C}_0 + 2^{-2}\mathbf{D}_0 + \mathbf{z}_1. \quad (5.29)$$

- **Strong interference:** Consider $Q = 8$, $N = 2$, $M = 1$. For Jafar we have: $x_1 = 64C_2 + 8C_1 + C_0$, where Jafar considers another constraint where $C_2 = C_0$. This is necessary for decoding. A lattice with a similar structure is given by $\Lambda(0, 11) = 64\mathbb{Z}^{212} + 32\text{RM}(11, 12) + 16\text{RM}(9, 12) + 8\text{RM}(7, 12) + 4\text{RM}(5, 12) + 2\text{RM}(3, 12) + \text{RM}(1, 12) = 64\mathbf{C}_6 + 32\mathbf{C}_5 + 16\mathbf{C}_4 + 8\mathbf{C}_3 + 4\mathbf{C}_2 + 2\mathbf{C}_1 + \mathbf{C}_0$. Then $\mathbf{x}_1 = 64\mathbf{C}_6 + 8\mathbf{C}_3 + \mathbf{C}_0$,

where $\mathbf{C}_5 = \mathbf{C}_4 = \mathbf{C}_2 = \mathbf{C}_1 = 0_{4096}$. Similarly to Jafar we consider $\mathbf{C}_6 = \mathbf{C}_0$. Then $\mathbf{x}_1 = 64\mathbf{C}_0 + 8\mathbf{C}_3 + \mathbf{C}_0$. In the same way $\mathbf{x}_2 = 64\mathbf{D}_0 + 8\mathbf{D}_3 + \mathbf{D}_0$. With the channel gain given by $g = 8$, at receiver 1 we have

$$\mathbf{y}_1 = 512\mathbf{D}_0 + 64(\mathbf{D}_3 + \mathbf{C}_0) + 8(\mathbf{D}_0 + \mathbf{C}_3) + \mathbf{C}_0 + \mathbf{z}_1. \quad (5.30)$$

5.4.2 Decoding

Again we use the low-complexity BDD algorithm for BW lattices proposed by Micciancio in [26, Algorithm 2]. The decoding procedure is the same as the one shown in Algorithm 5.2 where we define $\mathbf{s} = \mathbf{y}_1$ for very strong and strong interference, and $\mathbf{s} = Q^M \mathbf{y}_1$ for moderately weak and weak interference.

Using Algorithm 5.2, all levels have been estimated and we can obtain an estimated transmitted version of \mathbf{x}_1 .

For the case of strong and moderately weak interference using BW lattices we also consider Algorithm 5.2, with a small variation explained next.

To decode we do something slightly different to before, because there are levels that overlap. From (5.10) we consider that if $\mathbf{x}_1 \in \Lambda$ and $\mathbf{x}_2 \in \Lambda$, then $\mathbf{x}_1 + g\mathbf{x}_2$ is also in Λ . Therefore, we first decode the received signal to a point in Λ to eliminate the noise, with a BDD decoder like the one of Algorithm 5.2.

We then realize that in the levels in which the interference overlaps the signal we have

$$\text{RM}(j, m+1) + \text{RM}(i, m+1), \quad (5.31)$$

where $i > j$. Then [58]

$$\text{RM}(j, m+1) + \text{RM}(i, m+1) \subset \text{RM}(i, m+1) + \text{RM}(i, m+1) \quad (5.32)$$

$$= 2\text{RM}(i+2, m+1) + \text{RM}(i, m+1). \quad (5.33)$$

Note that the separation between the levels is big due to the construction of the

scheme (and the selection of Q). Thus, there is no overlap (carryovers) to other levels.

From the examples shown in section 5.4.1 we have:

- Very strong interference: From (5.28) we have

$$\mathbf{y}_1 = 64\mathbf{D}_2 + 16\mathbf{D}_0 + 4\mathbf{C}_2 + \mathbf{C}_0 + \mathbf{z}_1. \quad (5.34)$$

From $\mathbf{s} = \mathbf{y}_1$ the BDD computes the estimated transmitted RM code from RM(1, 4), to obtain $\hat{\mathbf{C}}_0$. Then, $\hat{\mathbf{C}}_2 = ((\mathbf{s} - \hat{\mathbf{C}}_0)/4) \bmod 2$. The estimated transmitted symbol from user 1 is $\hat{\mathbf{x}}_1 = 4\hat{\mathbf{C}}_2 + \hat{\mathbf{C}}_0$.

- Weak interference: From (5.29) we have

$$\mathbf{y}_1 = 16\mathbf{C}_4 + 4\mathbf{D}_4 + \mathbf{C}_0 + 2^{-2}\mathbf{D}_0 + \mathbf{z}_1. \quad (5.35)$$

From $\mathbf{s} = 4\mathbf{y}_1$ the BDD computes the estimated transmitted RM code from RM(1, 9) to obtain $\hat{\mathbf{D}}_0$. Then $\mathbf{s} = (\mathbf{s} - \hat{\mathbf{D}}_0)/4$ and proceeds to estimate the transmitted RM code from RM(1, 9) to obtain $\hat{\mathbf{C}}_0$. Then to obtain $\hat{\mathbf{D}}_4$ we say $\mathbf{s} = (\mathbf{s} - \hat{\mathbf{C}}_0)/4$ and $\hat{\mathbf{D}}_4 = \lfloor \mathbf{s} \rfloor \bmod 2$. Finally, we say $\mathbf{s} = (\mathbf{s} - \hat{\mathbf{D}}_4)/4$ and $\hat{\mathbf{C}}_4 = \lfloor \mathbf{s} \rfloor \bmod 2$. The estimated transmitted symbol from user 1 is $\hat{\mathbf{x}}_1 = 16\hat{\mathbf{C}}_4 + \hat{\mathbf{C}}_0$.

- Strong interference: From (5.30) we have

$$\mathbf{y}_1 = 512\mathbf{D}_0 + 64(\mathbf{D}_3 + \mathbf{C}_0) + 8(\mathbf{D}_0 + \mathbf{C}_3) + \mathbf{C}_0 + \mathbf{z}_1. \quad (5.36)$$

We first decode to a point in $\Lambda(0, 11)$ where

$$\Lambda(0, 11) = 64\mathbf{F}_6 + 32\mathbf{F}_5 + 16\mathbf{F}_4 + 8\mathbf{F}_3 + 4\mathbf{F}_2 + 2\mathbf{F}_1 + \mathbf{F}_0 \quad (5.37)$$

We use the BDD and the RM decoder for each \mathbf{F}_i to obtain an estimated noiseless version of \mathbf{y}_1 given by

$$\hat{\mathbf{y}}_1 = 64\hat{\mathbf{F}}_6 + 32\hat{\mathbf{F}}_5 + 16\hat{\mathbf{F}}_4 + 8\hat{\mathbf{F}}_3 + 4\hat{\mathbf{F}}_2 + 2\hat{\mathbf{F}}_1 + \hat{\mathbf{F}}_0 \quad (5.38)$$

Note that

$$\mathbf{D}_0 + \mathbf{C}_3 \in \text{RM}(1, 12) + \text{RM}(7, 12) \subset \text{RM}(7, 12) + \text{RM}(7, 12) \quad (5.39)$$

$$= 2\text{RM}(9, 12) + \text{RM}(7, 12) = 2\mathbf{A} + \mathbf{B} \quad (5.40)$$

and then $8(\mathbf{D}_0 + \mathbf{C}_3) = 16\mathbf{A} + 8\mathbf{B}$. From (5.37) we can match

$$\mathbf{F}_0 \rightarrow \mathbf{C}_0 \quad (5.41)$$

$$\mathbf{F}_3 \rightarrow \mathbf{B} \quad (5.42)$$

$$\mathbf{F}_4 \rightarrow \mathbf{A} \quad (5.43)$$

Similarly

$$\mathbf{D}_3 + \mathbf{C}_0 \subset 2\text{RM}(9, 12) + \text{RM}(7, 12) = 2\mathbf{G} + \mathbf{H}, \quad (5.44)$$

Then $64(\mathbf{D}_3 + \mathbf{C}_0) = 128\mathbf{G} + 64\mathbf{H}$. Finally, we know that $\mathbf{D}_0 \in \text{RM}(1, 12)$.

We can see that the (5.30) transforms to

$$\mathbf{y}_{1, \text{noiseless}} = 512\mathbf{D}_0 + 128\mathbf{G} + 64\mathbf{H} + 16\mathbf{A} + 8\mathbf{B} + \mathbf{C}_0. \quad (5.45)$$

Then from (5.37) we have

$$\mathbf{F}_6 \rightarrow 8\mathbf{D}_0 + 2\mathbf{G} + \mathbf{H} \quad (5.46)$$

In the last level, given by 64 in (5.37) we have a sum of codewords. Originally, $512\mathbf{D}_0 + 64(\mathbf{D}_3 + \mathbf{C}_0) \in 512\text{RM}(1, 12) + 64(\text{RM}(9, 12) + \text{RM}(7, 12))$. But since we have to decode each of these RM codes using the BDD, we need them to be nested. Therefore we can actually say that $\mathbf{D}_0 \in \text{RM}(11, 12)$. That way, we have $512\text{RM}(11, 12) + 128\text{RM}(9, 12) + 64\text{RM}(7, 12)$.

Equations (5.41), (5.42) and (5.43) can then be easily solved using the BDD with the RM decoders. For (5.46) we need to solve $64\text{RM}(7, 12)$, first to decode the next

one 128RM(9, 12) and finally 512RM(11, 12) simply using the BDD again.

With this we obtain \mathbf{D}_0 , and we can subtract it from $2\hat{\mathbf{B}} + \hat{\mathbf{A}}$, which is the estimated value of the sum given by $(\mathbf{D}_0 + \mathbf{C}_3)$. Thus, we obtain $\hat{\mathbf{C}}_3$, and we finally have $\hat{\mathbf{x}}_1 = 64\hat{\mathbf{C}}_0 + 8\hat{\mathbf{C}}_3 + \hat{\mathbf{C}}_0$.

5.4.3 General proposed scheme

In this section we explain the general design of a BW lattice given the parameters Q , M , N and α to mimic the Jafar schemes for each type of interference. We start by identifying which BW lattice can be used given those variables, and go on to explain how this lattice can be adapted to mimic Jafar's encoding and decoding.

5.4.4 Selecting the lattice that mimics the Jafar one-dimensional message

In this section we explain how to find the appropriate BW lattice given Q , M , N and α while leaving zeros, according to Jafar's encoding scheme.

Very strong interference

For the very strong interference, Jafar users constructs its symbol by

$$x_1 = Q^{N-1}C_{N-1} + \cdots + QC_1 + C_0 \quad (5.47)$$

for a given Q and N .

- Take $Q^{N-1} = 2^{\frac{m+1}{2}}$

$$m = (2 \log_2 Q^{N-1}) - 1, \quad (5.48)$$

where we are working with the case of m odd lattices, but we could easily work with m even². This means this is a lattice of dimension $2^{m+1} = 2^{(2 \log_2 Q^{N-1}) - 1}$. Here $M \geq N$.

²Working with odd lattices allow us to choose a slightly smaller dimensional lattice, which is useful for simulation purposes.

- Now we know which lattice we are working with, but we need to leave zeros in order to encode the same levels as Jafar. Recall (5.23) where the lattice is expressed as $m - r$ odd:

$$\begin{aligned} \Lambda(r, m) &= 2^{\frac{m-r+1}{2}} \mathbb{Z}^{2^{m+1}} \\ &+ \sum_{\substack{r+1 \leq r' \leq m \\ m-r' \text{ even}}} 2^{(r'-r-1)/2} \text{RM}(r', m+1) \end{aligned} \quad (5.49)$$

where $r = 0$. Disregarding the first term ($2^{\frac{m-r+1}{2}} \mathbb{Z}^{2^N}$), we can say that we have a sum of the form $\sum_j 2^{\frac{j-1}{2}} \text{RM}(j, m+1)$. Also, considering that the structure of Jafar's symbol for the very strong interference is very simple, we can say

$$2^{\frac{j-1}{2}} = Q^{N-q} \text{ for all values of } q = \{2, \dots, N\} \quad (5.50)$$

we have

$$j = (2 \log_2 Q^{N-q}) + 1 \text{ for } q = \{2, \dots, N\} \quad (5.51)$$

Finally,

$$\mathbf{x}_i \in 2^{\frac{m+1}{2}} \mathbb{Z}^{2^{m+1}} + \sum_j 2^{\frac{j-1}{2}} \text{RM}(j, m+1), \quad (5.52)$$

where m comes from (5.48) and j comes from (5.51).

Note that, we can take a smaller dimensional lattice if we choose $Q^{N-q} = 2^{\frac{m+1}{2}}$ for some $q \in \{1, \dots, N\}$ and $2^{\frac{j-1}{2}} = Q^{N-\bar{q}}$ where $\bar{q} = \{q+1, \dots, N\}$.

Example:

Take $N = 2$, $M = 4$ and $Q = 4$. Then we have $Q^{N-1} = 2^{\frac{m+1}{2}}$ and $m = 3$. The dimension is given by $2^{m+1} = 16$, $q = \{2\}$, and $j = \{1\}$. Thus:

$$\mathbf{x}_i \in 2^{\frac{m+1}{2}} \mathbb{Z}^{2^{m+1}} + \sum_j 2^{\frac{j-1}{2}} \text{RM}(j, m+1) = 4\mathbb{Z}^{16} + \text{RM}(1, 4) \quad (5.53)$$

Strong interference

The symbol given by Jafar is constructed as

$$x_1 = Q^{2N-M-1}C_{2N-M-1} + \sum_{p=2}^{N-M} Q^{2N-M-p}C_{2N-M-p} + \sum_{q=1}^N Q^{N-q}C_{N-q} \quad (5.54)$$

- Take $Q^{2N-M-1} = 2^{\frac{m+1}{2}}$, where again we are working with the case of m odd lattices.

Then

$$m = (2 \log_2 Q^{2N-M-1}) - 1. \quad (5.55)$$

This means this is a lattice of dimension $2^{m+1} = 2^{(2 \log_2 Q^{2N-M-1})-1}$. The dimension is normally quite big. This is because Q and M are big.

- Now we need to leave zeros to choose the same levels as Jafar. Similarly to the previous case we say

$$Q^{2N-M-p} = 2^{\frac{j_1-1}{2}}$$

$$j_1 = (2 \log_2 Q^{2N-M-p}) + 1 \quad (5.56)$$

where $p = \{2, \dots, N - M\}$. And for the second half we have

$$Q^{N-q} = 2^{\frac{j_2-1}{2}}$$

$$j_2 = (2 \log_2 Q^{N-q}) + 1, \quad (5.57)$$

where $q = \{1 \dots, N\}$.

Finally, the symbol transmitted from user i is given by

$$\mathbf{x}_i \in 2^{\frac{m+1}{2}}\mathbb{Z}^{2^{m+1}} + \sum_{j_1} 2^{\frac{j_1-1}{2}}\text{RM}(j_1, m+1) + \sum_{j_2} 2^{\frac{j_2-1}{2}}\text{RM}(j_2, m+1), \quad (5.58)$$

where m comes from (5.55), j_1 comes from (5.56) and j_2 comes from (5.57).

There is an extra constraint imposed by Jafar to enable decoding despite of the overlapping on some levels at the receivers. This is given by

$$C_{2N-M-i} = C_{i-1}, \quad (5.59)$$

for $i = \{1, \dots, N - M\}$.

To adapt condition (5.59) by Jafar to BW lattices we say

$$\mathbb{Z}^{2^{m+1}} = \text{RM}(1, m + 1) \quad (5.60)$$

$$\text{RM}(2 \log_2 Q^{2N-M-\tilde{p}} + 1, m + 1) = \text{RM}(2 \log_2 Q^{\tilde{p}-1} + 1, m + 1), \quad (5.61)$$

where $\tilde{p} = \{2, \dots, N - M\}$

Example:

Take $N = 4$, $M = 2$ and $Q = 8$. From that, Jafar builds the symbol as

$$x_{\text{Jafar}} = Q^5 C_5 + Q^4 C_4 + Q^3 C_3 + Q^2 C_2 + Q C_1 + C_0$$

Then, $m = 29$, the dimension of the lattice is 2^{30} . Since $p = \{2\}$, we only have $j_1 = 25$, and $q = \{1, 2, 3, 4\}$, then $j_2 = \{19, 13, 7, 1\}$. Thus, the BW lattice to choose is $\Lambda(0, 29)$, and more precisely

$$\begin{aligned} \mathbf{x}_i \in & 2^{15} \mathbb{Z}^{2^{30}} + 2^{12} \text{RM}(25, 30) \\ & + 2^9 \text{RM}(19, 30) + 2^6 \text{RM}(13, 30) + 2^3 \text{RM}(7, 30) + \text{RM}(1, 30). \end{aligned} \quad (5.62)$$

Moderately weak interference

The Jafar symbol is built as

$$\begin{aligned}
x_1 = & Q^{2N+3M-1}C_{2N+3M-1} + \sum_{p=2}^N Q^{2N+3M-p}C_{2N+3M-p} + \sum_{q=1}^M Q^{3M+N-q}C_{3M+N-q} \\
& + \sum_{t=1}^N Q^{2M+N-t}C_{2M+N-t} + \sum_{r=1}^M Q^{M-r}C_{M-r}
\end{aligned} \tag{5.63}$$

To find the *equivalent* BW lattice let

$$\begin{aligned}
Q^{2N+3M-1} &= 2^{\frac{m+1}{2}} \\
m &= (2 \log_2 Q^{2N+3M-1}) - 1,
\end{aligned} \tag{5.64}$$

and

$$j_1 = (2 \log_2 Q^{2N+3M-p}) + 1, \text{ for } p = \{2, \dots, N\} \tag{5.65}$$

$$j_2 = (2 \log_2 Q^{3M+N-q}) + 1, \text{ for } q = \{1, \dots, M\} \tag{5.66}$$

$$j_3 = (2 \log_2 Q^{2M+N-t}) + 1, \text{ for } t = \{1, \dots, N\} \tag{5.67}$$

$$j_4 = (2 \log_2 Q^{M-r}) + 1, \text{ for } r = \{1, \dots, M\} \tag{5.68}$$

The transmitted signal is given by

$$\mathbf{x}_1 \in 2^{\frac{m+1}{2}} \mathbb{Z}^{2^{m+1}} + \sum_{j_1} 2^{\frac{j_1-1}{2}} \text{RM}(j_1, m+1) \tag{5.69}$$

$$+ \sum_{j_2} 2^{\frac{j_2-1}{2}} \text{RM}(j_2, m+1) + \sum_{j_3} 2^{\frac{j_3-1}{2}} \text{RM}(j_3, m+1) \tag{5.70}$$

$$+ \sum_{j_4} 2^{\frac{j_4-1}{2}} \text{RM}(j_4, m+1) \tag{5.71}$$

where m comes from (5.64), j_1 from (5.65), j_2 from (5.66), j_3 from (5.67) and j_4 from (5.68).

As before, there is another constraint given by

$$C_{2N+3M-i} = C_{2M+i-1}, \quad (5.72)$$

for $i = \{1, \dots, N\}$.

Condition (5.72) can be adapted as

$$\mathbb{Z}^{2^{m+1}} = \text{RM}(2 \log_2 Q^{2^M} + 1, m + 1) \quad (5.73)$$

$$\text{RM}(2 \log_2 Q^{2N+3M-\tilde{p}} + 1, m + 1) = \text{RM}(2 \log_2 Q^{2N+\tilde{p}-1} + 1, m + 1) \quad (5.74)$$

where $\tilde{p} = \{2, \dots, N\}$

Example:

Take $N = 2$, $M = 1$ and $Q = 8$. We have $m = 35$, $j_1 = \{31\}$, $j_2 = \{25\}$, $j_3 = \{19, 13\}$, $j_4 = \{1\}$. Therefore, the transmitted symbol using BW lattices is given by:

$$\mathbf{x}_i \in 2^{18} \mathbb{Z}^{2^{36}} + 2^{15} \text{RM}(31, 36) + 2^{12} \text{RM}(25, 36) \quad (5.75)$$

$$+ 2^9 \text{RM}(19, 36) + 2^6 \text{RM}(13, 36) + \text{RM}(1, 36) \quad (5.76)$$

Weak interference

The Jafar symbol is built as

$$x_1 = Q^{2M+N-1} C_{2M+N-1} + \sum_{p=2}^N Q^{2M+N-p} C_{2M+N-p} + \sum_{q=1}^M Q^{M-q} C_{M-q} \quad (5.77)$$

To find the *equivalent* BW lattice take

$$Q^{2M+N-1} = 2^{\frac{m+1}{2}}$$

$$m = (2 \log_2 Q^{2M+N-1}) - 1, \quad (5.78)$$

and

$$j_1 = (2 \log_2 Q^{2M+N-p}) + 1, \text{ for } p = \{2, \dots, N\} \quad (5.79)$$

$$j_2 = (2 \log_2 Q^{M-q}) + 1, \text{ for } q = \{1, \dots, M\} \quad (5.80)$$

Thus, the transmitted signal is given by

$$\mathbf{x}_i \in 2^{\frac{m+1}{2}} \mathbb{Z}^{2^{m+1}} + \sum_{j_1} 2^{\frac{j_1-1}{2}} \text{RM}(j_1, m+1) \quad (5.81)$$

$$+ \sum_{j_2} 2^{\frac{j_2-1}{2}} \text{RM}(j_2, m+1) \quad (5.82)$$

where m comes from (5.78), j_1 from (5.79) and j_2 from (5.80).

Example:

Take $N = 2$, $M = 4$ and $Q = 4$. We have $m = 35$, $j_1 = \{33\}$, $j_2 = \{13, 9, 5, 1\}$. Therefore, the transmitted symbol using BW lattices is given by:

$$\mathbf{x}_i \in 2^{18} \mathbb{Z}^{2^{19}} + 2^{16} \text{RM}(33, 36) + 2^6 \text{RM}(13, 36) \quad (5.83)$$

$$+ 2^4 \text{RM}(9, 36) + 2^2 \text{RM}(5, 36) + \text{RM}(1, 36) \quad (5.84)$$

5.4.5 Simulations

In this section we show some simulations that compare the Jafar schemes and the proposed schemes based on BW lattices. The average symbol energy is defined as in [5] per type of interference and we consider the following: for the very strong interference case $\mathbb{E}([x_i]^2) < Q^{2N}$, for the weak interference case $\mathbb{E}([x_i]^2) < (Q^{N+2M})^2$ and for the strong interference case $\mathbb{E}([x_i]^2) < (Q^{2N-M})^2$. We assume the same for the BW lattices since we consider the energy per dimension.

We observe, as expected, that when higher dimensional lattices are used, the asymptotic performance is improved. However, the trick is to find the correct lattice to mimic the code construction given by Jafar for any channel and any type of interference. Note that, due to the computation complexity we are not able to generate all the cases

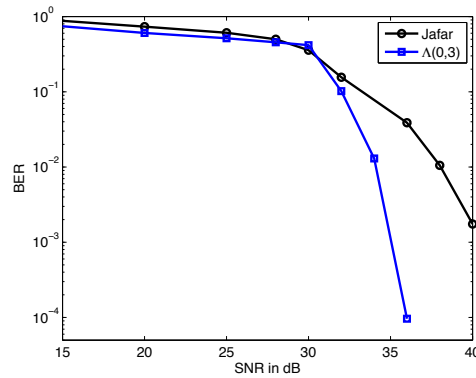


Figure 5.1: Error rate for very strong interference, when $Q = 4$, $M = 2$, $N = 2$

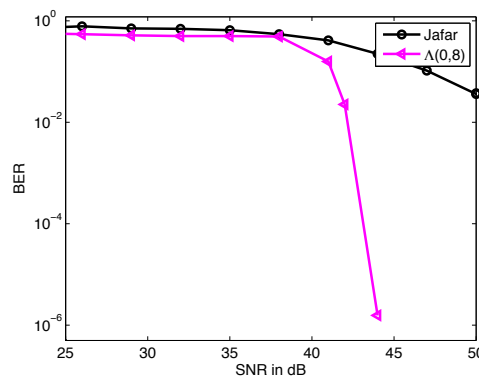


Figure 5.2: Error rate for weak interference, when $Q = 4$, $M = 1$, $N = 1$

and therefore we only compute the case for the examples shown for very strong, weak and strong interference. However, since the scheme is similar for all cases we can project the same results for all types of interference.

5.5 Barnes-Wall lattices for the K -user symmetric interference channel

The above is valid for two users, but is extendible to $K > 2$. We first begin with an example. The Jafar weak interference example seen previously when $Q = 4$, implies that $C_i = \{1, \dots, Q-2\} = \{1, 2\}$. Since C_i does not depend on the number of users, it should be possible to allocate K users. But we can see this is not true. If the codes transmitted

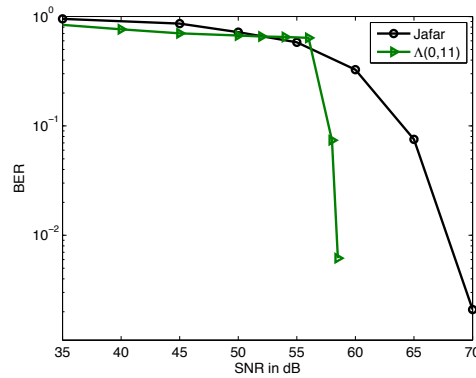


Figure 5.3: Error rate for strong interference, when $Q = 8$, $M = 1$, $N = 2$

from transmitter 3 are expressed as E_i , at receiver 1 we have

$$y_1 = 16C_2 + 4(D_2 + E_2) + C_0 + 2^{-2}(D_0 + E_0) + z_1. \quad (5.85)$$

Take $D_2 + E_2$ and consider the case where $D_2 = E_2 = 2$, then we have a carryover to the next level. To overcome this problem for this specific example, consider that the codewords are still defined in $\{1, 2\}$ but $Q = 8$. In that case there are no carryovers and we can proceed.

Thus, take $Q = 8$, $N = 1$ and $M = 1$ as before and let us select the corresponding BW lattice generated signals as

$$\mathbf{x}_1 = 64\mathbf{C}_6 + \mathbf{C}_0 \quad (5.86)$$

$$\mathbf{x}_2 = 64\mathbf{D}_6 + \mathbf{D}_0 \quad (5.87)$$

$$\mathbf{x}_3 = 64\mathbf{E}_6 + \mathbf{E}_0, \quad (5.88)$$

where $\mathbf{x}_1, \mathbf{x}_2, \mathbf{x}_3 \in \Lambda(0, 11)$. At receiver 1 we have

$$\mathbf{y}_1 = 64\mathbf{C}_6 + 8(\mathbf{D}_6 + \mathbf{E}_6) + \mathbf{C}_0 + 8^{-1}(\mathbf{D}_0 + \mathbf{E}_0) + \mathbf{z}_1. \quad (5.89)$$

To decode let

$$\bar{\mathbf{y}}_1 = Q\mathbf{y}_1 = 512\mathbf{C}_6 + 64(\mathbf{D}_6 + \mathbf{E}_6) + 8\mathbf{C}_0 + (\mathbf{D}_0 + \mathbf{E}_0) + 8\mathbf{z}_1, \quad (5.90)$$

and decode to a point in the lattice $\Lambda(0, 11)$

$$\Lambda(0, 11) = 64\mathbb{Z}^{2^{12}} + 32\mathbf{RM}(11, 12) + 16\mathbf{RM}(9, 12) + 8\mathbf{RM}(7, 12) \quad (5.91)$$

$$+ 4\mathbf{RM}(5, 12) + 2\mathbf{RM}(3, 12) + \mathbf{RM}(1, 12)$$

$$= 64\mathbf{F}_6 + 32\mathbf{F}_5 + 16\mathbf{F}_4 + 8\mathbf{F}_3 + 4\mathbf{F}_2 + 2\mathbf{F}_1 + \mathbf{F}_0 \quad (5.92)$$

We obtain

$$\hat{\mathbf{y}}_1 = 64\hat{\mathbf{F}}_6 + 32\hat{\mathbf{F}}_5 + 16\hat{\mathbf{F}}_4 + 8\hat{\mathbf{F}}_3 + 4\hat{\mathbf{F}}_2 + 2\hat{\mathbf{F}}_1 + \hat{\mathbf{F}}_0 \quad (5.93)$$

Observing equation (5.90) take

$$\begin{aligned} (\mathbf{D}_0 + \mathbf{E}_0) &\in \mathbf{RM}(1, 12) + \mathbf{RM}(1, 12) \in 2\mathbf{RM}(3, 12) + \mathbf{RM}(1, 12) \\ &= 2\mathbf{A} + \mathbf{B} \end{aligned}$$

Then

$$\hat{\mathbf{F}}_0 = \hat{\mathbf{B}} \quad (5.94)$$

$$\hat{\mathbf{F}}_1 = \hat{\mathbf{A}} \quad (5.95)$$

$$\hat{\mathbf{F}}_3 = \hat{\mathbf{C}}_0 \quad (5.96)$$

Thus we have

$$512\mathbf{C}_6 + 64(\mathbf{D}_6 + \mathbf{E}_6) \in 64\mathbb{Z}^{2^{12}} \quad (5.97)$$

Therefore, $8\mathbf{C}_6 + (\mathbf{D}_6 + \mathbf{E}_6)$ are all estimated to $\hat{\mathbf{F}}_6$. To decode this part, since none of these codewords are in a RM code, we decode the sum of $\mathbf{D}_6 + \mathbf{E}_6$ by saying $\hat{\mathbf{F}}_{6n} = \hat{\mathbf{F}}_6 \bmod 8$, then decode $\hat{\mathbf{C}}_6 = \frac{\hat{\mathbf{F}}_6 - \hat{\mathbf{F}}_{6n}}{8}$.

Fig. 5.4 shows the simulation of this system. We can see that asymptotically, BW lattices have better performance than the one-dimensional Jafar scheme.

Again due to the computation complexity in this section we have worked only with

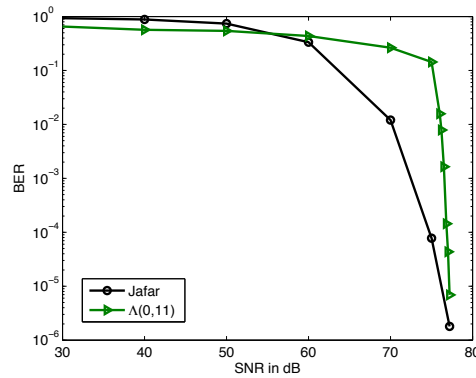


Figure 5.4: Error rate for weak interference, when $Q = 8$, $M = 1$, $N = 1$ and $K = 3$

one example in weak interference. However, again since the scheme is similar for all cases we can deduce that the same result is valid for all types of interference. On the other hand, the purpose of this example is simply to illustrate the extension to a higher number of user.

We can generalize the encoding and decoding with $K > 2$ with the following rule. Given \tilde{K} overlapping codewords in a level, take the one with the biggest RM order. Let us call this $\text{RM}(i, m + 1)$, and say that the sum of codewords is contained in

$$\sum_{j=1}^K 2^{j-1} \text{RM}(i + 2^{j-1}, m + 1). \quad (5.98)$$

With this we can see that for the strong and moderately weak interference scenarios, where at some levels interference and desired signal overlap, we can allocate up to $\tilde{K} = K < \log_2(Q) + 1$ users with BW lattices. On the other hand, for the weak interference scenario where the interference and the desired signal do not overlap in each level, we can allocate $\tilde{K} + 1 = K < \log_2(Q) + 2$ users with BW lattices. Naturally, for the very strong interference case K can take any number.

5.6 Conclusions

In this chapter, we have shown how the work of Jafar eliminates the interference by building a clever scheme for each type of interference. Inspired by this, we used BW

lattices due to their resemblance as multilevel codes, and because of the extension that lattices imply in higher dimensions. We show that with a proper selection of the lattices, we can improve the performance of the schemes proposed by Jafar. Further, we show that for any given values of parameters Q , M and N we can construct symbols with BW lattices, and we can decode them using a multilevel BDD. We have also shown the extension to more than two users is simple, but for both this scheme and the original Jafar scheme, it is restricted to the value of Q . Namely, the number of users that can be allocated depends directly on said parameters. Since we are constructing the signals in the same manner as Jafar we believe the GDoF is still valid for this scheme, but with the benefit of performance improvement given by the BW lattices. The schemes presented are for the symmetric interference channel, for a particular type of channel gain g . If the channel is asymmetric, we cannot guarantee that the schemes will work, unless there is some structure in the channel model. If the indirect channel gains are given by g_{ij} (from transmitter j to receiver i) and they are powers of 2, then the schemes have the potential to be adapted to align and suppress interference as the ones proposed in [5].

Chapter 6

Generalized degrees of freedom of a two-user symmetric interference channel using lattice Gaussian distribution

6.1 Introduction

In this section we analyse the GDoF of the two-user symmetric interference channel using lattices. In [2], Etkin found the GDoF for a two-user symmetric interference channel and the well known GDoF W curve is explained as well as how the GDoF is achieved using Gaussian codes. Since we want to use the potential of lattices to align interference, in this chapter we propose to use lattice codes. We use lattice Gaussian distribution [27] to demonstrate that we can achieve the GDoF for all types of interference.

6.2 Preliminary

The paper by Etkin [2] finds the capacity of the two-user interference channel within one bit of the achievable region found by HK. For the case where the power of the interference is smaller than the power of the desired signal, a range of values is found in which the

HK rate is contained. Normalizing this rate by the capacity of the point-to-point AWGN channel and taking the limit of this ratio when the SNR, $\text{INR} \rightarrow \infty$, they are able to find the GDoF. In order to do this, random Gaussian codes and a simple HK scheme are used. In this section we show their results for noisy, weak and moderately weak interference, and we also show the GDoF for the very strong and strong interference cases. This was briefly discussed in Chapter 2. Here we present it in more detail.

6.2.1 Generalized degrees of freedom with random codes [2]

In [2] and [5] a symmetric interference channel is studied. Consider a two-user interference channel model:

$$y_1 = x_1 + gx_2 + z_1 \quad (6.1)$$

$$y_2 = gx_1 + x_2 + z_2, \quad (6.2)$$

where y_k is the received signal at receiver k ($k = 1, 2$), g is the real indirect channel coefficient, x_k is the signal transmitted by transmitter k , x_j is the interference signal from transmitter j , and z_k is the AWGN with variance σ^2 and zero mean. In [5] the channel is defined as $g = \sqrt{\frac{\text{INR}}{\text{SNR}}}$.

From [2] and as explained in Chapter 2, (2.30) shows the achievable rate of the very simple HK scheme. Two regions are found which are defined by either $\text{SNR}(\text{SNR} + \text{INR}) < \text{INR}^2(\text{INR} + 1)$ or $\text{SNR}(\text{SNR} + \text{INR}) > \text{INR}^2(\text{INR} + 1)$. The rate (2.30) is normalized by the point-to-point capacity of the AWGN channel, to obtain

$$\frac{R_{\text{HK}}}{C_{\text{AWGN}}} \approx \min \left\{ 1 - \frac{1}{2} \frac{\log \text{INR}}{\log \text{SNR}}, \max \left\{ \frac{\log \text{INR}}{\log \text{SNR}}, 1 - \frac{\log \text{INR}}{\log \text{SNR}} \right\} \right\} \quad (6.3)$$

To simplify the expression, the parameter α is defined as $\alpha \triangleq \frac{\log \text{INR}}{\log \text{SNR}}$. Then:

$$\frac{R_{\text{HK}}}{C_{\text{AWGN}}} \approx \min \left\{ 1 - \frac{\alpha}{2}, \max\{\alpha, 1 - \alpha\} \right\} \quad (6.4)$$

Equation (6.4) is important because three regimes can be identified

$$\frac{R_{\text{HK}}}{C_{\text{AWGN}}} = \begin{cases} 1 - \frac{\alpha}{2}, & \text{for } \frac{2}{3} < \alpha < 1 \\ \alpha, & \text{for } \frac{1}{2} < \alpha < \frac{2}{3} \\ 1 - \alpha, & \text{for } 0 < \alpha < \frac{1}{2} \end{cases} \quad (6.5)$$

These regimes are of weak interference with respect to the desired signal. Since the result shown in (6.5) is within one bit of the upper bound found in [2], and using that $\text{SNR}, \text{INR} \rightarrow \infty$, the GDoF is also given by (6.5) and is defined as d_{sym} . For the completeness of the result, they also find the GDoF for the very strong and strong interference cases.

When $\text{INR} \geq \text{SNR}^2 + \text{SNR}$, the interference is said to be very strong. In this case the user can decode the interference before the desired message, and then subtract it from the received signal, to obtain the desired signal at that receiver. The receiver sees then an AWGN channel. Therefore, the symmetric capacity is given by¹

$$C_{\text{sym}} = \log(1 + \text{SNR}) \approx \log(\text{SNR}), \quad (6.6)$$

where we assume $\text{SNR}, \text{INR} \gg 1$, and $\text{INR} \geq \text{SNR}^2$. Then

$$d_{\text{sym}} = 1. \quad (6.7)$$

To find the symmetric capacity of the strong interference channel, the intersection of the capacity regions of the two-user MAC explained in Chapter 2 are considered. In particular, for the MAC we have [2]

$$R_1 + R_2 \leq I(x_1, x_2|y) \quad (6.8)$$

¹Note that in [2] the signals are defined as complex. In this chapter we consider real signals.

Then for the interference channel and assuming $R_1 = R_2$,

$$C_{\text{sym}} = \frac{1}{2} I(x_1, x_2 | y) \quad (6.9)$$

$$\begin{aligned} &= \frac{1}{2} (\mathbf{H}(y) - \mathbf{H}(y | x_1, x_2)) \\ &= \frac{1}{2} (\mathbf{H}(x_1 + g x_2 + z) - \mathbf{H}(z)) \\ &= \frac{1}{2} \log(1 + \text{SNR} + \text{INR}) \end{aligned} \quad (6.10)$$

Since the interference is strong, the following condition is given:

$$\text{SNR} \leq \text{INR} \leq \text{SNR}^2. \quad (6.11)$$

From (6.10) and (6.11) C_{sym} is approximated by [2]

$$C_{\text{sym}} \approx \frac{1}{2} \log(\text{INR}) \quad (6.12)$$

and using that $\text{INR} = \text{SNR}^\alpha$ we have

$$d_{\text{sym}} = \frac{\log(\text{SNR})^{\frac{\alpha}{2}}}{\log(\text{SNR})} = \frac{\alpha}{2} \quad (6.13)$$

With these results, the GDoF is computed for each type of interference, and is given by [2]

$$d_{\text{sym}} = \begin{cases} 1 - \alpha & \text{for } 0 \leq \alpha \leq 1/2 & \text{Noisy;} \\ \alpha & \text{for } 1/2 \leq \alpha \leq 2/3 & \text{Weak;} \\ 1 - \frac{\alpha}{2} & \text{for } 2/3 \leq \alpha < 1 & \text{Moderately Weak;} \\ \frac{\alpha}{2} & \text{for } 1 < \alpha \leq 2 & \text{Strong;} \\ 1 & \text{for } \alpha \geq 2 & \text{Very Strong.} \end{cases}$$

The GDoF for the symmetric interference channel is shown in Fig 6.1.

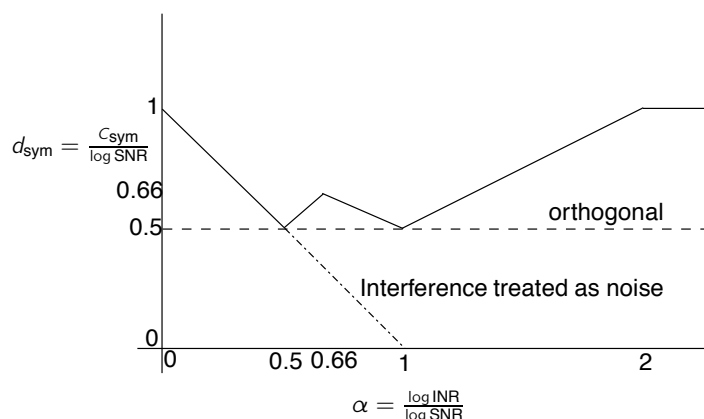


Figure 6.1: W curve (adapted from [2])

6.2.2 Lattice Gaussian Coding

The idea of using lattices seems appealing because of the extension in higher dimensions, and the fact that some lattices are said to be AWGN good if they are good for AWGN channels. Also, there is the potential of using lattice alignment for any number of users in an interference channel. We note that the randomness of the codewords is useful particularly when part of the codeword has to be treated as noise. Also the capacity demonstrated in [2] and the GDoF, are based on Gaussian random codes. Therefore, lattice Gaussian codes [27] are considered, to use randomness within the structure of the lattice.

In this section we show the main results in this area. Namely, we show here the definitions, Lemmas and Theorems from [59], [27], [60] and [61]. In the next section we see how to apply them in order to obtain the GDoF for the symmetric two-user interference channel with lattices.

Definition 1 (AWGN-good [59] [27]). *Let an n -dimensional lattice Λ , $\varepsilon > 0$ and W^n an i.i.d. Gaussian random vector of variance σ_ε^2 with $\mathbb{P}\{W^n \notin \mathcal{V}(\Lambda)\} = \varepsilon$, where $\mathcal{V}(\Lambda)$ is the Voronoi cell of Λ . Consider $\gamma_\Lambda(\sigma_\varepsilon) = \frac{(\mathcal{V}(\Lambda))^{\frac{2}{n}}}{\sigma_\varepsilon^2}$. The lattice Λ is AWGN-good if, $\forall \varepsilon \in (0, 1)$,*

$$\lim_{n \rightarrow \infty} \gamma_{\Lambda^{(n)}}(\sigma_\varepsilon) = 2\pi e \quad (6.14)$$

and if, for a fixed $\gamma_\Lambda(\sigma_\epsilon) > e$, the quantity

$$\mathbb{P}\{W^n \notin \mathcal{V}(\Lambda)\} \quad (6.15)$$

vanishes exponentially fast with n .

Definition 2 (Gaussian distribution [27]). For $\sigma > 0$ and $\mathbf{c} \in \mathbb{R}^n$, the Gaussian distribution of variance σ^2 centered at $\mathbf{c} \in \mathbb{R}^n$ is defined as

$$f_{\sigma,\mathbf{c}}(\mathbf{x}) = \frac{1}{(\sqrt{2\pi}\sigma)^n} e^{-\frac{\|\mathbf{x}-\mathbf{c}\|^2}{2\sigma^2}}, \quad (6.16)$$

for all $\mathbf{x} \in \mathbb{R}^n$. For convenience, $f_\sigma(\mathbf{x}) = f_{\sigma,0}(\mathbf{x})$.

Definition 3 (Discrete Gaussian distribution [27]). The discrete Gaussian distribution over Λ centered at $\mathbf{c} \in \mathbb{R}^n$ is defined as:

$$D_{\Lambda,\sigma,\mathbf{c}}(\lambda) = \frac{f_{\sigma,\mathbf{c}}(\lambda)}{f_{\sigma,\mathbf{c}}(\Lambda)} \quad \forall \lambda \in \Lambda, \quad (6.17)$$

where $f_{\sigma,\mathbf{c}}(\Lambda) \triangleq \sum_{\lambda \in \Lambda} f_{\sigma,\mathbf{c}}(\lambda)$, and again for convenience, $D_{\Lambda,\sigma} = D_{\Lambda,\sigma,0}$.

Definition 4 (Discrete Gaussian distribution over a coset [27]). The discrete Gaussian distribution over a coset of Λ is defined as:

$$D_{\Lambda-\mathbf{c},\sigma}(\lambda - \mathbf{c}) = \frac{f_\sigma(\lambda - \mathbf{c})}{f_{\sigma,\mathbf{c}}(\Lambda)} \quad \forall \lambda \in \Lambda. \quad (6.18)$$

Note that $D_{\Lambda-\mathbf{c},\sigma}(\lambda - \mathbf{c})$ is a shifted version of $D_{\Lambda,\sigma,\mathbf{c}}(\lambda)$.

The following lemma comes from the definition of the flatness factor (1.66).

Lemma 1. [27] For all $\mathbf{c} \in \mathbb{R}^n$ and $\sigma > 0$, we have:

$$f_{\sigma,\mathbf{c}}(\Lambda) \in [1 - \epsilon_\Lambda(\sigma), 1 + \epsilon_\Lambda(\sigma)] \frac{1}{V(\Lambda)} \quad (6.19)$$

The following result shows that when the flatness factor is small, the mean and variance per dimension of the discrete Gaussian distribution $D_{\Lambda,\sigma,\mathbf{c}}$ is not so far from the mean and variance of the continuous Gaussian distribution.

Lemma 2. [60] Let \mathbf{x} be sampled from the Gaussian distribution $D_{\Lambda, \sigma, \mathbf{c}}$. If $\varepsilon \triangleq \varepsilon_{\Lambda}(\sigma/2) < 1$, then

$$\|\mathbb{E}[\mathbf{x} - \mathbf{c}]\| \leq \frac{\sqrt{2\pi\varepsilon}}{1-\varepsilon}\sigma \quad (6.20)$$

$$\left| \mathbb{E}[\|\mathbf{x} - \mathbf{c}\|^2] - n\sigma^2 \right| \leq \frac{2\pi\varepsilon}{1-\varepsilon}\sigma^2. \quad (6.21)$$

Lemma 3 (Entropy of discrete Gaussian [60]). Let $\mathbf{x} \sim D_{\Lambda, \sigma, \mathbf{c}}$. If $\varepsilon \triangleq \varepsilon_{\Lambda}(\sigma/2) < 1$, then the entropy rate of \mathbf{x} satisfies

$$\left| \frac{1}{n} \mathbb{H}(\mathbf{x}) - \left[\log(\sqrt{2\pi e}\sigma) - \frac{1}{n} \log V(\Lambda) \right] \right| \leq \varepsilon', \quad (6.22)$$

where $\varepsilon' = -\frac{\log(1-\varepsilon)}{n} + \frac{\pi\varepsilon}{n(1-\varepsilon)}$.

The following Lemma shows that the sum of the discrete Gaussian distribution and a continuous Gaussian distribution is very close to a continuous Gaussian distribution if the flatness factor is small.

Lemma 4. [27]: Let $\tilde{\sigma} = \frac{\sigma\sigma_0}{\sqrt{\sigma^2 + \sigma_0^2}}$ where $\sigma_0, \sigma > 0$, and let \mathbf{c} any vector in \mathbb{R}^n . Consider the continuous distribution g on \mathbb{R}^n obtained by adding a continuous Gaussian of variance σ^2 to a discrete Gaussian $D_{\Lambda - \mathbf{c}, \sigma_0}$:

$$g(\mathbf{x}) = \frac{1}{f_{\sigma_0}(\Lambda - \mathbf{c})} \sum_{\mathbf{t} \in \Lambda + \mathbf{c}} f_{\sigma_0}(\mathbf{t}) f_{\sigma}(\mathbf{x} - \mathbf{t}), \quad \mathbf{x} \in \mathbb{R}^n \quad (6.23)$$

If $\varepsilon = \varepsilon_{\Lambda}(\tilde{\sigma}) < \frac{1}{2}$, then $\frac{g(\mathbf{x})}{f_{\sqrt{\sigma_0^2 + \sigma^2}}(\mathbf{x})}$ is uniformly close to 1:

$$\forall \mathbf{x} \in \mathbb{R}^n, \quad \left| \frac{g(\mathbf{x})}{f_{\sqrt{\sigma_0^2 + \sigma^2}}(\mathbf{x})} - 1 \right| \leq 4\varepsilon. \quad (6.24)$$

The next lemma shows that the probability of a lattice Gaussian distribution falling outside of a ball of radius larger than $\sqrt{n}\sigma$ is exponentially small [27].

Lemma 5. [27] Let $\mathbf{x} \sim D_{\Lambda, \sigma, \mathbf{c}}$ and $\varepsilon \triangleq \varepsilon_{\Lambda}(\sigma) < 1$. Then for any $\rho > 1$, the probability

$$\mathbb{P}(\|\mathbf{x} - \mathbf{c}\| > \rho \cdot \sqrt{n}\sigma) \leq \frac{1 + \varepsilon}{1 - \varepsilon} \cdot \beta^n \quad (6.25)$$

where $\beta = \rho \cdot e^{(1-\rho^2)/2} < 1$.

Definition 5 (Semi-spherical noise [61]). *Let $\mathcal{B}(0, r)$ be a ball of radius r centered at zero. A sequence \mathbf{Z}_n is semi-spherical if $\forall \delta > 0$*

$$\mathbb{P}(\mathbf{Z}_n \in \mathcal{B}(0, (1 + \epsilon)\sqrt{n}\sigma)) > 1 - \delta \quad (6.26)$$

for sufficiently large n .

Therefore, $\mathbf{x} \sim D_{\Lambda, \sigma, \mathbf{c}}$ can be seen as semi-spherical noise. It is known that the sum of semi-spherical noise and AWGN is semi-spherical [61].

Finally, it is shown in [27], that the discrete Gaussian distribution is capacity achieving in an AWGN channel.

Theorem 1. [27] *Consider an AWGN channel, a signal which as a discrete Gaussian distribution $D_{\Lambda - \mathbf{c}, \sigma_0}$ for arbitrary $\mathbf{c} \in \mathbb{R}^n$, and noise with variance given by σ^2 , and let the average signal power be P so that $\text{SNR} = P/\sigma^2$. Let $\tilde{\sigma} = \frac{\sigma_0 \sigma}{\sqrt{\sigma_0^2 + \sigma^2}}$. Then if $\epsilon = \epsilon_{\Lambda}(\tilde{\sigma}) < \frac{1}{2}$ and $\frac{\pi \epsilon_{\Lambda}(\sigma_0/2)}{1 - \epsilon_{\Lambda}(\sigma_0/2)} \leq \epsilon$, the discrete Gaussian signalling achieves the capacity*

$$C_D \geq \frac{1}{2} \log(1 + \text{SNR}) - \frac{6\epsilon}{n}, \quad (6.27)$$

per channel use.

The following definition states that some lattices are good for capacity, since the gap $\frac{6\epsilon}{n}$ to the AWGN capacity vanishes.

Definition 6 (Capacity-good lattices [27]). *A lattice Λ is capacity good if*

$$\epsilon_{\Lambda}(\tilde{\sigma}) < \frac{1}{2}, \quad (6.28)$$

where $\tilde{\sigma} = \frac{\sigma_0 \sigma}{\sqrt{\sigma_0^2 + \sigma^2}}$.

6.3 Achieving the generalized degrees of freedom for the two-user symmetric interference channel using lattice Gaussian distribution

Consider the two-user interference channel as shown in Fig. 6.2.

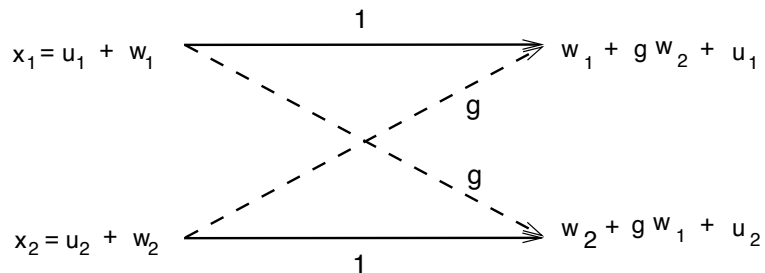


Figure 6.2: System model

The channel model is given by

$$y_1 = x_1 + gx_2 + z_1 \tag{6.29}$$

$$y_2 = x_2 + gx_1 + z_2. \tag{6.30}$$

The transmitted symbols are constructed using a common and a private message

$$x_1 = w_1 + u_1 \tag{6.31}$$

$$x_2 = w_2 + u_2 \tag{6.32}$$

where w_i and u_i are the common and private messages of user $i = 1, 2$ respectively. At receiver 1 w_1 , gw_2 and u_1 are decoded, while gu_2 is considered as noise. Similarly, at receiver 2 w_2 , gw_1 and u_2 are decoded, while gu_1 is treated as noise.

Etkin in [2] works with a simple HK scheme for a two-user interference channel where Gaussian codebooks are used. Therefore, it seems natural to use the idea of Gaussian distribution if we apply lattices. Consider that $w_i \in D_{\Lambda_{w_i}, \sigma_{w_i}}$, $gw_i \in D_{g\Lambda_{w_i}, g\sigma_{w_i}}$, $u_i \in D_{\Lambda_{u_i}, \sigma_{u_i}}$ and $gu_i \in D_{g\Lambda_{u_i}, g\sigma_{u_i}}$.

At receiver 1, we have

$$\mathbf{y}_1 \in D_{\Lambda_{w_1}, \sigma_{w_1}} + D_{g\Lambda_{w_2}, g\sigma_{w_2}} + D_{\Lambda_{u_1}, \sigma_{u_1}} + D_{g\Lambda_{u_2}, g\sigma_{u_2}} + \mathbf{z}_1, \quad (6.33)$$

where \mathbf{z}_1 is AWGN with variance σ^2 and zero mean. Since we treat \mathbf{u}_2 as noise, then $D_{g\Lambda_{u_2}, g\sigma_{u_2}} + \mathbf{z}_1$ is considered as noise. From Lemma 5, if the flatness factor $\epsilon_{g\Lambda_{u_2}}(g\sigma_{u_2}/2) < 1$ then $D_{g\Lambda_{u_2}, g\sigma_{u_2}} + \mathbf{z}_1$ is not so far from a continuous distribution. With this, we can treat the new noise $\tilde{\mathbf{z}}_1 = \alpha D_{g\Lambda_{u_2}, g\sigma_{u_2}} + \mathbf{z}_1$ as AWGN with variance $g^2\sigma_{u_2}^2 + \sigma^2$. We consider that the power of the private messages at transmitter 1 is $\sigma_{u_1}^2$ and $\sigma_{u_2}^2$ at transmitter 2, and the power of the common messages at transmitter 1 is $\sigma_{w_1}^2$ and $\sigma_{w_2}^2$ at transmitter 2. Further, we consider $\sigma_u^2 = \sigma_{u_1}^2 = \sigma_{u_2}^2$ and $\sigma_w^2 = \sigma_{w_1}^2 = \sigma_{w_2}^2$. We also define $\text{SNR}_c = \frac{\sigma_w^2}{\sigma^2}$, $\text{SNR}_p = \frac{\sigma_u^2}{\sigma^2}$, $\text{INR}_c = \frac{g^2\sigma_w^2}{\sigma^2}$ and $\text{INR}_p = \frac{g^2\sigma_u^2}{\sigma^2} \triangleq 1$. Then $\text{SNR} = \text{SNR}_c + \text{SNR}_p$ and $\text{INR} = \text{INR}_c + \text{INR}_p$.

In the following subsections we show that it is possible to achieve the GDoF for each type of interference using the lattice Gaussian distribution.

6.3.1 Very strong and strong interference scenarios

In this subsection we consider the case for the very strong and strong interference. The interference is said to be very strong when $\text{INR} > \text{SNR}^2$. The strong interference case corresponds to $\text{SNR} < \text{INR} < \text{SNR}^2$. In the very strong and strong interference cases both signals \mathbf{x}_1 and \mathbf{x}_2 are entirely common messages, and there is no private message. Then $\mathbf{x}_1 = \mathbf{w}_1 \in D_{\Lambda_{w_1}, \sigma_{w_1}}$, and $\mathbf{x}_2 = \mathbf{w}_2 \in D_{\Lambda_{w_2}, \sigma_{w_2}}$. We will decode with successive cancellation for both cases without yet defining the type of interference.

Consider the interference channel given by

$$\mathbf{y}_1 = \mathbf{x}_1 + g\mathbf{x}_2 + \mathbf{z}_1 \quad (6.34)$$

$$\mathbf{y}_2 = \mathbf{x}_2 + g\mathbf{x}_1 + \mathbf{z}_2. \quad (6.35)$$

or

$$\mathbf{y}_1 = \mathbf{w}_1 + g\mathbf{w}_2 + \mathbf{z}_1 \quad (6.36)$$

$$\mathbf{y}_2 = \mathbf{w}_2 + g\mathbf{w}_1 + \mathbf{z}_2. \quad (6.37)$$

To decode, we divide the problem in the following two MAC regions.

MAC1

The first MAC is formed by transmitter 1 and 2, and receiver 1. Thus, at the receiver we have (6.36). The decoding procedure is the following

- Decode $\mathbf{y}_1 = \mathbf{w}_1 + \check{\mathbf{z}}_1$ where $\check{\mathbf{z}}_1 = g\mathbf{w}_2 + \mathbf{z}_1$ is treated as the new AWGN noise. This is valid from Lemma 5 if

$$\epsilon_{\Lambda_{g\mathbf{w}_2}}(g\sigma_{\mathbf{w}_2}) < 1. \quad (6.38)$$

Since this transforms into an AWGN channel, by Theorem 1 we have that if

$$\epsilon_{\Lambda_{\mathbf{w}_1}} = \epsilon_{\Lambda_{\mathbf{w}_1}} \left(\frac{\sigma_{\mathbf{w}_1} \sqrt{g^2 \sigma_{\mathbf{w}_2}^2 + \sigma^2}}{\sqrt{\sigma_{\mathbf{w}_1}^2 + g^2 \sigma_{\mathbf{w}_2}^2 + \sigma^2}} \right) < \frac{1}{2}, \quad (6.39)$$

and

$$\frac{\pi \epsilon_{\Lambda_{\mathbf{w}_1}}(\sigma_{\mathbf{w}_1}/2)}{1 - \epsilon_{\Lambda_{\mathbf{w}_1}}(\sigma_{\mathbf{w}_1}/2)} < \epsilon_{\Lambda_{\mathbf{w}_1}} \quad (6.40)$$

then

$$R_{w1,1} = \frac{1}{2} \log \left(1 + \frac{\sigma_{\mathbf{w}_1}^2}{g^2 \sigma_{\mathbf{w}_2}^2 + \sigma^2} \right) - \frac{6\epsilon}{n}, \quad (6.41)$$

where in this case $\epsilon = \epsilon_{\Lambda_{\mathbf{w}_1}} \left(\frac{\sigma_{\mathbf{w}_1} \sqrt{g^2 \sigma_{\mathbf{w}_2}^2 + \sigma^2}}{\sqrt{\sigma_{\mathbf{w}_1}^2 + g^2 \sigma_{\mathbf{w}_2}^2 + \sigma^2}} \right)$. Now, from definition 6 we can say

that the gap $\frac{6\epsilon}{n}$ vanishes as

$$\epsilon_{\Lambda_{w_1}} \left(\frac{\sigma_{w_1} \sqrt{g^2 \sigma_{w_2}^2 + \sigma^2}}{\sqrt{\sigma_{w_1}^2 + g^2 \sigma_{w_2}^2 + \sigma^2}} \right) < \frac{1}{2} \quad (6.42)$$

which is the same condition as (6.39). Therefore, we can say that

$$R_{w_1,1} \approx \frac{1}{2} \log \left(1 + \frac{\sigma_{w_1}^2}{g^2 \sigma_{w_2}^2 + \sigma^2} \right) \quad (6.43)$$

- Then decode $\tilde{\mathbf{y}}_1 = \mathbf{y}_1 - \hat{\mathbf{w}}_1 = g\mathbf{w}_2 + \mathbf{z}_1$. Again we can apply Theorem 1

$$R_{w_2,1} \approx \frac{1}{2} \log \left(1 + \frac{g^2 \sigma_{w_2}^2}{\sigma^2} \right) \quad (6.44)$$

where the following conditions must be fulfilled

$$\epsilon_{g\Lambda_{w_2}} = \epsilon_{g\Lambda_{w_2}} \left(\frac{g\sigma_{w_2}\sigma}{\sqrt{g^2 \sigma_{w_2}^2 + \sigma^2}} \right) < \frac{1}{2}, \quad (6.45)$$

and

$$\frac{\pi \epsilon_{g\Lambda_{w_2}} (\sigma_{g w_2} / 2)}{1 - \epsilon_{g\Lambda_{w_2}} (\sigma_{g w_2} / 2)} < \epsilon_{g\Lambda_{w_2}} \quad (6.46)$$

- In a similar way we can decode the signal from user 2 first by saying, $\mathbf{y}_1 = g\mathbf{w}_2 + \check{\mathbf{z}}_1$ where from Lemma 4, $\check{\mathbf{z}}_1 = \mathbf{w}_1 + \mathbf{z}_1$ is treated as the new AWGN noise. Since this transforms into an AWGN channel, by Theorem 1 we have

$$R_{w_2,2} \approx \frac{1}{2} \log \left(1 + \frac{g^2 \sigma_{w_2}^2}{\sigma_{w_1}^2 + \sigma^2} \right) \quad (6.47)$$

where the required conditions are

$$\epsilon_{\Lambda_{w_1}} \left(\frac{\sigma_{w_1} \sigma}{\sqrt{\sigma_{w_1}^2 + \sigma^2}} \right) < \frac{1}{2}, \quad (6.48)$$

$$\tau_{g\Lambda_{w_2}} = \epsilon_{g\Lambda_{w_2}} \left(\frac{g\sigma_{w_2} \sqrt{\sigma_{w_1}^2 + \sigma^2}}{\sqrt{\sigma_{w_1}^2 + g^2\sigma_{w_2}^2 + \sigma^2}} \right) < \frac{1}{2}, \quad (6.49)$$

and

$$\frac{\pi \epsilon_{g\Lambda_{w_2}} (\sigma_{g w_2} / 2)}{1 - \epsilon_{g\Lambda_{w_2}} (g\sigma_{w_2} / 2)} < \tau_{g\Lambda_{w_2}} \quad (6.50)$$

- As above we proceed to decode $\tilde{\mathbf{y}}_1 = \mathbf{y}_1 - g\hat{\mathbf{w}}_2 = \mathbf{w}_1 + \mathbf{z}_1$. Again we can apply Theorem 1

$$R_{w_{1,2}} \approx \frac{1}{2} \log \left(1 + \frac{\sigma_{w_1}^2}{\sigma^2} \right) \quad (6.51)$$

where we need

$$\tau_{\Lambda_{w_1}} = \epsilon_{\Lambda_{w_1}} \left(\frac{\sigma_{w_1} \sigma}{\sqrt{\sigma_{w_1}^2 + \sigma^2}} \right) < \frac{1}{2}, \quad (6.52)$$

and

$$\frac{\pi \epsilon_{\Lambda_{w_1}} (\sigma_{w_1} / 2)}{1 - \epsilon_{\Lambda_{w_1}} (\sigma_{w_1} / 2)} < \tau_{\Lambda_{w_1}} \quad (6.53)$$

MAC2

In a similar way we can obtain the rates for the MAC2 through the following steps

- Decode $\mathbf{y}_2 = \mathbf{w}_2 + \check{\mathbf{z}}_2$ where $\check{\mathbf{z}}_2 = g\mathbf{w}_1 + \mathbf{z}_2$ is the new AWGN noise. This is valid from Lemma 5. Since this transforms into an AWGN channel, by Theorem 1 we have

$$\bar{R}_{w_{2,2}} \approx \frac{1}{2} \log \left(1 + \frac{\sigma_{w_2}^2}{g^2\sigma_{w_1}^2 + \sigma^2} \right) \quad (6.54)$$

where we need

$$\epsilon_{g\Lambda_{w_1}} (g\sigma_{w_1}) < 1, \quad (6.55)$$

$$\epsilon_{\Lambda_{w_2}} = \epsilon_{\Lambda_{w_2}} \left(\frac{\sigma_{w_2} \sqrt{g^2 \sigma_{w_1}^2 + \sigma^2}}{\sqrt{g^2 \sigma_{w_1}^2 + \sigma_{w_2}^2 + \sigma^2}} \right) < \frac{1}{2}, \quad (6.56)$$

and

$$\frac{\pi \epsilon_{\Lambda_{w_2}} (\sigma_{w_2}/2)}{1 - \epsilon_{\Lambda_{w_2}} (\sigma_{w_2}/2)} < \epsilon_{\Lambda_{w_2}} \quad (6.57)$$

- Then decode $\tilde{\mathbf{y}}_2 = \mathbf{y}_2 - \hat{\mathbf{w}}_2 = g\mathbf{w}_1 + \mathbf{z}_2$. Again we can apply Theorem 1

$$\bar{R}_{w_{1,2}} \approx \frac{1}{2} \log \left(1 + \frac{g^2 \sigma_{w_1}^2}{\sigma^2} \right) \quad (6.58)$$

where we require

$$\epsilon_{g\Lambda_{w_1}} = \epsilon_{g\Lambda_{w_1}} \left(\frac{g\sigma_{w_1}\sigma}{\sqrt{g^2 \sigma_{w_1}^2 + \sigma^2}} \right) < \frac{1}{2}, \quad (6.59)$$

and

$$\frac{\pi \epsilon_{g\Lambda_{w_1}} (g\sigma_{w_1}/2)}{1 - \epsilon_{g\Lambda_{w_1}} (g\sigma_{w_1}/2)} < \epsilon_{g\Lambda_{w_1}} \quad (6.60)$$

- In a similar way we can decode the signal from user 1 first by saying $\mathbf{y}_2 = g\mathbf{w}_1 + \check{\mathbf{z}}_2$ where $\check{\mathbf{z}}_2 = \mathbf{w}_2 + \mathbf{z}_2$ is the new AWGN noise. This is valid from Lemma 4. Since this transforms into an AWGN channel, by Theorem 1 we have

$$\bar{R}_{w_{1,1}} \approx \frac{1}{2} \log \left(1 + \frac{g^2 \sigma_{w_1}^2}{\sigma_{w_2}^2 + \sigma^2} \right) \quad (6.61)$$

where

$$\epsilon_{\Lambda_{w_2}} \left(\frac{\sigma_{w_2}\sigma}{\sqrt{\sigma_{w_2}^2 + \sigma^2}} \right) < \frac{1}{2}, \quad (6.62)$$

$$\tau_{g\Lambda_{w_1}} = \epsilon_{g\Lambda_{w_1}} \left(\frac{g\sigma_{w_1} \sqrt{\sigma_{w_2}^2 + \sigma^2}}{\sqrt{g^2 \sigma_{w_1}^2 + \sigma_{w_2}^2 + \sigma^2}} \right) < \frac{1}{2}, \quad (6.63)$$

and

$$\frac{\pi \epsilon_{g\Lambda_{w_1}}(g\sigma_{w_1}/2)}{1 - \epsilon_{g\Lambda_{w_1}}(g\sigma_{w_1}/2)} < \tau_{g\Lambda_{w_1}} \quad (6.64)$$

- As above we then proceed to decode $\tilde{\mathbf{y}}_2 = \mathbf{y}_2 - g\hat{\mathbf{w}}_1 = \mathbf{w}_2 + \mathbf{z}_2$. Again we can apply Theorem 1

$$\bar{R}_{w_{2,1}} \approx \frac{1}{2} \log \left(1 + \frac{\sigma_{w_2}^2}{\sigma^2} \right) \quad (6.65)$$

with the following conditions

$$\epsilon_{\Lambda_{w_2}} = \epsilon_{\Lambda_{w_2}} \left(\frac{\sigma_{w_2}\sigma}{\sqrt{\sigma_{w_2}^2 + \sigma^2}} \right) < \frac{1}{2}, \quad (6.66)$$

and

$$\frac{\pi \epsilon_{\Lambda_{w_2}}(\sigma_{w_2}/2)}{1 - \epsilon_{\Lambda_{w_2}}(\sigma_{w_2}/2)} < \epsilon_{\Lambda_{w_2}} \quad (6.67)$$

Since we are working with a symmetric interference channel, we can change the rates obtained above by the following rates:

$$R_{1A} = R_{w_{1,1}} \approx \frac{1}{2} \log \left(1 + \frac{\text{SNR}}{\text{INR} + 1} \right) \quad (6.68)$$

$$R_{2A} = R_{w_{2,1}} \approx \frac{1}{2} \log (1 + \text{INR}) \quad (6.69)$$

$$R_{2B} = R_{w_{2,2}} \approx \frac{1}{2} \log \left(1 + \frac{\text{INR}}{\text{SNR} + 1} \right) \quad (6.70)$$

$$R_{1B} = R_{w_{1,2}} \approx \frac{1}{2} \log (1 + \text{SNR}) \quad (6.71)$$

$$R_{2E} = \bar{R}_{w2,2} \approx \frac{1}{2} \log \left(1 + \frac{\text{SNR}}{\text{INR} + 1} \right) \quad (6.72)$$

$$R_{1E} = \bar{R}_{w1,2} \approx \frac{1}{2} \log (1 + \text{INR}) \quad (6.73)$$

$$R_{1D} = \bar{R}_{w1,1} \approx \frac{1}{2} \log \left(1 + \frac{\text{INR}}{\text{SNR} + 1} \right) \quad (6.74)$$

$$R_{2D} = \bar{R}_{w2,1} \approx \frac{1}{2} \log (1 + \text{SNR}) \quad (6.75)$$

The achievable rates are depicted in Fig. 6.3 and 6.4.

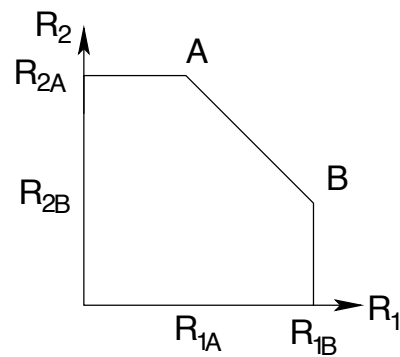


Figure 6.3: MAC1

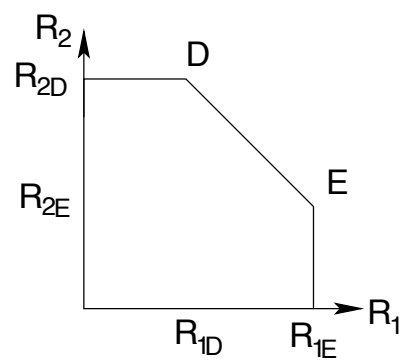


Figure 6.4: MAC2

Very strong interference

In this case, since the interference is very strong ($\text{INR} > \text{SNR}^2$) we can approximate the rates and easily find the maximum achievable rate, which is given by

$$R_{\text{maxreg1}} = R_{1B} = R_{2D} \approx \frac{1}{2} \log(1 + \text{SNR}) \quad (6.76)$$

and is shown in Fig. 6.5.

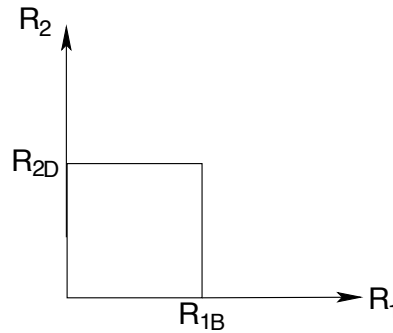


Figure 6.5: Intersection region for the very strong interference case

From the definition of the flatness factor, the following must be true since $\epsilon_{\Lambda} > 0$

$$\epsilon_{\Lambda_{w_1}}(\sigma_{w_1}/2) < \frac{\pi \epsilon_{\Lambda_{w_1}}(\sigma_{w_1}/2)}{1 - \epsilon_{\Lambda_{w_1}}(\sigma_{w_1}/2)} < \tau_{\Lambda_{w_1}} \quad (6.77)$$

Therefore, from equations (6.52) and (6.53) (conditions for point R_{1B} in Fig. 6.5) we also have

$$\epsilon_{\Lambda_{w_1}}(\sigma_{w_1}/2) < \epsilon_{\Lambda_{w_1}}\left(\frac{\sigma_{w_1}\sigma}{\sqrt{\sigma_{w_1}^2 + \sigma^2}}\right). \quad (6.78)$$

This implies the following

$$\begin{aligned} \frac{\sigma_{w_1}}{2} &> \frac{\sigma_{w_1}\sigma}{\sqrt{\sigma_{w_1}^2 + \sigma^2}} \\ \sigma_{w_1}^2 &> 3\sigma^2 \\ \text{SNR} &> 3, \end{aligned} \tag{6.79}$$

which is valid since we can assume that for the GDoF, SNR and INR $\gg 1$.

This condition is not contradictory to the very strong interference case. Since the channel is symmetric, we will obtain the same if we consider (6.66) and (6.67), which are the conditions for R_{2D} .

Strong interference

In this case the final intersection is shown in Fig. 6.6.

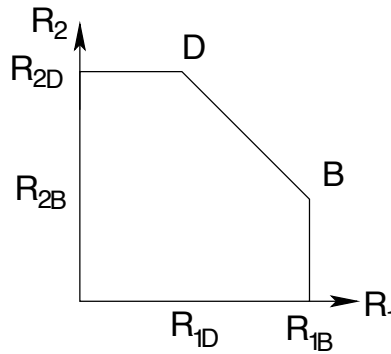


Figure 6.6: Intersection region for the strong interference case

From the definition of the flatness factor the following must be true

$$\epsilon_{g\Lambda_{w_2}}(g\sigma_{w_2}/2) < \frac{\pi\epsilon_{g\Lambda_{w_2}}(\sigma_{g w_2}/2)}{1 - \epsilon_{g\Lambda_{w_2}}(g\sigma_{w_2}/2)} < \tau_{g\Lambda_{w_2}} \tag{6.80}$$

Therefore, from equations (6.49) and (6.50) (conditions for point R_{2B} in Fig. 6.6) we also have that

$$\epsilon_{g\Lambda_{w_2}}(g\sigma_{w_2}/2) < \epsilon_{g\Lambda_{w_2}}\left(\frac{g\sigma_{w_2}\sqrt{\sigma_{w_1}^2 + \sigma^2}}{\sqrt{\sigma_{w_1}^2 + g^2\sigma_{w_2}^2 + \sigma^2}}\right) \quad (6.81)$$

This means the following

$$\begin{aligned} \frac{g\sigma_{w_2}}{2} &> \frac{g\sigma_{w_2}\sqrt{\sigma^2 + \sigma^2}}{\sqrt{\sigma_{w_1}^2 + g^2\sigma_{w_2}^2 + \sigma^2}} \\ \frac{1}{4} &> \frac{\sigma_{w_1}^2 + \sigma^2}{\sigma_{w_1}^2 + g^2\sigma_{w_2}^2 + \sigma^2} \\ \text{INR} &> 3\text{SNR} \\ \alpha &> 1 + \frac{\log(3)}{\log(\text{SNR})} \end{aligned} \quad (6.82)$$

From equations (6.52) and (6.53)(conditions for point R_{1B} in Fig. 6.6) and (6.48) we also have

$$\epsilon_{\Lambda_{w_1}}(\sigma_{w_1}/2) < \epsilon_{\Lambda_{w_1}}\left(\frac{\sigma_{w_1}\sigma}{\sqrt{\sigma_{w_1}^2 + \sigma^2}}\right) \quad (6.83)$$

Then

$$\begin{aligned} \frac{\sigma_{w_1}^2}{4} &> \frac{\sigma_{w_1}^2\sigma^2}{\sigma_{w_1}^2 + \sigma^2} \\ \sigma_{w_1}^2 &> 3\sigma^2 \\ \text{SNR} &> 3. \end{aligned} \quad (6.84)$$

Neither (6.82) nor (6.84) are contradictory to the strong interference case. Since the channel is symmetric, we obtain the same if we consider equations (6.62), (6.63) and (6.64), (6.66) and (6.67), which are the conditions for point D in Fig. 6.6.

Therefore, we can find the maximum achievable rate

$$\begin{aligned}
 R_{\max} &\approx \frac{\frac{1}{2} \log \left(1 + \frac{\text{INR}}{\text{SNR}_{+1}} \right) + \frac{1}{2} \log (1 + \text{SNR})}{2} \\
 &\approx \frac{1}{4} \log \left(\left(\frac{1 + \text{INR} + \text{SNR}}{1 + \text{SNR}} \right) (1 + \text{SNR}) \right) \\
 &\approx \frac{1}{4} \log ((1 + \text{INR} + \text{SNR})). \tag{6.85}
 \end{aligned}$$

Then to obtain the GDoF we say as, in the previous section $\frac{R_{\max}}{R_{\text{AWGN}}}$, where $R_{\text{AWGN}} = \frac{1}{2} \log(1 + \text{SNR})$:

$$d_{\text{sym}} \approx \frac{\frac{1}{4} \log ((1 + \text{INR} + \text{SNR}))}{\frac{1}{2} \log(1 + \text{SNR})} \tag{6.86}$$

Applying the same strong interference conditions (6.11) as in the previous section, we obtain

$$\begin{aligned}
 d_{\text{sym}} &\approx \frac{\frac{1}{2} \log (\text{INR})}{\log(\text{SNR})} \\
 &= \frac{\alpha}{2} \tag{6.87}
 \end{aligned}$$

6.3.2 Moderately weak and weak interference

To find the GDoF for the cases of moderately weak and weak interference, we need to work with both common and private messages. The system is given by

$$\mathbf{y}_1 = \mathbf{w}_1 + g\mathbf{w}_2 + \mathbf{u}_1 + g\mathbf{u}_2 + \mathbf{z}_1 \tag{6.88}$$

$$\mathbf{y}_2 = \mathbf{w}_2 + g\mathbf{w}_1 + \mathbf{u}_2 + g\mathbf{u}_1 + \mathbf{z}_2. \tag{6.89}$$

Again, we consider the problem as the intersection of two MAC regions. The decoding strategy is to decode the common messages first, then the desired private message, always leaving the interference private message as noise.

MAC1

The MAC system is given by (6.88). The decoding procedure is the following:

- Decode $\mathbf{y}_1 = \mathbf{w}_1 + \tilde{\mathbf{z}}_1$ where $\tilde{\mathbf{z}}_1 = g\mathbf{w}_2 + \mathbf{u}_1 + g\mathbf{u}_2 + \mathbf{z}_1$ is the new AWGN noise. This is valid from Lemmas 4 and 5 and since it transforms into an AWGN channel, by Theorem 1 we have

$$R_{w1,1} \approx \frac{1}{2} \log \left(1 + \frac{\sigma_{w1}^2}{g^2\sigma_{w2}^2 + \sigma_{u1}^2 + g^2\sigma_{u2}^2 + \sigma^2} \right) \quad (6.90)$$

with the following set of conditions

$$\epsilon_{g\Lambda_{w2}} \left(\frac{g\sigma_{w2}\sigma}{\sqrt{g^2\sigma_{w2}^2 + \sigma^2}} \right) < \frac{1}{2}, \quad (6.91)$$

$$\epsilon_{g\Lambda_{u2}} \left(\frac{g\sigma_{u2}\sigma}{\sqrt{g^2\sigma_{u2}^2 + \sigma^2}} \right) < \frac{1}{2}, \quad (6.92)$$

$$\epsilon_{\Lambda_{u1}}(\sigma_{u1}) < 1, \quad (6.93)$$

$$\epsilon_{\Lambda_{w1}} = \epsilon_{\Lambda_{w1}} \left(\frac{\sigma_{w1} \sqrt{g^2\sigma_{w2}^2 + g^2\sigma_{u2}^2 + \sigma_{u1}^2 + \sigma^2}}{\sqrt{\sigma_{w1}^2 + g^2\sigma_{w2}^2 + g^2\sigma_{u2}^2 + \sigma_{u1}^2 + \sigma^2}} \right) < \frac{1}{2}, \quad (6.94)$$

and

$$\frac{\pi \epsilon_{\Lambda_{w1}}(\sigma_{w1}/2)}{1 - \epsilon_{\Lambda_{w1}}(\sigma_{w1}/2)} < \epsilon_{\Lambda_{w1}} \quad (6.95)$$

- Then decode $\tilde{\mathbf{y}}_1 = \mathbf{y}_1 - \hat{\mathbf{w}}_1 = g\mathbf{w}_2 + \tilde{\mathbf{z}}_1$, where $\tilde{\mathbf{z}}_1 = \mathbf{u}_1 + g\mathbf{u}_2 + \mathbf{z}_1$ is treated as noise from Lemmas 4 and 5. Again we can apply Theorem 1

$$R_{w2,1} \approx \frac{1}{2} \log \left(1 + \frac{g^2\sigma_{w2}^2}{\sigma_{u1}^2 + g^2\sigma_{u2}^2 + \sigma^2} \right) \quad (6.96)$$

with the following conditions

$$\epsilon_{g\Lambda_{u_2}} \left(\frac{g\sigma_{u_2}\sigma}{\sqrt{g^2\sigma_{u_2}^2 + \sigma^2}} \right) < \frac{1}{2}, \quad (6.97)$$

$$\epsilon_{\Lambda_{u_1}}(\sigma_{u_1}) < 1, \quad (6.98)$$

$$\epsilon_{g\Lambda_{w_2}} = \epsilon_{g\Lambda_{w_2}} \left(\frac{g\sigma_{w_2}\sqrt{g^2\sigma_{u_2}^2 + \sigma_{u_1}^2 + \sigma^2}}{\sqrt{g^2\sigma_{w_2}^2 + g^2\sigma_{u_2}^2 + \sigma_{u_1}^2 + \sigma^2}} \right) < \frac{1}{2}, \quad (6.99)$$

and

$$\frac{\pi\epsilon_{g\Lambda_{w_2}}(g\sigma_{w_2}/2)}{1 - \epsilon_{g\Lambda_{w_2}}(g\sigma_{w_2}/2)} < \epsilon_{g\Lambda_{w_2}} \quad (6.100)$$

- In a similar way, we can start by decoding the signal from user 2 first by saying, $\mathbf{y}_1 = g\mathbf{w}_2 + \mathbf{z}_1$ where $\mathbf{z}_1 = \mathbf{w}_1 + g\mathbf{u}_2 + \mathbf{u}_1 + \mathbf{z}_1$ is treated as noise from Lemmas 5 and 4. Since this transforms into an AWGN channel, by Theorem 1 we have

$$R_{w_2,2} \approx \frac{1}{2} \log \left(1 + \frac{g^2\sigma_{w_2}^2}{\sigma_{w_1}^2 + \sigma_{u_1}^2 + g^2\sigma_{u_2}^2 + \sigma^2} \right) \quad (6.101)$$

with the following

$$\epsilon_{\Lambda_{w_1}}(\sigma_{w_1}) < 1, \quad (6.102)$$

$$\epsilon_{\Lambda_{u_1}}(\sigma_{u_1}) < 1, \quad (6.103)$$

$$\epsilon_{g\Lambda_{u_2}} \left(\frac{g\sigma_{u_2}\sigma}{\sqrt{g^2\sigma_{u_2}^2 + \sigma^2}} \right) < \frac{1}{2}, \quad (6.104)$$

$$\tau_{g\Lambda_{w_2}} = \epsilon_{g\Lambda_{w_2}} \left(\frac{g\sigma_{w_2} \sqrt{\sigma_{w_1}^2 + g^2\sigma_{u_2}^2 + \sigma_{u_1}^2 + \sigma^2}}{\sqrt{g^2\sigma_{w_2}^2 + \sigma_{w_1}^2 + g^2\sigma_{u_2}^2 + \sigma_{u_1}^2 + \sigma^2}} \right) < \frac{1}{2}, \quad (6.105)$$

and

$$\frac{\pi\epsilon_{g\Lambda_{w_2}}(g\sigma_{w_2}/2)}{1 - \epsilon_{g\Lambda_{w_2}}(g\sigma_{w_2}/2)} < \tau_{g\Lambda_{w_2}} \quad (6.106)$$

- As above, we proceed to decode $\tilde{\mathbf{y}}_1 = \mathbf{y}_1 - g\hat{\mathbf{w}}_2 = \mathbf{w}_1 + \tilde{\mathbf{z}}_1$ where $\tilde{\mathbf{z}}_1 = \mathbf{u}_1 + g\mathbf{u}_2 + \mathbf{z}_1$ from Lemmas 5 and 4. Again we can apply Theorem 1

$$R_{w_1,2} \approx \frac{1}{2} \log \left(1 + \frac{\sigma_{w_1}^2}{\sigma_{u_1}^2 + g^2\sigma_{u_2}^2 + \sigma^2} \right) \quad (6.107)$$

with the following

$$\epsilon_{\Lambda_{u_1}}(\sigma_{u_1}) < 1, \quad (6.108)$$

$$\epsilon_{g\Lambda_{u_2}} \left(\frac{g\sigma_{u_2}\sigma}{\sqrt{g^2\sigma_{u_2}^2 + \sigma^2}} \right) < \frac{1}{2}, \quad (6.109)$$

$$\epsilon_{\Lambda_{w_1}} = \epsilon_{\Lambda_{w_1}} \left(\frac{\sigma_{w_1} \sqrt{\sigma_{u_1}^2 + g^2\sigma_{u_2}^2 + \sigma^2}}{\sqrt{\sigma_{w_1}^2 + \sigma_{u_1}^2 + g^2\sigma_{u_2}^2 + \sigma^2}} \right) < \frac{1}{2}, \quad (6.110)$$

and

$$\frac{\pi\epsilon_{\Lambda_{w_1}}(\sigma_{w_1}/2)}{1 - \epsilon_{\Lambda_{w_1}}(\sigma_{w_1}/2)} < \epsilon_{\Lambda_{w_1}} \quad (6.111)$$

MAC2

This MAC corresponds to (6.89). The decoding procedure is the following

- Decode $\mathbf{y}_2 = g\mathbf{w}_1 + \tilde{\mathbf{z}}_2$ where $\tilde{\mathbf{z}}_2 = \mathbf{w}_2 + \mathbf{u}_2 + g\mathbf{u}_1 + \mathbf{z}_2$ is treated as the new AWGN noise. This is valid from Lemma 5 and Lemma 4. Since this transforms into an

AWGN channel, by Theorem 1 we have

$$\bar{R}_{w1,1} \approx \frac{1}{2} \log \left(1 + \frac{g^2 \sigma_{w1}^2}{\sigma_{w2}^2 + g^2 \sigma_{u1}^2 + \sigma_{u2}^2 + \sigma^2} \right) \quad (6.112)$$

with

$$\epsilon_{\Lambda_{w2}}(\sigma_{w2}) < 1, \quad (6.113)$$

$$\epsilon_{\Lambda_{u2}}(\sigma_{u2}) < 1, \quad (6.114)$$

$$\epsilon_{g\Lambda_{u1}} \left(\frac{g\sigma_{u1}\sigma}{\sqrt{g^2\sigma_{u1}^2 + \sigma^2}} \right) < \frac{1}{2}, \quad (6.115)$$

$$\epsilon_{g\Lambda_{w1}} = \epsilon_{g\Lambda_{w1}} \left(\frac{g\sigma_{w1}\sqrt{\sigma_{w2}^2 + \sigma_{u2}^2 + g^2\sigma_{u1}^2 + \sigma^2}}{\sqrt{g^2\sigma_{w1}^2 + g^2\sigma_{u1}^2 + \sigma_{w2}^2 + \sigma_{u2}^2 + \sigma^2}} \right) < \frac{1}{2}, \quad (6.116)$$

and

$$\frac{\pi \epsilon_{g\Lambda_{w1}}(g\sigma_{w1}/2)}{1 - \epsilon_{g\Lambda_{w1}}(g\sigma_{w1}/2)} < \epsilon_{g\Lambda_{w1}} \quad (6.117)$$

- Then decode $\tilde{\mathbf{y}}_2 = \mathbf{y}_2 - g\hat{\mathbf{w}}_1 = \mathbf{w}_2 + \tilde{\mathbf{z}}_2$, where $\tilde{\mathbf{z}}_2 = g\mathbf{u}_1 + \mathbf{u}_2 + \mathbf{z}_2$, from Lemmas 4 and 5. Again we can apply Theorem 1

$$\bar{R}_{w2,1} \approx \frac{1}{2} \log \left(1 + \frac{\sigma_{w2}^2}{g^2\sigma_{u1}^2 + \sigma_{u2}^2 + \sigma^2} \right) \quad (6.118)$$

with

$$\epsilon_{\Lambda_{u2}}(\sigma_{u2}) < 1, \quad (6.119)$$

$$\epsilon_{g\Lambda_{u_1}} \left(\frac{g\sigma_{u_1}\sigma}{\sqrt{g^2\sigma_{u_1}^2 + \sigma^2}} \right) < \frac{1}{2}, \quad (6.120)$$

$$\epsilon_{\Lambda_{w_2}} = \epsilon_{\Lambda_{w_2}} \left(\frac{\sigma_{w_2} \sqrt{g^2\sigma_{u_1}^2 + \sigma_{u_2}^2 + \sigma^2}}{\sqrt{g^2\sigma_{w_1}^2 + g^2\sigma_{u_1}^2 + \sigma_{u_2}^2 + \sigma_{w_2}^2\sigma^2}} \right) < \frac{1}{2}, \quad (6.121)$$

and

$$\frac{\pi\epsilon_{\Lambda_{w_2}}(\sigma_{w_2}/2)}{1 - \epsilon_{\Lambda_{w_2}}(\sigma_{w_2}/2)} < \epsilon_{\Lambda_{w_2}} \quad (6.122)$$

- In a similar way we can start by decoding the signal from user 2 first by saying $\mathbf{y}_2 = \mathbf{w}_2 + \mathbf{z}_2$ where $\mathbf{z}_2 = g\mathbf{w}_1 + g\mathbf{u}_1 + \mathbf{u}_2 + \mathbf{z}_2$ is the new AWGN noise. This is valid from Lemmas 4 and 5. Since this transforms into an AWGN channel, by Theorem 1 we have

$$\bar{R}_{w_2,2} \approx \frac{1}{2} \log \left(1 + \frac{\sigma_{w_2}^2}{g^2\sigma_{w_1}^2 + g^2\sigma_{u_1}^2 + \sigma_{u_2}^2 + \sigma^2} \right) \quad (6.123)$$

with

$$\epsilon_{g\Lambda_{w_1}} \left(\frac{g\sigma_{w_1}\sigma}{\sqrt{g^2\sigma_{w_1}^2 + \sigma^2}} \right) < \frac{1}{2}, \quad (6.124)$$

$$\epsilon_{g\Lambda_{u_1}} \left(\frac{g\sigma_{u_1}\sigma}{\sqrt{g^2\sigma_{u_1}^2 + \sigma^2}} \right) < \frac{1}{2}, \quad (6.125)$$

$$\epsilon_{\Lambda_{u_2}}(\sigma_{u_2}) < 1, \quad (6.126)$$

$$\tau_{\Lambda_{w_2}} = \epsilon_{\Lambda_{w_2}} \left(\frac{\sigma_{w_2} \sqrt{g^2\sigma_{w_1}^2 + g^2\sigma_{u_1}^2 + \sigma_{u_2}^2 + \sigma^2}}{\sqrt{\sigma_{w_2}^2 + g^2\sigma_{w_1}^2 + g^2\sigma_{u_1}^2 + \sigma_{u_2}^2 + \sigma^2}} \right) < \frac{1}{2}, \quad (6.127)$$

and

$$\frac{\pi \epsilon_{\Lambda_{w_2}}(\sigma_{w_2}/2)}{1 - \epsilon_{\Lambda_{w_2}}(\sigma_{w_2}/2)} < \tau_{\Lambda_{w_2}} \quad (6.128)$$

- As before, we decode $\tilde{\mathbf{y}}_2 = \mathbf{y}_2 - \hat{\mathbf{w}}_2 = g\mathbf{w}_1 + \tilde{\mathbf{z}}_2$, where $\tilde{\mathbf{z}}_2 = g\mathbf{u}_1 + \mathbf{u}_2 + \mathbf{z}_2$. This is valid from Lemmas 4 and 5. Applying Theorem 1

$$\bar{R}_{w_{1,2}} \approx \frac{1}{2} \log \left(1 + \frac{g^2 \sigma_{w_1}^2}{g^2 \sigma_{u_1}^2 + \sigma_{u_2}^2 + \sigma^2} \right) \quad (6.129)$$

with

$$\epsilon_{g\Lambda_{u_1}} \left(\frac{g\sigma_{u_1}\sigma}{\sqrt{g^2\sigma_{u_1}^2 + \sigma^2}} \right) < \frac{1}{2}, \quad (6.130)$$

$$\epsilon_{\Lambda_{u_2}}(\sigma_{u_2}) < 1, \quad (6.131)$$

$$\epsilon_{g\Lambda_{w_1}} = \epsilon_{g\Lambda_{w_1}} \left(\frac{g\sigma_{w_1}\sqrt{g^2\sigma_{u_1}^2 + \sigma_{u_2}^2 + \sigma^2}}{\sqrt{g^2\sigma_{w_1}^2 + g^2\sigma_{u_1}^2 + \sigma_{u_2}^2 + \sigma^2}} \right) < \frac{1}{2}, \quad (6.132)$$

and

$$\frac{\pi \epsilon_{g\Lambda_{w_1}}(g\sigma_{w_1}/2)}{1 - \epsilon_{g\Lambda_{w_1}}(g\sigma_{w_1}/2)} < \epsilon_{g\Lambda_{w_1}} \quad (6.133)$$

Since we are working with the symmetric interference channel we can change the rates obtained above with the following rates, and say

$$R_{1A} = R_{w1,1} \approx \frac{1}{2} \log \left(1 + \frac{\text{SNR}_c}{\text{INR}_c + \text{INR}_p + \text{SNR}_p + 1} \right) \quad (6.134)$$

$$R_{2A} = R_{w2,1} \approx \frac{1}{2} \log \left(1 + \frac{\text{INR}_c}{\text{SNR}_p + \text{INR}_p + 1} \right) \quad (6.135)$$

$$R_{2B} = R_{w2,2} \approx \frac{1}{2} \log \left(1 + \frac{\text{INR}_c}{\text{SNR}_p + \text{INR}_p + \text{SNR}_c + 1} \right) \quad (6.136)$$

$$R_{1B} = R_{w1,2} \approx \frac{1}{2} \log \left(1 + \frac{\text{SNR}_c}{\text{SNR}_p + \text{INR}_p + 1} \right) \quad (6.137)$$

$$R_{1D} = \bar{R}_{w1,1} \approx \frac{1}{2} \log \left(1 + \frac{\text{INR}_c}{\text{SNR}_p + \text{INR}_p + \text{SNR}_c + 1} \right) \quad (6.138)$$

$$R_{2D} = \bar{R}_{w2,1} \approx \frac{1}{2} \log \left(1 + \frac{\text{SNR}_c}{\text{INR}_p + \text{SNR}_p + 1} \right) \quad (6.139)$$

$$R_{2E} = \bar{R}_{w2,2} \approx \frac{1}{2} \log \left(1 + \frac{\text{SNR}_c}{\text{INR}_c + \text{INR}_p + \text{SNR}_p + 1} \right) \quad (6.140)$$

$$R_{1E} = \bar{R}_{w1,2} \approx \frac{1}{2} \log \left(1 + \frac{\text{INR}_c}{\text{SNR}_p + \text{INR}_p + 1} \right) \quad (6.141)$$

The intersection of these two regions, unlike the strong interference case, has two possibilities. These depend on whether $R_{1A} \leq R_{1E}$ or $R_{1A} > R_{1E}$. Suppose $R_{1A} \leq R_{1E}$ (region 1), then we have

$$\begin{aligned}
 \frac{\text{SNR}_c}{\text{INR}_c + \text{INR}_p + \text{SNR}_p + 1} &\leq \frac{\text{INR}_c}{\text{SNR}_p + \text{INR}_p + 1} \\
 \frac{(\text{SNR}_c)(\text{INR}_c + 1)}{(\text{INR}_c + \text{INR}_p + \text{SNR}_p + 1)(\text{INR}_c + 1)} &\leq \frac{(\text{INR}_c)(\text{INR}_c + 1)}{(\text{SNR}_p + \text{INR}_p + 1)} \\
 \frac{\text{INR}_c \text{SNR}}{\text{INR}_c^2 + \text{INR}_c + (\text{SNR} + 2\text{INR})} &\leq \frac{\text{INR}_c^2 + \text{INR}_c}{\text{SNR} + 2\text{INR}} \\
 \text{SNR}(\text{SNR} + 2\text{INR}) &\leq (\text{INR}_c + 1)(\text{INR}_c(\text{INR}_c + 1) + \text{SNR} + 2\text{INR}) \\
 \text{SNR}(\text{SNR} + 2\text{INR}) &\leq (\text{INR})(\text{INR}_c \text{INR} + \text{SNR} + 2\text{INR}) \\
 \text{SNR}(\text{SNR} + 2\text{INR}) &\leq (\text{INR})(\text{INR}(\text{INR}_c + 2) + \text{SNR}) \\
 \text{SNR}(\text{SNR} + 2\text{INR}) &\leq (\text{INR})(\text{INR}(\text{INR} + 1) + \text{SNR}) \\
 \text{SNR}^2 + 2\text{SNR} \cdot \text{INR} &\leq \text{INR}^2(\text{INR} + 1) + \text{SNRINR} \\
 \text{SNR}^2 + \text{SNR} \cdot \text{INR} &\leq \text{INR}^2(\text{INR} + 1) \\
 \text{SNR}(\text{SNR} + \text{INR}) &\leq \text{INR}^2(\text{INR} + 1) \tag{6.142}
 \end{aligned}$$

Obviously, the case for $R_{1A} > R_{1E}$ (region 2) is given by

$$\text{SNR}(\text{SNR} + \text{INR}) > \text{INR}^2(\text{INR} + 1). \tag{6.143}$$

We can see that these are the same regions obtained in [2]. These are illustrated in Figs. 6.7 and 6.8

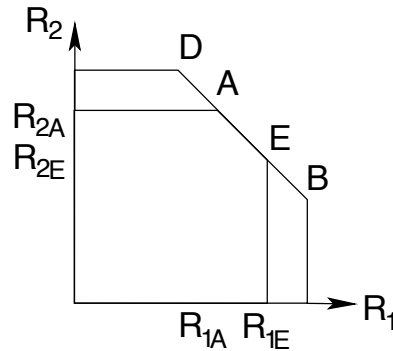


Figure 6.7: Intersection region for the weak interference case, region 1

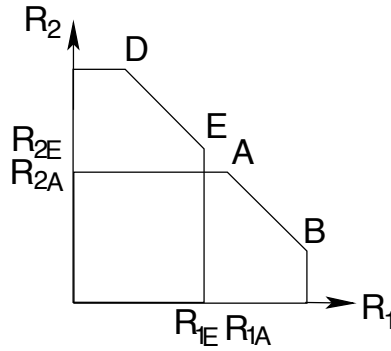


Figure 6.8: Intersection region for the weak interference case, region 2

Similar to the very strong and strong interference cases we verify the flatness factor conditions. Again from the definition of the flatness factor, $\epsilon_{\Lambda} > 0$ must be true. Thus, from (6.94) and (6.95) (which corresponds to the point R_{1A}) we have

$$\frac{\pi \epsilon_{\Lambda_{w_1}}(\sigma_{w_1}/2)}{1 - \epsilon_{\Lambda_{w_1}}(\sigma_{w_1}/2)} < \epsilon_{\Lambda_{w_1}} \left(\frac{\sigma_{w_1} \sqrt{g^2 \sigma_{w_2}^2 + g^2 \sigma_{u_2}^2 + \sigma_{u_1}^2 + \sigma^2}}{\sqrt{\sigma_{w_1}^2 + g^2 \sigma_{w_2}^2 + g^2 \sigma_{u_2}^2 + \sigma_{u_1}^2 + \sigma^2}} \right), \quad (6.144)$$

we also need

$$\epsilon_{\Lambda_{w_1}}(\sigma_{w_1}/2) < \epsilon_{\Lambda_{w_1}} \left(\frac{\sigma_{w_1} \sqrt{g^2 \sigma_{w_2}^2 + g^2 \sigma_{u_2}^2 + \sigma_{u_1}^2 + \sigma^2}}{\sqrt{\sigma_{w_1}^2 + g^2 \sigma_{w_2}^2 + g^2 \sigma_{u_2}^2 + \sigma_{u_1}^2 + \sigma^2}} \right). \quad (6.145)$$

Then

$$\begin{aligned} \frac{\sigma_{w_1}^2}{2} &> \frac{\sigma_{w_1} \sqrt{g^2 \sigma_{w_2}^2 + g^2 \sigma_{u_2}^2 + \sigma_{u_1}^2 + \sigma^2}}{\sqrt{\sigma_{w_1}^2 + g^2 \sigma_{w_2}^2 + g^2 \sigma_{u_2}^2 + \sigma_{u_1}^2 + \sigma^2}} \\ \frac{1}{4} &> \frac{g^2 \sigma_{w_2}^2 + g^2 \sigma_{u_2}^2 + \sigma_{u_1}^2 + \sigma^2}{\sigma_{w_1}^2 + g^2 \sigma_{w_2}^2 + g^2 \sigma_{u_2}^2 + \sigma_{u_1}^2 + \sigma^2} \\ \sigma_{w_1}^2 &> 3g^2 \sigma_{w_2}^2 + 3g^2 \sigma_{u_2}^2 + 3\sigma_{u_1}^2 + 3\sigma^2 \\ \text{SNR}_c &> 3\text{INR}_c + 3\text{INR}_p + 3\text{SNR}_p + 3 \\ \text{SNR} &> 3\text{INR} + 4\text{SNR}_p + 3 \\ \text{SNR} \cdot \text{INR} &> 3\text{INR}^2 + 4\text{SNR} + 3\text{INR}. \end{aligned} \quad (6.146)$$

We also verify (6.99) and (6.100), (which corresponds to the point R_{2A})

$$\epsilon_{g\Lambda_{w_2}}(g\sigma_{w_2}/2) < \epsilon_{g\Lambda_{w_2}}\left(\frac{g\sigma_{w_2}^2\sqrt{(g^2\sigma_{u_2}^2 + \sigma_{u_1}^2 + \sigma^2)}}{\sqrt{g^2\sigma_{w_2}^2 + g^2\sigma_{u_2}^2 + \sigma_{u_1}^2 + \sigma^2}}\right), \quad (6.147)$$

then

$$\begin{aligned} \frac{g^2\sigma_{w_2}^2}{4} &> \frac{g^2\sigma_{w_2}^2(g^2\sigma_{u_2}^2 + \sigma_{u_1}^2 + \sigma^2)}{g^2\sigma_{w_2}^2 + g^2\sigma_{u_2}^2 + \sigma_{u_1}^2 + \sigma^2} \\ \frac{1}{4} &> \frac{(g^2\sigma_{u_2}^2 + \sigma_{u_1}^2 + \sigma^2)}{g^2\sigma_{w_2}^2 + g^2\sigma_{u_2}^2 + \sigma_{u_1}^2 + \sigma^2} \\ g^2\sigma_{w_2}^2 &> 3g^2\sigma_{u_2}^2 + 3\sigma_{u_1}^2 + 3\sigma^2 \\ \text{INR}_c &> 3\text{INR}_p + 3\text{SNR}_p + 3 \\ \text{INR}^2 &> 4\text{INR} + 3\text{SNR} + 3\text{INR}. \end{aligned} \quad (6.148)$$

We have two more restrictions given by the relationship between (6.99) and (6.127). Let us say that (6.99) is bigger than (6.127). We can verify that $\epsilon_{\Lambda}(\sigma) = \epsilon_{g\Lambda}(g\sigma)$ (see Appendix B), then

$$\begin{aligned} \epsilon_{\Lambda_{w_2}}\left(\frac{\sigma_{w_2}\sqrt{g^2\sigma_{w_1}^2 + g^2\sigma_{u_1}^2 + \sigma_{u_2}^2 + \sigma^2}}{\sqrt{\sigma_{w_2}^2 + g^2\sigma_{w_1}^2 + g^2\sigma_{u_1}^2 + \sigma_{u_2}^2 + \sigma^2}}\right) &< \epsilon_{g\Lambda_{w_2}}\left(\frac{g\sigma_{w_2}\sqrt{g^2\sigma_{u_2}^2 + \sigma_{u_1}^2 + \sigma^2}}{\sqrt{g^2\sigma_{w_2}^2 + g^2\sigma_{u_2}^2 + \sigma_{u_1}^2 + \sigma^2}}\right), \\ \frac{g^2\sigma_{u_2}^2 + \sigma_{u_1}^2 + \sigma^2}{g^2\sigma_{w_2}^2 + g^2\sigma_{u_2}^2 + \sigma_{u_1}^2 + \sigma^2} &< \frac{g^2\sigma_{w_1}^2 + g^2\sigma_{u_1}^2 + \sigma_{u_2}^2 + \sigma^2}{\sigma_{w_2}^2 + g^2\sigma_{w_1}^2 + g^2\sigma_{u_1}^2 + \sigma_{u_2}^2 + \sigma^2} \\ \frac{\text{INR}_p + \text{SNR}_p + 1}{\text{INR}_c + \text{INR}_p + \text{SNR}_p + 1} &< \frac{\text{INR}_c + \text{INR}_p + \text{SNR}_p + 1}{\text{SNR}_c + \text{INR}_c + \text{INR}_p + \text{SNR}_p + 1} \\ (\text{INR}_p + \text{SNR}_p + 1)(\text{SNR} + \text{INR} + 1) &< (\text{INR} + \text{SNR}_p + 1)^2 \\ \text{SNR} + \text{INR}_p + \text{SNR}_p \cdot \text{SNR} &< \text{INR}^2 + \text{SNR}_p^2 + \text{SNR}_p \\ \text{SNR} \cdot \text{INR}^2 + \text{INR}^2 + \text{SNR}_p \text{SNR} \cdot \text{INR}^2 &< \text{INR}^4 + \text{SNR}_p^2 \text{INR}^2 + \text{SNR}_p \cdot \text{INR}^2. \\ \frac{\text{INR}}{\text{SNR}} + \frac{\text{INR}}{\text{SNR}^2} + 1 &< \frac{\text{INR}^3}{\text{SNR}^2} + \frac{1}{\text{INR} \text{SNR}} + \frac{1}{\text{SNR}}, \end{aligned} \quad (6.149)$$

We will see later that this corresponds to region 1.

Obviously when (6.99) is smaller than (6.127), we have

$$\frac{\text{INR}}{\text{SNR}} + \frac{\text{INR}}{\text{SNR}^2} + 1 > \frac{\text{INR}^3}{\text{SNR}^2} + \frac{1}{\text{INRSNR}} + \frac{1}{\text{SNR}} \quad (6.150)$$

which corresponds to region 2.

Since the channel is symmetric, we will obtain the same if we consider equations (6.127) and (6.128), (6.132) and (6.133), which are the conditions for point E in Fig. 6.7 or 6.8 and (6.132) and (6.94).

The maximum common rate can now be calculated from these two regions. For the first region we have

$$\begin{aligned} R_{\max\text{reg1}} &\approx \frac{R_{1A} + R_{1E}}{2} \\ &\approx \frac{1}{4} \log \left(1 + \frac{\text{SNR}_c}{\text{INR}_c + \text{INR}_p + \text{SNR}_p + 1} \right) + \frac{1}{2} \log \left(1 + \frac{\text{INR}_c}{\text{SNR}_p + \text{INR}_p + 1} \right) \\ &\approx \frac{1}{4} \log \left(\left(\frac{\text{SNR} + \text{INR} + 1}{\text{INR} + \text{SNR}_p + 1} \right) \left(\frac{\text{SNR}_p + \text{INR} + 1}{\text{INR}_p + \text{SNR}_p + 1} \right) \right) \\ &\approx \frac{1}{4} \log \left(\frac{\text{SNR} + \text{INR} + 1}{\text{SNR}_p + \text{INR}_p + 1} \right) \\ &\approx \frac{1}{4} \log \left(\frac{(\text{SNR} + \text{INR} + 1)(\text{INR}_c + 1)}{\text{SNR} + 2\text{INR}} \right) \\ &\approx \frac{1}{4} \log \left(1 + \frac{(\text{SNR} + \text{INR})(\text{INR} - 1)}{\text{SNR} + 2\text{INR}} \right) \end{aligned} \quad (6.151)$$

Due to the symmetry of the channel, $\frac{R_{2A} + R_{2E}}{2}$ gives the same result.

For the second region we have

$$\begin{aligned}
 R_{\max \text{reg}2} &\approx R_{2A} = R_{1E} \\
 &\approx \frac{1}{2} \log \left(1 + \frac{\text{INR}_c}{\text{SNR}_p + \text{INR}_p + 1} \right) \\
 &\approx \frac{1}{2} \log \left(\frac{\text{SNR}_p + \text{INR} + 1}{\text{SNR}_p + \text{INR}_p + 1} \right) \\
 &\approx \frac{1}{2} \log \left(\frac{(\text{SNR}_p + \text{INR} + 1)(\text{INR}_c + 1)}{(\text{SNR}_p + \text{INR}_p + 1)(\text{INR}_c + 1)} \right) \\
 &\approx \frac{1}{2} \log \left(\frac{\text{SNR} + \text{INR} + \text{INR}^2}{\text{SNR} + 2\text{INR}} \right) \\
 &\approx \frac{1}{2} \log \left(1 + \frac{\text{INR}(\text{INR} - 1)}{\text{SNR} + 2\text{INR}} \right) \tag{6.152}
 \end{aligned}$$

Since we have already found \mathbf{w}_1 and \mathbf{w}_2 , to find the private message we simply do the following: for user 1 and from Lemma 4 we consider $g\mathbf{u}_2$ as noise and say $\mathbf{y}_1 - \hat{\mathbf{w}}_1 - g\hat{\mathbf{w}}_2 = \mathbf{u}_1 + (g\mathbf{u}_2 + \mathbf{z}_1)$. Then

$$R_{u1} \approx \frac{1}{2} \log \left(1 + \frac{\sigma_{u1}^2}{g^2\sigma_{u2}^2 + \sigma^2} \right) \tag{6.153}$$

with the set of conditions

$$\epsilon_{g\Lambda_{u2}} \left(\frac{g\sigma_{u2}\sigma}{\sqrt{g^2\sigma_{u2}^2 + \sigma^2}} \right) < \frac{1}{2}, \tag{6.154}$$

$$\epsilon_{\Lambda_{u1}} = \epsilon_{\Lambda_{u1}} \left(\frac{\sigma_{u1}\sqrt{g^2\sigma_{u2}^2 + \sigma^2}}{\sqrt{\sigma_{u1}^2 + g^2\sigma_{u2}^2 + \sigma^2}} \right) < \frac{1}{2}, \tag{6.155}$$

and

$$\frac{\pi\epsilon_{\Lambda_{u1}}(\sigma_{u1}/2)}{1 - \epsilon_{\Lambda_{u1}}(\sigma_{u1}/2)} < \epsilon_{\Lambda_{u1}} \tag{6.156}$$

And for user 2, we consider $g\mathbf{u}_1$ as noise from Lemma 4 and say $\mathbf{y}_2 - \hat{\mathbf{w}}_2 - g\hat{\mathbf{w}}_1 = \mathbf{u}_2 + (g\mathbf{u}_1 + \mathbf{z}_2)$. Then

$$R_{u2} \approx \frac{1}{2} \log \left(1 + \frac{\sigma_{u2}^2}{g^2\sigma_{u1}^2 + \sigma^2} \right). \quad (6.157)$$

with the following set of conditions

$$\epsilon_{g\Lambda_{u1}} \left(\frac{g\sigma_{u1}\sigma}{\sqrt{g^2\sigma_{u1}^2 + \sigma^2}} \right) < \frac{1}{2}, \quad (6.158)$$

$$\epsilon_{\Lambda_{u2}} = \epsilon_{\Lambda_{u2}} \left(\frac{\sigma_{u2}\sqrt{g^2\sigma_{u1}^2 + \sigma^2}}{\sqrt{\sigma_{u2}^2 + g^2\sigma_{u1}^2 + \sigma^2}} \right) < \frac{1}{2}, \quad (6.159)$$

and

$$\frac{\pi\epsilon_{\Lambda_{u2}}(\sigma_{u2}/2)}{1 - \epsilon_{\Lambda_{u2}}(\sigma_{u2}/2)} < \epsilon_{\Lambda_{u2}} \quad (6.160)$$

Again since we are working with a symmetric channel, the maximum private rate is given by

$$R_u \approx \frac{1}{2} \log \left(1 + \frac{\text{SNR}_p}{\text{INR}_p + 1} \right). \quad (6.161)$$

From the conditions (6.155) and (6.156) we have

$$\epsilon_{\Lambda_{u1}}(\sigma_{u1}/2) < \epsilon_{\Lambda_{u1}} \left(\frac{\sigma_{u1}\sqrt{g^2\sigma_{u2}^2 + \sigma^2}}{\sqrt{\sigma_{u1}^2 + g^2\sigma_{u2}^2 + \sigma^2}} \right) \quad (6.162)$$

Then

$$\begin{aligned}
 \frac{\sigma_{u_1}^2}{4} &> \frac{\sigma_{u_1}^2 (g^2 \sigma_{u_2}^2 + \sigma^2)}{\sigma_{u_1}^2 + g^2 \sigma_{u_2}^2 + \sigma^2} \\
 \sigma_{u_1}^2 &> 3g^2 \sigma_{u_2}^2 + 3\sigma^2 \\
 \text{SNR}_p &> 3\text{INR}_p + 3 \\
 \text{SNR} &> 6\text{INR} \\
 \alpha &< 1 + \frac{\log(6)}{\log(\text{SNR})} \tag{6.163}
 \end{aligned}$$

Because of the symmetry of the channel conditions (6.159) and (6.160) give the same result as (6.163).

We also see that equations (6.126) and (6.131) are the same, and smaller than (6.92). Equation (6.92) is the same as (6.97) and (6.154), and smaller than $\epsilon_{g\Lambda_{u_2}}(g\sigma_{u_2}/2)$, which is smaller than (6.159). Thus

$$\epsilon_{\Lambda_{u_2}}(\sigma_{u_2}) < \epsilon_{\Lambda_{u_2}}\left(\frac{\sigma_{u_2} \sqrt{g^2 \sigma_{u_1}^2 + \sigma^2}}{\sqrt{\sigma_{u_2}^2 + g^2 \sigma_{u_1}^2 + \sigma^2}}\right) < \frac{1}{2}. \tag{6.164}$$

It is important to verify these equations to be sure there are no contradictions with the flatness factor conditions. This is similar for (6.93), (6.98),(6.125),(6.130),(6.158) and (6.155) due to the symmetry of the channel.

Therefore, we have the following conditions

$$\text{INR}^2 > 4\text{INR} + 3\text{SNR} + 3\text{INR}, \text{ for any region} \tag{6.165}$$

$$\text{SNR} \cdot \text{INR} > 3\text{INR}^2 + 4\text{SNR} + 3\text{INR}, \text{ for region 1} \tag{6.166}$$

$$\frac{\text{INR}}{\text{SNR}} + \frac{\text{INR}}{\text{SNR}^2} + 1 < \frac{\text{INR}^3}{\text{SNR}^2} + \frac{1}{\text{INRSNR}} + \frac{1}{\text{SNR}}, \text{ for region 1} \tag{6.167}$$

$$\frac{\text{INR}}{\text{SNR}} + \frac{\text{INR}}{\text{SNR}^2} + 1 > \frac{\text{INR}^3}{\text{SNR}^2} + \frac{1}{\text{INRSNR}} + \frac{1}{\text{SNR}}, \text{ for region 2} \tag{6.168}$$

$$\text{SNR} > 6\text{INR}, \text{ for any region} \tag{6.169}$$

From (6.165) we have

$$\begin{aligned} \text{INR}^2 &> 7\text{INR} + 3\text{SNR} \\ \text{INR}^3 &> 7\text{INR}^2 + 3\text{SNR}\text{INR} \\ \frac{\text{INR}^3}{\text{SNR}^2} &> \frac{7\text{INR}^2}{\text{SNR}^2} + \frac{3\text{INR}}{\text{SNR}} \end{aligned} \quad (6.170)$$

this approximates to

$$\text{INR} > 7. \quad (6.171)$$

From (6.166) we have

$$\begin{aligned} \text{SNR} \cdot \text{INR} &> 3\text{INR}^2 + 4\text{SNR} + 3\text{INR} \\ 1 &> \frac{3\text{INR}}{\text{SNR}} + \frac{4}{\text{INR}} + \frac{3}{\text{SNR}} \end{aligned} \quad (6.172)$$

this approximates to

$$\begin{aligned} \text{SNR} &> 3\text{INR}. \\ 1 &> \frac{\log 3}{\log \text{SNR}} + \frac{\log \text{INR}}{\log \text{SNR}} \\ \alpha &< 1 - \frac{\log 3}{\log \text{SNR}}. \end{aligned} \quad (6.173)$$

From (6.167) we have

$$\begin{aligned} \frac{\text{INR}}{\text{SNR}} + \frac{\text{INR}}{\text{SNR}^2} + 1 &< \frac{\text{INR}^3}{\text{SNR}^2} + \frac{1}{\text{INR}\text{SNR}} + \frac{1}{\text{SNR}} \\ \frac{\text{INR}}{\text{SNR}} + \frac{\text{INR}}{\text{SNR}^2} + 1 &< \frac{\text{INR}^3}{\text{SNR}^2} + \frac{1}{\text{SNR}\text{INR}} + \frac{1}{\text{SNR}} \end{aligned} \quad (6.174)$$

which approximates to

$$\begin{aligned} 1 &< \frac{\text{INR}^3}{\text{SNR}^2} \\ \alpha &> \frac{2}{3}. \end{aligned} \quad (6.175)$$

From (6.168) we have

$$\begin{aligned} 1 &> \frac{\text{INR}^3}{\text{SNR}^2} \\ \alpha &< \frac{2}{3}. \end{aligned} \tag{6.176}$$

From (6.169) we have

$$\begin{aligned} \text{SNR} &> 6\text{INR} \\ \log \text{SNR} &> \log \text{INR} + \log 6 \\ \alpha &< 1 - \frac{\log 6}{\log \text{INR}} \end{aligned} \tag{6.177}$$

We will see shortly that (6.165), (6.166), (6.167), (6.168) and (6.169) are not contradictory to the weak or moderately weak interference channels.

For the two possible maximum rates of the common messages and the private rate, we can find the total rate and derive the GDoF.

$$\frac{R_{\max}}{R_{\text{AWGN}}} \approx \frac{\min\{R_u + R_{\max\text{reg}1}, R_u + R_{\max\text{reg}2}\}}{\frac{1}{2} \log(1 + \text{SNR})}$$

$$\begin{aligned} R_{\max} &\approx \min\left\{\frac{1}{4} \log \left(\left(1 + \frac{\text{SNR}}{2\text{INR}}\right)^2 \left(1 + \frac{(\text{SNR} + 1)(\text{INR} - 1)}{\text{SNR} + 2\text{INR}}\right)\right)\right. \\ &\quad \left., \frac{1}{2} \log \left(\left(1 + \frac{\text{INR}(\text{INR} - 1)}{\text{SNR} + 2\text{INR}}\right) \left(1 + \frac{\text{SNR}}{2\text{INR}}\right)\right)\right\} \\ &\approx \min\left\{\frac{1}{4} \log \left(\left(\frac{2\text{INR} + \text{SNR}}{4\text{INR}}\right) (\text{INR} + \text{SNR} + 1)\right), \frac{1}{2} \log \left(\frac{\text{SNR} + \text{INR} + \text{INR}^2}{2\text{INR}}\right)\right\} \\ &\approx \min\left\{\frac{1}{4} \log \left((\text{INR} + \text{SNR} + 1) \left(1 + \frac{\text{SNR}}{\text{INR}}\right) \frac{1}{4}\right), \frac{1}{2} \log \left(\left(\frac{\text{SNR}}{\text{INR}} + \text{INR} + 1\right) \frac{1}{2}\right)\right\} \\ &\approx \min\left\{\frac{1}{4} \log ((\text{INR} + \text{SNR} + 1)) + \frac{1}{4} \log \left(1 + \frac{\text{SNR}}{\text{INR}}\right) - \frac{1}{2}, \frac{1}{2} \log \left(1 + \text{INR} + \frac{\text{INR}}{\text{SNR}}\right) - 1\right\}. \end{aligned} \tag{6.178}$$

Then

$$\begin{aligned} \frac{R_{\max}}{R_{\text{AWGN}}} &\approx \frac{\min\{\frac{1}{4} \log((\text{INR} + \text{SNR} + 1)) + \frac{1}{4} \log\left(1 + \frac{\text{SNR}}{\text{INR}}\right) - \frac{1}{2}, \frac{1}{2} \log\left(1 + \text{INR} + \frac{\text{INR}}{\text{SNR}}\right) - 1\}}{\frac{1}{2} \log(1 + \text{SNR})} \\ &\approx \frac{\min\{\frac{1}{4} \log(\text{SNR}) + \frac{1}{4} \log(\text{SNR}) - \frac{1}{4} \log(\text{INR}), \frac{1}{2} \log(\text{INR})\}}{\frac{1}{2} \log(\text{SNR})} \end{aligned} \quad (6.179)$$

where we have considered that $\text{SNR} < \text{INR}^2$.

$$\frac{R_{\max}}{R_{\text{AWGN}}} \approx \min\left\{1 - \frac{1}{2} \frac{\log(\text{INR})}{\log(\text{SNR})}, \frac{\log(\text{INR})}{\log(\text{SNR})}\right\} \quad (6.180)$$

As seen previously $\alpha \triangleq \frac{\log(\text{INR})}{\log(\text{SNR})}$, then

$$\frac{R_{\text{HK}}}{R_{\text{AWGN}}} \approx \min\left\{1 - \frac{1}{2}\alpha, \alpha\right\} \quad (6.181)$$

Here we have two results, depending on the level of interference. The first one, $1 - \frac{1}{2}\alpha$ is valid when $\text{SNR} (\text{SNR} + \text{INR}) \leq \text{INR}^2 (\text{INR} + 1)$ (represented in Fig. 6.7), and can be further simplified if we consider that $\text{SNR}, \text{INR} \gg 1$ and $\text{SNR} > \text{INR}$. We obtain that

$$\frac{2}{3} < \frac{\log(\text{INR})}{\log(\text{SNR})} = \alpha, \quad (6.182)$$

which is the same as condition (6.175). For the other region $\alpha < \frac{2}{3}$, which is the same as condition (6.176). Obviously, for these two region conditions (6.171), (6.173) and (6.177) are achievable.

6.3.3 Noisy interference

For noisy interference we only have the private messages. Then $\mathbf{x}_1 = \mathbf{u}_1$, and $\mathbf{x}_2 = \mathbf{u}_2$. Consider that both $\mathbf{u}_1 \in D_{\Lambda_{u_1}, \sigma_{u_1}}$ and $\mathbf{u}_2 \in D_{\Lambda_{u_2}, \sigma_{u_2}}$, and that for noisy interference $\text{INR}^2 < \text{SNR}$. This case is very similar to the very strong interference, except here we use private messages instead of common messages. The rates are the same as the ones obtained for the very strong and strong interference cases except here we can approximate them as follows

$$R_{1A} = R_{w1,1} \approx \frac{1}{2} \log \left(\frac{\text{SNR}}{\text{INR}} \right) \quad (6.183)$$

$$R_{2A} = R_{w2,1} \approx \frac{1}{2} \log (\text{INR}) \quad (6.184)$$

$$R_{2B} = R_{w2,2} \approx \frac{1}{2} \log (1) \quad (6.185)$$

$$R_{1B} = R_{w1,2} \approx \frac{1}{2} \log (\text{SNR}) \quad (6.186)$$

$$R_{2E} = \bar{R}_{w2,2} \approx \frac{1}{2} \log \left(\frac{\text{SNR}}{\text{INR}} \right) \quad (6.187)$$

$$R_{1E} = \bar{R}_{w1,2} \approx \frac{1}{2} \log (\text{INR}) \quad (6.188)$$

$$R_{1D} = \bar{R}_{w1,1} \approx \frac{1}{2} \log (1) \quad (6.189)$$

$$R_{2D} = \bar{R}_{w2,1} \approx \frac{1}{2} \log (\text{SNR}) \quad (6.190)$$

The intersection of both MAC regions is shown in Fig. 6.9.

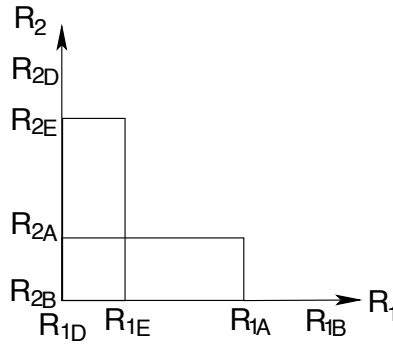


Figure 6.9: Intersection region for the noisy interference case

Therefore, the maximum achievable rate is given by

$$R_{\max} = R_{1A} = R_{2E} \approx \frac{1}{2} \log \left(\frac{\text{SNR}}{\text{INR}} \right) = \log (\text{SNR}) - \log (\text{INR}). \quad (6.191)$$

And the GDoF is given by

$$d_{\text{sym}} \approx \frac{\frac{1}{2} \log (\text{SNR}) - \frac{1}{2} \log (\text{INR})}{\frac{1}{2} \log (\text{SNR})} \approx 1 - \alpha. \quad (6.192)$$

To conclude the chapter, we can summarize that we have obtained as

$$\frac{R_{\text{HK}}}{C_{\text{AWGN}}} \approx \begin{cases} 1 - \alpha & \text{for } 0 \leq \alpha \leq 1/2 & \text{Noisy;} \\ \alpha & \text{for } 1/2 \leq \alpha \leq 2/3 & \text{Weak;} \\ 1 - \frac{\alpha}{2} & \text{for } 2/3 \leq \alpha < 1 & \text{Moderately Weak;} \\ \frac{\alpha}{2} & \text{for } 1 < \alpha \leq 2 & \text{Strong;} \\ 1 & \text{for } \alpha \geq 2 & \text{Very Strong.} \end{cases}$$

With these results we demonstrate that we have obtained the same regions as Etkin and that the final GDoF using Gaussian lattices is the same as when random codebooks are used.

6.4 Conclusions

In this chapter, we have found the GDoF of a two-user symmetric interference channel with lattices. The GDoF for this scenario has been demonstrated before using random coding. Here we use lattice Gaussian distribution to put randomness in the structure of the lattice. We demonstrate that using lattice Gaussian distribution, and by considering some properties of the flatness factor of the lattices, we can find the same GDoF for all types of interference as was found using the random coding technique, with a HK scheme where private and common messages are used. We can conjecture that this could be extended to a K -user symmetric interference channel because of the use of lattices, since the interference will automatically be aligned at the receivers.

Chapter 7

Conclusion and Future Work

7.1 Conclusions

This thesis focuses on interference management techniques for the interference channel. We mainly worked with the interference alignment technique, which allows to align all interference at the receivers, and leave $1/2$ of the signal space for the desired signal. We approached the problem from two perspectives. The first is addressed in Chapter 3. Here we worked with interference alignment from the signal space perspective as the one originally proposed in the renowned paper by Cadambe and Jafar [10]. We noted that many papers deal with the interference alignment method proposed by [10] in terms of rate and DoF achievability for many scenarios, but few have focused on the performance of the technique. We therefore applied some precoding techniques such as SVD and THP along with bit and power loading techniques to show that the performance of the Cadambe and Jafar interference alignment scheme can be improved. Later in Chapter 4, we focused our work on the signal scale perspective of interference alignment. In that chapter, we still used Cadambe and Jafar's original scheme but we assumed the matrices that jointly represent the channel and the precoding are the generator matrices of a lattice. Here we worked with a three user many-to-one interference channel and aligned interference by designing the precoding matrices along with unimodular matrices. After that, and using the properties of the lattice, we derived a bound for the probability of error considering a maximum likelihood decoder. We found a result that relates the theta series

of the joint received lattice and the theta series of the interference lattice. Since the theta series is closely related to the flatness factor of the lattice, we verified the hypothesis that to minimize the error probability, the interference lattice must have a big flatness factor. We also presented some design criteria for the lattices for the direct channels 2 and 3. In Chapter 5, we continued to work with lattices. In this case we used BW lattices for the symmetric (fully connected) interference channel. We mimicked the work presented in [5] where a multilevel strategy is used to achieve the GDoF for the symmetric interference channel. However, their strategy only considers one-dimensional codes, leaving the possibility for improvement. For that reason we decided to use lattices, in particular BW lattices, not only because of the better performance that we can obtain with lattices but also because of their similarities since they can be built using a multilevel construction similar to the one used in [5]. We showed that we can improve the error rate and, since we followed their design in the construction of the codewords, we can also conjecture we can achieve the GDoF. In Chapter 6, we continued to work with lattices to achieve the GDoF with general lattices. In this chapter we focused our attention on [2], the first paper to work with the GDoF for every type of interference, although only for two users. Their strategy involves using random Gaussian codewords. Since the proofs for capacity and DoF normally use random codes, we worked with the lattice Gaussian distribution [27] to take advantage of the higher dimension of the lattice and of the randomness that the Gaussian distribution can provide. We found that under some constraints of the flatness factor of the lattices we can also achieve the GDoF for all types of interference.

7.2 Future work

We see that there are still many open questions to be answered on interference alignment. We simplified our research by working with special channels, to contribute to the understanding of the interference alignment problem. Our work showed an improvement in error probability and designed a path to obtain methods to implement codes for interference alignment.

In particular, an open issue is to find optimal precoders for interference alignment

in the signal space. One idea is to rotate the signals at the transmitters such that at the desired receiver, most of the signal is projected into the desired subspace. We believe this would improve the performance of the Cadambe and Jafar scheme. However, finding this rotation matrix is not trivial.

In terms of error probability and its bounds, we found a result for the many-to-one interference channel with lattices. The extension to fully connected channels is an open problem, using the properties of lattices such as the flatness factor.

We also showed that using Jafar's Q -base representation idea and BW lattices it is possible to improve the performance of the interference channel. However, a new idea would be to extend this either by using any construction D lattice or by using nested lattices in each level.

For the last chapter, the design of a practical working scheme with Gaussian lattices for interference is still an open issue.

One of the big open problem corresponds to the global channel knowledge that interference alignment requires. For this, some authors are working on the subject of the Grassmannian manifold. In those papers, the channel is estimated at the receivers and a truncated unitary matrix that spans the same subspace of the estimated channels is fed back. The receiver quantizes this subspace into codewords whose codebooks are known at both the receivers and transmitters. The receivers then broadcast the index of this quantized codeword to the transmitters. The quantized codeword is the closest point on the Grassmannian manifold. We wonder if these codebooks can be constructed using structured codes.

Bibliography

- [1] G. Bresler, A. Parekh, and D. Tse, "The approximate capacity of the many-to-one and one-to-many Gaussian interference channels," *IEEE Transactions on Information Theory*, vol. 56, pp. 4566–4592, Sep. 2010.
- [2] R. H. Etkin, D. N. C. Tse, and H. Wang, "Gaussian interference channel capacity to within one bit," *IEEE Transactions on Information Theory*, vol. 54, pp. 5534–5562, Dec. 2008.
- [3] S. D. S. Avestimehr and D. Tse, "Wireless network information flow," *Allerton Conference on Communication, Control, and Computing*, Sep. 2007.
- [4] V. Cadambe, S. Jafar, and S. Shamai, "Interference alignment on the deterministic channel and application to fully connected Gaussian interference networks," *IEEE Transactions on Information Theory*, vol. 55, pp. 269–274, Jan. 2009.
- [5] S. A. Jafar and S. Vishwanath, "Generalized degrees of freedom of the symmetric Gaussian K user interference channel," *IEEE Transactions on Information Theory*, vol. 56, pp. 3297–3303, Jul. 2010.
- [6] A. Carleial, "A case where interference does not reduce capacity," *IEEE Transactions on Information Theory*, vol. 21, pp. 569–570, Sept. 1975.
- [7] T.S.Han and K. Kobayashi, "A new achievable rate region for the interference channel," *IEEE Transactions on Information Theory*, vol. 27, pp. 49–60, Jan. 1981.
- [8] H. Sato, "The capacity of the gaussian interference channel under strong interference," *IEEE Transactions on Information Theory*, vol. 27, pp. 786–788, Nov. 1981.

- [9] M. Costa, "On the Gaussian interference channel," *IEEE Transactions on information theory*, vol. 31, pp. 607–615, Sep. 1985.
- [10] V. Cadambe and S. A. Jafar, "Interference alignment and degrees of freedom of the K -user interference channel," *IEEE Transactions on Information Theory*, vol. 54, pp. 3425–3441, Aug. 2008.
- [11] S. A. Jafar, "Interference alignment - a new look at signal dimensions in a communications network," *Foundations and Trends in Communications and Information Theory*, vol. 7, pp. 1–136, 2011.
- [12] S. Jafar and S. S. (Shitz), "Degrees of freedom for the MIMO X channel," *IEEE Transactions on Information Theory*, vol. 54, pp. 151–170, Jan. 2008.
- [13] M. Maddah-Ali, A. Motahari, and A. Khandani, "Communication over the MIMO X channel: Signaling and performance analysis," *University of California, Berkeley, Tech, Rep.*, 2007.
- [14] K. Gomadam, V. Cadambe, and S. Jafar, "Approaching the capacity of wireless networks through distributed interference alignment," *IEEE Global Telecommunications Conference*, pp. 1–6, Dec. 2008.
- [15] F. Oggier and E. Viterbo, "Algebraic number theory and code design for rayleigh fading channels," *Foundations and Trends® in Communications and Information Theory*, vol. 1, pp. 333–415, Dec. 2004.
- [16] J. Conway and N. Sloane, *Sphere Packings, Lattices and Groups*. Springer-Verlag, 1988.
- [17] R. Fischer, *Precoding and Signal Shaping for Digital transmission*. Wiley-IEEE Press, 2002.
- [18] J. J. D. Forney, "Coset codes - part I: Introduction and geometrical classification," *IEEE Transactions on Information Theory*, vol. 34, pp. 1123–1151, Sept. 1998.

- [19] J.-C. Belfiore and F. Oggier, "Secrecy gain: a wiretap lattice code design," *International Symposium on Information Theory and its Applications*, pp. 174–178, Oct 2010.
- [20] J.-C. Belfiore, "Lattice codes for the compute and forward protocol: the flatness factor," *IEEE Information Theory Workshop*, pp. 3425–3441, Aug. 2011.
- [21] C. Ling, L. Luzzi, and J.-C. Belfiore, "Lattice codes achieving strong secrecy over the mod- Λ Gaussian channel," in *IEEE International Symposium on Information Theory*, submitted for publication, 2012.
- [22] J. D. Forney, "Coset codes - part II: Binary lattices and related codes," *IEEE Transactions on Information Theory*, vol. 34, pp. 1152–1187, Sept. 1998.
- [23] A. J. Salomon and O. Amrani, "Generalized multilevel constructions for reed-muller codes and barnes-wall lattices," *International Symposium on Information Theory*, pp. 896–900, July 2006.
- [24] E. S. Barnes and G. E. Wall, "Some extreme forms defined in terms of Abelian groups," *J. Austral. Math. Soc.*, 1959.
- [25] A. J. Salomon and O. Amrani, "Augmented product codes and lattices: Reed-Muller codes and Barnes-Wall lattices," *IEEE Transactions on Information Theory*, vol. 51, pp. 3918–3930, Nov. 2005.
- [26] D. Micciancio and A. Nicolosi, "Efficient bounded distance decoders for Barnes-Wall lattices," *IEEE International Symposium on Information Theory, 2008*, pp. 2484–2488, Jul. 2008.
- [27] C. Ling and J.-C. Belfiore, "Achieving the AWGN channel capacity with lattice gaussian coding," *Submitted to IEEE Transactions on Information Theory*, 2013. [Online]. Available: <http://arxiv.org/abs/1302.5906>
- [28] R. Fischer and J. Huber, "A new loading algorithm for discrete multitone transmission," *IEEE Global Telecommunications Conference*, pp. 724–728, Nov. 1996.

- [29] S. W. Peters and R. W. Heath Jr., "Interference alignment via alternating minimization," *IEEE International Conference on Acoustics, Speech, and Signal Processing*, pp. 2445–2448, Apr. 2009.
- [30] R. Tresch, M. Guillaud, and E. Riegler, "On the achievability of interference alignment in the k -user constant MIMO interference channel," *IEEE Workshop on Statistical Signal Processing*, pp. 277–280, Sept. 2009.
- [31] H. Sung, S. H. Park, K. J. Lee, and I. Lee, "Linear precoder designs for k -user interference channels," *IEEE Transactions on Wireless Communications*, vol. 9, pp. 291–301, Jan. 2010.
- [32] S. W. Choi, S. A. Jafar, and S. Y. Chung, "On the beamforming design for efficient interference alignment," *IEEE Communications Letters*, vol. 13, pp. 847–849, Nov. 2009.
- [33] M. Shen, A. Host-Madsen, and J. Vidal, "An improved interference alignment scheme for frequency selective channels," *IEEE International Symposium on Information Theory*, pp. 559–563, July 2008.
- [34] A. Sezgin, S. Jafar, and H. Jafarkhani, "Optimal use of antennas in interference networks: A tradeoff between rate, diversity and interference alignment," *Global Telecommunications Conference, GLOBECOM 2009*, Nov.- Dec. 2009.
- [35] M. Yuksel and E. Erkip, "Diversity-multiplexing tradeoff in cooperative wireless systems," *40th Annual Conference on Information Sciences and Systems, Princeton*, pp. 1062–1067, Mar. 2006.
- [36] C. Yetis, T. Gou, S. Jafar, and A. Kayran, "Feasibility conditions for interference alignment," *Global telecommunications conference, 2009*, pp. 1–6, Nov. 2009.
- [37] H. Ning, C. Ling, and K. Leung, "Feasibility conditions for interference alignment with diversity," *IEEE Transactions on Information Theory*, vol. 57, pp. 2902–2912, May. 2011.

- [38] S. Sridharan, S. Vishwanath, and S. A. Jafar, "Capacity of the symmetric K -user Gaussian very strong interference channels," *Proc. IEEE Global Telecommun. Conf.*, vol. 56, Dec. 2008.
- [39] S. Sridharan, A. Jafarian, S. Vishwanath, S. Jafar, and S. Shamai, "A layered lattice coding scheme for a class of three user Gaussian interference channel," *46th Annual Allerton Conference on Communication, Control, and Computing, 2008*, pp. 531–538, Sep. 2008.
- [40] J. Choi, "Interference alignment over lattices for MIMO interference channels," *IEEE Communications Letters*, vol. 15, pp. 374–376, Apr. 2011.
- [41] R. Tresch and M. Guillaud, "Cellular interference alignment with imperfect channel knowledge," *IEEE International Conference on Communications Workshops*, pp. 1–5, Jun. 2009.
- [42] S. A. Jafar, "Blind interference alignment," *IEEE Journal of Selected Topics in Signal Processing*, pp. 216–227, Jun. 2012.
- [43] M. Rezaee and M. Guillaud, "Limited feedback for interference alignment in the K -user MIMO interference channel," *IEEE Information Theory Workshop*, pp. 667 – 671, Sept. 2012.
- [44] D. J. Love and R. W. Heath Jr, "Grassmannian beamforming for the multiple input multiple output wireless systems," *IEEE Transaction on Information Theory*, vol. 49, pp. 2735–2747, Oct. 2003.
- [45] B. Mondal, R. W. Heath Jr, and L. Hanlen, "Quantization on the grassmann manifold: Applications to precoded MIMO wireless systems," *IEEE International Conference on Acoustics, Speech, and Signal Processing*, Mar. 2005.
- [46] R.-A. Pitaval, H.-L. Maattanen, K. Schobel, O. Tirkkonen, and R. Wichman, "Beamforming codebooks for two transmit antenna systems based on optimum grassmannian packings," *IEEE Transaction on Information Theory*, vol. 57, pp. 6591–6602, 2011.

- [47] Z. Utkovski, P.-C. Chen, and J. Lindner, "Some geometric methods for construction of space-time codes in grassmann manifold," *Forty-sixth annual Allerton Conference*, Sept. 2008.
- [48] J. Conway, R. Hardin, and N. Sloane, "Packings lines, planes, etc: Packing in grassmannian spaces," *Exp. Math.*, vol. 5, Apr. 1996.
- [49] C. Windpassinger, R. Fischer, T. Vencel, and J. Huber, "Precoding in multiantenna and multiuser communications," *IEEE Transactions on Wireless Communications*, vol. 3, pp. 1305–1316, Jul. 2004.
- [50] C. Vencel, C. Windpassinger, and R. Fischer, "Sorting in the v-blast algorithm and loading," *Communications Systems and Networks*, pp. 304–309, Sept. 2002.
- [51] H. Wang and Z. Zhao, "Designs and performance analysis on ML-decoders in a two user's interference channel," *International Conference on Wireless Communications and Signal Processing*, Nov. 2011.
- [52] P. Razaghi and G. Caire, "Interference alignment, carrier pairing, and lattice decoding," *8th International Symposium on Wireless Communication Systems*, No. 2011.
- [53] O. Ordentlich and E. Erez, "Interference alignment at finite SNR for time-invariant channels," *IEEE Information Theory Workshop*, pp. 442–446, Oct. 2011.
- [54] W. Ebeling, *Lattices and Codes: a course partially based on lectures by Friedrich Hirzebruch*. Springer Spektrum, 2013.
- [55] M. Atiyah and I. Macdonald, *Introduction to commutative algebra*. Addison-Wesley publishing, 1969.
- [56] G. Poltyrev, "On coding without restrictions for the AWGN channel," *IEEE Transactions on Information Theory*, vol. 40, pp. 409–417, Mar. 1994.
- [57] G. D. Forney, "A bounded-distance decoding algorithm for the Leech lattice, with generalizations," *IEEE Transactions on Information Theory*, vol. 35, pp. 906–909, Jul. 1989.

-
- [58] W. Kositwattanarerk and F. Oggier, “Connections between construction D and related constructions of lattices,” 2013. [Online]. Available: <http://arxiv.org/abs/1308.6175v1>
- [59] C. Ling and J.-C. Belfiore, “Achieving the AWGN channel capacity with lattice gaussian coding,” *IEEE International Symposium on Information Theory*, pp. 1416–1420, Jul. 2013.
- [60] C. Ling, L. Luzzi, J.-C. Belfiore, and D. Stehlé, “Semantically secure lattice codes for the Gaussian wiretap channel,” *submitted to IEEE Transactions on Information Theory*, 2012. [Online]. Available: <http://arxiv.org/abs/1210.6673>
- [61] R. Zamir, *Lattice Coding for Signal and Networks*. Cambridge, U.K.: Cambridge University Press, book in preparation, 1988.

Appendix A

Fisher-Huber optimization

In this appendix, we will solve the FH optimization. Recall the optimization problem given by equations (3.14)-(3.15):

Thus, the optimization transforms into:

$$\text{SNR}_0 = \frac{3S_T}{\sum_{i=1}^D N_i 2^{R_i}} \quad (\text{A.1})$$

subject to:

$$R_T = \sum R_i = \text{constant} \quad (\text{A.2})$$

Using Lagrange

$$L : \frac{3S_T}{\sum_{i=1}^D N_i 2^{R_i}} - \lambda \left(R_T - \sum_{i=1}^D R_i \right) \quad (\text{A.3})$$

without loss of generality, let us consider that we will find the differential for R_1 .

$$\frac{\partial L}{\partial R_1} = 0 \quad (\text{A.4})$$

$$\frac{\partial}{\partial R_1} \left(\frac{3S_T}{N_1 2^{R_1} + N_2 2^{R_2} + \dots + N_D 2^{R_D}} - \lambda (R_T - R_1 - R_2 - \dots - R_D) \right) = 0 \quad (\text{A.5})$$

Assigning the following variables $P_1 = 2^{R_1}$, $B_1 = N_1 P_1 + \sum_{i=2}^D N_i 2^{R_i}$, $A_1 = \frac{3S_T}{B_1}$, and using

the chain rule

$$\frac{\partial L}{\partial R_1} = \frac{\partial L}{\partial A_1} \frac{\partial A_1}{\partial B_1} \frac{\partial B_1}{\partial P_1} \frac{\partial P_1}{\partial R_1} + \lambda \quad (\text{A.6})$$

$$\frac{\partial L}{\partial R_1} = 1 \cdot \frac{-3S_T}{(N_1 2^{R_1} + N_2 2^{R_2} + \dots + N_D 2^{R_D})^2} \cdot N_1 \cdot 2^{R_1} \log(2) + \lambda = 0 \quad (\text{A.7})$$

Which transforms to

$$\frac{\text{SNR}_0}{\sum_{i=1}^D N_i 2^{R_i}} \cdot N_1 \cdot 2^{R_1} \log(2) = \lambda \quad (\text{A.8})$$

But we define SNR_0 to be constant. Clearly $3S_T$ is constant too, and then $\sum N_i 2^{R_i}$ is also constant. Hence:

$$N_1 \cdot 2^{R_1} = \text{constant}_2 \quad (\text{A.9})$$

But, now if we run the same derivation on R_2 we will get

$$\frac{\text{SNR}_0}{\sum_{i=1}^D N_i 2^{R_i}} \cdot N_2 \cdot 2^{R_2} \log(2) = \lambda, \quad (\text{A.10})$$

which is exactly the same as before. Hence

$$N_i 2^{R_i} = \text{constant} \quad (\text{A.11})$$

With these, the rate and energy are obtained in [28].

Appendix B

Proof of $\epsilon_{\Lambda}(\sigma) = \epsilon_{g\Lambda}(g\sigma)$

Given the theta series of a lattice

$$\theta_{\Lambda} \left(\exp^{-\frac{1}{2\sigma^2}} \right) = \sum_{x \in \Lambda} \exp^{-\frac{\|x\|^2}{2\sigma^2}}, \quad (\text{B.1})$$

and the definition of the theta series

$$\epsilon_{\Lambda}(\sigma) = \frac{V(\Lambda)}{(\sqrt{2\pi}\sigma)^n} \theta_{\Lambda} \left(\exp^{-\frac{1}{2\sigma^2}} \right) - 1, \quad (\text{B.2})$$

Then

$$\theta_{g\Lambda} \left(\exp^{-\frac{1}{2\sigma^2}} \right) = \sum_{\tilde{x} \in g\Lambda} \exp^{-\frac{\|\tilde{x}\|^2}{2\sigma^2}} = \sum_{x \in \Lambda} \exp^{-\frac{g^2\|x\|^2}{2\sigma^2}} \quad (\text{B.3})$$

Consider now

$$\theta_{g\Lambda} \left(\exp^{-\frac{1}{2g^2\sigma^2}} \right) = \sum_{x \in \Lambda} \exp^{-\frac{g^2\|x\|^2}{2g^2\sigma^2}} = \sum_{x \in \Lambda} \exp^{-\frac{\|x\|^2}{2\sigma^2}} = \theta_{\Lambda} \left(\exp^{-\frac{1}{2\sigma^2}} \right) \quad (\text{B.4})$$

Also

$$V(\Lambda) = \sqrt{\det(\mathbf{M}'\mathbf{M})}, \quad (\text{B.5})$$

where \mathbf{M} is the generator matrix of Λ , whose dimension is n . Then

$$\mathbf{V}(g\Lambda) = \sqrt{g^{2n} \det(\mathbf{M}'\mathbf{M})} = g^n \mathbf{V}(\Lambda). \quad (\text{B.6})$$

And

$$\epsilon_{g\Lambda}(g\sigma) = \frac{g^n \mathbf{V}(\Lambda)}{(\sqrt{2\pi}g\sigma)^n} \theta_\Lambda \left(\exp^{-\frac{1}{2\sigma^2}} \right) - 1 = \frac{\mathbf{V}(\Lambda)}{(\sqrt{2\pi}\sigma)^n} \theta_\Lambda \left(\exp^{-\frac{1}{2\sigma^2}} \right) - 1 = \epsilon_\Lambda(\sigma). \quad (\text{B.7})$$